

Aus dem Universitätsklinikum Heidelberg

Leitende Ärztliche Direktorin und Vorstandsvorsitzende: Prof. Dr. Annette
Grüters-Kieslich

Klinik für Kardiologie, Angiologie und Pneumologie

Innere Medizin III

Ärztlicher Direktor: Prof. Dr. med. Hugo A. Katus

**Influence of the SUMOylation pathway on adeno-associated virus vector
transduction**

Inauguraldissertation

zur Erlangung des Doctor scientiarum humanarum (Dr. sc. hum.)

an der

Medizinischen Fakultät Heidelberg

der

Ruprecht-Karls-Universität

vorgelegt von

Qingxin Chen

aus

Heilongjiang, China

2018

Dekan: Herr Prof. Dr. med. Andreas Draguhn
Doktorvater: Herr Prof. Dr. med. Oliver Müller

Table of contents

List of Symbols and Abbreviations	VI
Table of Figures	1
1 Introduction.....	1
1.1 Biology of Adeno-Associated Virus	1
1.1.1 Adeno-Associated Virus genome structure	3
1.1.2 Genetic engineering of the Adeno-Associated Virus	5
1.1.3 Adeno-Associated Virus Trafficking	7
1.1.4 Adeno-Associated Virus packaging mechanism	12
1.2 Biology of SUMOylation	13
1.2.1 SUMOylation Catalytic Pathway	13
1.2.2 The SUMOylation consensus sequence	15
1.2.3 SUMOylation in virus life cycles	18
1.3 Previous work.....	20
1.4 Aim of study	21
2 Materials	23
2.1 Biological materials	23
2.1.1 Eukaryotic Cells	23
2.1.2 Prokaryotic Cells	23
2.1.3 Virus.....	24
2.1.4 Media and Supplements	25
2.2 Molecular biology materials	27
2.2.1 Plasmid	27
2.2.2 Oligonucleotides for mutagenesis or normal PCR	28
2.2.3 oligonucleotides for siRNA knockdown	29
2.2.4 Enzymes	29
2.3 Virologic materials	29
2.3.1 Solutions for AAV production.....	29
2.3.2 Sucrose gradient for AAV separation	30
2.4 Buffers and Solutions for DNA extraction and analysis	30

2.4.1	DNA plasmid extraction by phenol-chloroform	30
2.4.2	Agarose gel electrophoresis	31
2.5	Buffers and Solutions for protein analysis	31
2.5.1	Protein concentration determination	31
2.5.2	Electrophoresis	32
2.5.3	SDS-polyacrylamide gels	32
2.5.4	Western blot analysis	33
2.6	Immunological materials	33
2.6.1	Antibody	33
2.6.2	Immunoprecipitation.....	34
2.6.3	Immunofluorescence.....	35
2.7	General buffer and solutions	35
2.8	Chemicals	36
2.9	Kits	37
2.10	Laboratory equipment	37
2.10.1	Electrical Equipment	37
2.10.2	Common use Equipment	41
2.10.3	Software.....	42
3	Methods.....	43
3.1	Cultivation and manipulation of cells.....	43
3.1.1	Cultivation and manipulation of prokaryotic cells	43
3.1.2	Cultivation and manipulation of eukaryotic cells	44
3.2	Molecular biology methods.....	46
3.2.1	Polymerase chain reaction (PCR).....	46
3.2.2	PCR product purification	47
3.2.3	StrataClone™ Blunt TOPO cloning	48
3.2.4	Gateway cloning	48
3.2.5	Site-directed mutagenesis QuikChange® cloning.....	49
3.2.6	Agarose gel-electrophoresis	50
3.2.7	DNA extraction from agarose gels	50
3.2.8	Enzyme restriction	51

3.2.9	Dephosphorylation of DNA backbone 5'	51
3.2.10	Ligation	51
3.2.11	Transformation of <i>E. coli</i> bacteria	52
3.2.12	DNA extraction from bacterial cultures	53
3.2.13	DNA quantification	54
3.2.14	DNA-Sequencing	54
3.3	Protein analysis methods	54
3.3.1	Bradford assay	54
3.3.2	SDS-Polyacrylamide gel electrophoresis (SDS-PAGE)	54
3.3.3	Western Blot analysis	55
3.3.4	Dot Blot	55
3.4	Immunological methods	56
3.4.1	Immunoprecipitation of virus	56
3.4.2	Immunofluorescence	57
3.5	Virological methods	58
3.5.1	Production of AAV particles in HEK293TT cells	58
3.5.2	AAV particle purification from 293TT cell extracts	59
3.5.3	AAV particle separation by continuous sucrose gradient.	59
3.5.4	AAV particle quantification	60
3.5.5	Viral transduction assay (for Firefly and Gaussia luciferase assay)	60
3.5.6	Viral transduction assay (qPCR)	60
3.5.7	Luciferase assay	61
4	Results	63
4.1	The role of SUMO as host restriction factors effecting AAV transduction	63
4.1.1	Knockdown of SUMOylation results in increased AAV transduction	63
4.1.2	Inhibition of AAV transduction by SUMOylation depends on the time point of the knockdown	64
4.1.3	SUMOylation affects transduction of single stranded and self-complementary AAV vectors	66
4.1.4	Total SUMOylation activity increases after AAV transduction	67

4.2	SUMOylation influences infection efficiency by affecting the AAV capsid	69
4.2.1	AAV2 particles can be SUMOylated.....	69
4.2.2	AAV2 particles cannot be SUMOylated in a SUMO-inhibited cell line.....	71
4.2.3	Empty AAV2 particles are SUMOylated to a higher extent in comparison to full AAV2 particles	72
4.2.4	K142/143 and/or K169 residues play a role in AAV particles SUMOylation	75
4.2.5	AAV2 capsid protein VP2 is SUMOylated but not VP1	79
4.2.6	AAV2 capsid protein SUMOylation related to the VP2 spatial structure.....	80
4.3	The effect of SUMOylation pathway on AAV trafficking <i>in vitro</i>	82
4.3.1	AAV transduction after SUMOylation knockdown is not due to increased binding or uptake.....	82
4.3.2	Inhibition of SUMOylation does not affect the AAV2 vector DNA distribution in cell membrane, cytoplasm or nucleus	84
4.3.3	SUMOylation inhibition can enhance AAV accumulation in the nucleus	86
4.4	SUMOylation is linked to other existing host cell restriction factors that affect AAV transduction	89
4.4.1	AAV transduction increased in a Daxx knock out cell line	89
4.4.2	SUMOylation and Daxx may work in the same pathway.....	91
5	Discussion	93
5.1	SUMOylation affects AAV transduction in a host cell dependent manner	93
5.2	What is the target of SUMOylation?	94
5.3	Which step of the AAV transduction is affected by SUMOylation?	98
5.4	The Daxx protein affects AAV transduction via the SUMOylation pathway	101
5.5	AAV gene therapy	105
5.6	Conclusion	107

6	Summary	109
7	Zusammenfassung	111
8	References	113
9	Publication	131
10	Curriculum Vitae	133
11	Acknowledgement	135
12	Thesis Declaration.....	137

List of Symbols and Abbreviations

Symbol and Abbreviation	Description
α	anti
#	number
%	percent
Ψ	hydrophobic amino acid
$^{\circ}\text{C}$	degree Celsius
aa	amino acid
Ad	adenovirus
AAP	assembly-activating protein
AAV	adeno-associated virus
AAVR	AAV receptor
Amp	Ampicillin
APS	ammonium peroxydisulfate
ATP	adenosine triphosphate
ATRX	alpha-thalassemia retardation syndrome x-linked
bp	base pairs
BSA	bovine serum albumin
CAR-T	chimeric antigen receptor T-cell immunotherapy
CBS	human cystathionine β -synthase
CDC73	cellular PAF1 complex component parafibromin
CLIC/GEEC	clathrin-independent carriers/ GPI-enriched early endosomal compartment
c-MET	hepatocyte growth factor receptor
CNS	central nervous system
CO ₂	carbon dioxide
CELO	chicken embryo lethal orphan
Daxx	Death domain associated protein

List of Symbols and Abbreviations

DDR	DNA damage response
DNA	deoxyribonucleic acid
DMEM	dulbecco's Modified Eagle Medium
DMSO	dimethyl sulfoxide
dsDNA	double stranded DNA
ECL	enhanced chemiluminescence
EDTA	ethylenediaminetetraacetic acid
Eer1	endoplasmic reticulum-associated degradation inhibitors
EGFR	epidermal growth factor receptor
EGFR-PTK	epidermal growth factor receptor tyrosine kinase
ER	endoplasmic reticulum
ERAD	ER-associated degradation
EV71	intestinal virus type 71
FGFR1	fibroblast growth factor receptor 1
g	gravitational
GAMPO	goat- anti- rabbit, coupled with peroxidase
GARPO	goat- anti- mouse, coupled with peroxidase
GFP	Green fluorescent protein
h	hour
H ₂ O	water
HA	Human influenza hemagglutinin
HCMV	human cytomegalovirus
HDF	host cell dependency factors
HEK 293TT	human embryonic kidney cells 293 with double T antigen
HGFR	hepatocyte growth factor receptor
HPV58	human papillomavirus type 58
HRF	host cell restriction factors
HRP	horseradish peroxidase
HSPG	heparan sulfate proteoglycans

List of Symbols and Abbreviations

HSV	herpes simplex virus
ITR	inverted terminal repeats
KCl	potassium chloride
kDa	kilo Dalton
KH ₂ PO ₄	monopotassium phosphate
LamR	laminin receptor
LV	lentivirus
LB	Luria-Bertani broth
LLnL	N-acetyl-I-leucinyI-I-leucinyI-norleucinal
LR	laminin receptor
nm	Nano meter
M	molar
min	minute
MOI	multiplicity of infection
nm	Nano meter
Na ₂ HPO ₄	disodium hydrogen phosphate
NaCl	sodium chloride
NaOH	sodium hydroxide
NLS	nuclear localizing signal
NPC	nuclear pore complex
ORF	open reading frame
PCR	Polymerase chain reaction
PBS	phosphate buffered saline
PDGFR	platelet-derived growth factor receptor
PBS-MK	PBS-magnesium-potassium
PBS-T	PBS-Tween
PIAS	protein inhibitor of activated STAT
PLA2	phospholipase A2 domain
PML	promyelocytic leukemia protein
PML-NBs	PML nuclear bodies

List of Symbols and Abbreviations

PODs	PML oncogenic domains
rAAV	recombinant adeno-associated virus
RdRp	RNA-dependent RNA polymerase
RING	really interesting new gene
RLU	relative light units
RNA	ribonucleic acid
RNAi	RNA interference
RV	retrovirus
RanBP2	nuclear pore protein
rpm	revolutions per minute
RT	room temperature
Sae1	subunit 1 of SUMO-activating enzyme E1
Sae2	subunit 2 of SUMO-activating enzyme E1
SDS	sodium dodecyl sulfate
SENp	sentrin-specific proteases
scAAV	self-complementary DNA in AAV
SIMs	SUMO-interacting motifs
siRNA	small interfering RNA
ssAAV	single-stranded DNA in AAV
SUMO	small ubiquitin-like modifier
TAE	Tris-acetate-EDTA
TBS-T	TBS-Tween
TE	Tris EDTA
TEMED	N,N,N',N'-tetramethylethylenediamin
TGF β	transforming growth factor beta
TGN	trans GOLGI network
TGS	Tris-glycine-SDS
TIF1 γ	transcriptional intermediary factor 1- γ
TNF	tumor necrosis factor
TRIM	tripartite motif containing

List of Symbols and Abbreviations

Tris	tris(hydroxymethyl)-aminomethan
U	unit
UV	Ultraviolet
UBA2	ubiquitin-like modifier activating enzyme 2
Ubc9	Ubiquitin-conjugating enzyme E2
V	volt
VP	virus protein
VP1	viral capsid protein 1
VP2	viral capsid protein 2
VP3	viral capsid protein 3
YFP	yellow fluorescent protein
wt	wild type

Table of Figures

Figure 1	The divergence of susceptibility with AAV serotypes in different tissues.	2
Figure 2	Adeno-Associated Virus genome structure.....	4
Figure 3	Single-strand AAV (ssAAV) and self-complementary AAV (scAAV) conformations.....	7
Figure 4	Schematic representation of Adeno-Associated Virus life cycle.	11
Figure 5	The Adeno-Associated Virus particle assembly process.....	12
Figure 6	The SUMOylation pathway.....	14
Figure 7	SUMO-interaction motifs (SIMs) role in protein SUMOylation.	16
Figure 8	SUMO consensus sequences a surrounding residue.	17
Figure 9	Two genome-wide siRNA libraries screen indicate that AAV transduction affected with SUMOylation pathway.	21
Figure 10	SUMOylation knockdown increases AAV transduction.....	64
Figure 11	Influence of the time point of Sae2 knockdown on AAV transduction... 	65
Figure 12	Sae2 or Ubc9 knockdown enhances transduction of ssAAV and scAAV vectors.....	67
Figure 13	Total SUMOylation activity increases after AAV transduction.	68
Figure 14	AAV2 purified particles SUMOylation specificity confirmation..	70
Figure 15	SUMO cannot be detected on purified AAV2 particles produced in Gam1 expressing (SUMO inhibited) cells.	72
Figure 16	Empty AAV2 particles are SUMOylated more than full (DNA-containing) AAV2 particles.....	74
Figure 17	SUMO detection of wt and modified AAV2 indicate K142/143 and K169 are not SUMOylated, and their transduction efficiency is not greatly affected by SUMO knockdown.....	78

Table of Figures

Figure 18 SUMO cannot be detected on AAV2- VP1+VP3 particles lacking VP2. .	80
Figure 19 AAV2- VP1/GFP-VP2/VP3 and AAV2- VP1/HA-VP2/VP3 capsids are not SUMOylated.....	81
Figure 20 Enhanced AAV transduction by inhibition of SUMOylation is not due to increased binding or uptake of capsids.....	83
Figure 21 Inhibition of SUMOylation does not lead to gross changes in subcellular localization of AAV vectors.....	85
Figure 22 Detection of Gam1 expression in HeLa-Gam1 cells which increases AAV transduction.....	87
Figure 23 SUMOylation inhibition by Gam1 expression can direct more AAV particle accumulation in the nucleus.	88
Figure 24 AAV2 infectivity enhanced in HeLa-Daxx knockout cell.....	90
Figure 25 SUMO protein and Daxx protein work in the same pathway controlling AAV transduction.....	92
Figure 26 Hypothetical infectious pathway of AAV2 impairment of SUMOylation by Sae2 knockdown.....	100
Figure 27 Hypothetical model of SUMOylation interfering with AAV.....	103
Figure 28 Multiple factors control AAV2 transduction.....	104
Figure 29 Coinfection with AAV2- Gam1 increases transduction efficacy of AAV2 vectors..	107

1 Introduction

1.1 Biology of Adeno-Associated Virus

Adeno-associated virus (AAV) is a nonpathogenic member of the *Parvoviridae* family which's members are characterized as small and non-enveloped. The AAV capsid has an icosahedral symmetry of approximately 20 to 30 nm diameter and contains a linear single-stranded DNA genome around 4.8 kb. In the 1960s, AAV was found and defined as a contaminant of purified adenovirus (Atchison *et al.* 1965; Hoggan *et al.* 1966) and now AAV has been widely concerned and used in recent decades. AAV is a dependovirus and there are two proposed names for this species: Adeno-associated dependoparvovirus A (primate dependoparvovirus, including most of AAV serotypes) and Adeno-associated dependoparvovirus B (serotype AAV5 only).

Different AAV serotypes are isolated from different species. There are 12 human AAV serotypes and more than 120 serotypes of non-human primates have been investigated so far. Most of AAV serotypes can infect diverse tissues but with significant divergence of transduction efficiency, showing different organizational affinity (Figure 1) (Chiorini *et al.* 1997; Chiorini *et al.* 1999; Gao *et al.* 2002; Gao *et al.* 2004; Mori *et al.* 2004; Muramatsu *et al.* 1996; Rutledge *et al.* 1998; Samulski *et al.* 1982; Schmidt *et al.* 2008; Srivastava *et al.* 1983; Xiao *et al.* 1999).

Although most people are infected with AAV it is considered non-pathogenic (Mingozzi and High 2013). On the contrary, AAV infection has been proposed to be benefit to people in some cases. AAV2 infection causes apoptosis of human cervical cancer cells (Alam and Meyers 2009), as well as the apoptosis in multiple breast cancer cells but has no effect on normal cells (Alam *et al.* 2011).

Furthermore, because of the low immunogenicity and site-specific integration, AAV is considered as a highly promising and prevalent gene therapy vector.

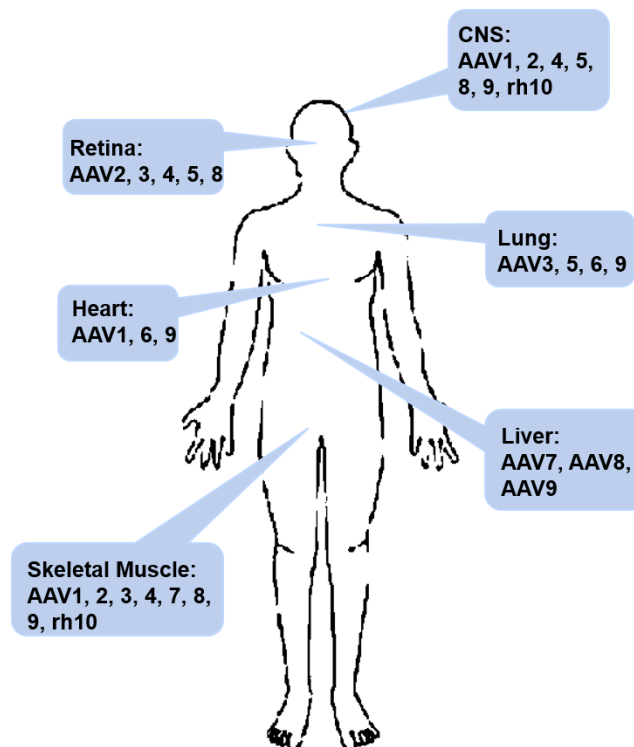


Figure 1 The divergence of susceptibility with AAV serotypes in different tissues. These serotypes differ in their tropism, or the types of cells they infect, making AAV a very useful system for preferentially transducing specific cell types. The chart gives a summary of the tropism of AAV serotypes, indicating the optimal serotype(s) for transduction of a given organ. CNS= central nervous system (adapted from Asokan *et al.* 2012)

In the very beginning AAV was recognized as a defective virus because it would not infect cells successfully unless a helper virus exist, e.g. adenovirus (Ad), herpes simplex virus type 1 and 2 (HSV1, HSV2), human cytomegalovirus (HCMV) or human papillomavirus (HPV) were present (Atchison *et al.* 1965; Buller *et al.* 1981; Georg-Fries *et al.* 1984; McPherson *et al.* 1985; Ogston *et al.* 2000; Walz *et al.* 1998).

Helper functions are performed from E1a, E1b, E2a, E4 and VA RNA in

adenovirus (Muzyczka 1992), or ICP0, ICP4, as well as UL5, UL8, UL52 and UL29 in herpes virus (Weindler and Heilbronn 1991). In addition, DNA damage caused by UV radiation, gamma irradiation or chemical treatment results in AAV activation. The helper virus co-infection could be performed before, after or simultaneously with AAV infection. When there is no helper virus, the viral DNA will be integrated into the host genome but will not undergo viral DNA replication or transcription. The AAV genome integrates into the specific position of the q-arm of chromosome 19 of the human genome (19q13.3-qter) (Cheung *et al.* 1980; Daya and Berns 2008; Kotin *et al.* 1990; Snyder *et al.* 1993). When helper virus functions are present, AAV infectious proliferation will be performed when cells are stimulated by the external cofactors supported from helper virus

1.1.1 Adeno-Associated Virus genome structure

The adenovirus-associated virus type 2 (AAV2) genome is a single-stranded DNA (ssDNA) with 4781 bp nucleotides including inverted terminal repeats (ITR) and two ORFs. It is known that that both sense or antisense strand DNA can be packaged into AAV particle. The ITRs are cis-acting elements that regulate AAV replication, integration, rescue and packaging. The first 125 bases of the ITRs form a T-shaped hairpin structure with two small palindromes (B and C) and a larger configuration (A), and the residual 20 bases remain as unpaired D-sequences (Figure 2b). The ssDNA is flanked by ITRs and contains two open reading frames (ORFs): Rep and Cap. The left ORF Rep encodes 4 non-structural proteins (Rep78, Rep68, Rep52 and Rep40) and their expression is controlled by the p5 and p19 promoters; the right ORF Cap encodes 3 capsid proteins (VP1, VP2, VP3) as well as the Assembly- Activating Protein (AAP) (Figure 2a).

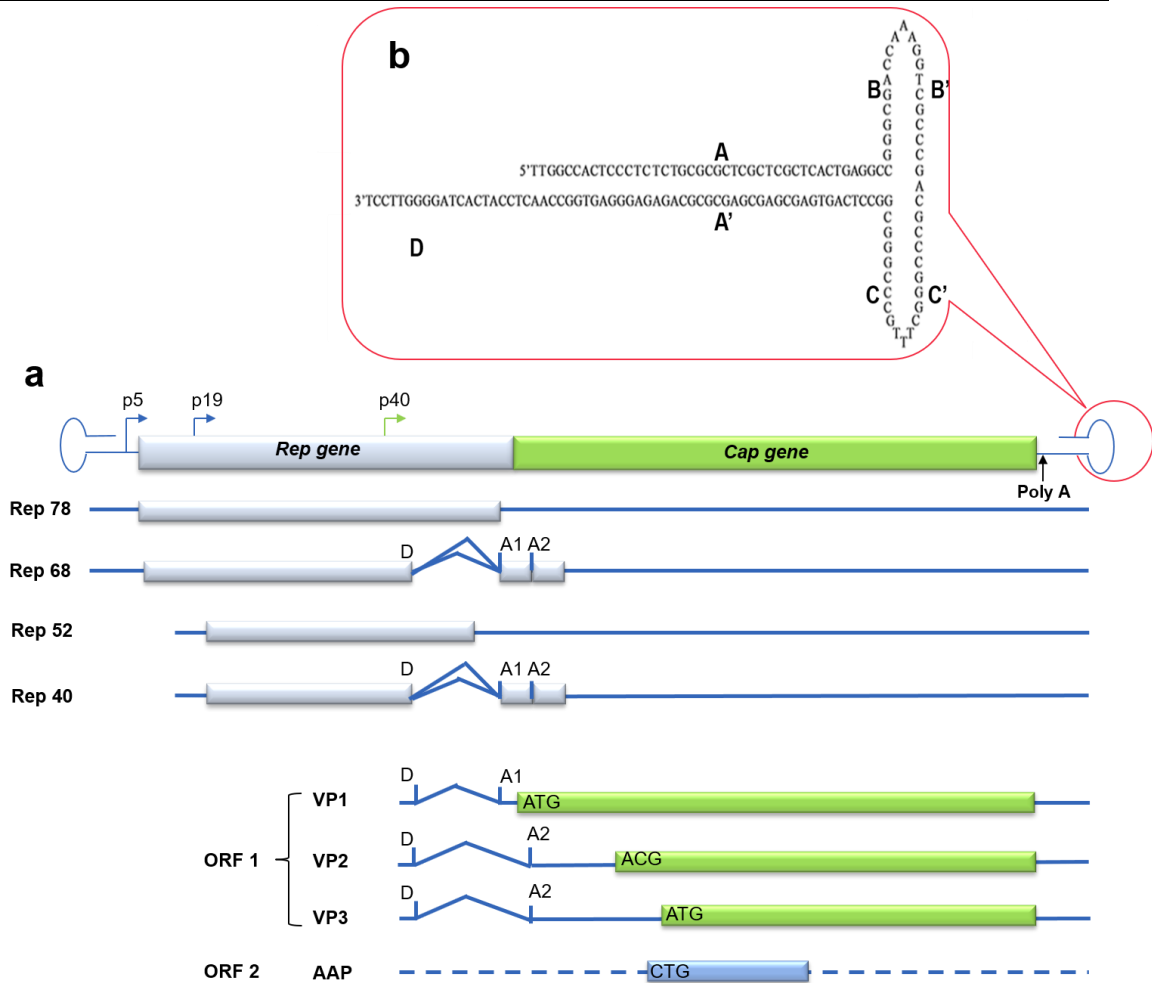


Figure 2 Adeno-Associated Virus genome structure. (a) The 4.7 kb AAV2 genome contains Rep (white) and Cap genes (green) flanked by two ITRs (blue). Promoters p5 and p19 will guide two mRNAs transcription which are spliced differentially to produce 4 non- structural proteins (rep78, rep68, rep52, rep40). The capsid proteins (VP1, VP2, VP3) are initiated from the p40 promoter and are generated from two mRNAs via alternative splicing and start codon usage. The blue bar represents AAP which is translated from the second ORF of cap gene. (b) ITR structure. 125 bases of the ITRs form a T-shaped hairpin structure with two small palindromes (B and C) and a larger configuration (A), and the residual 20 bases remain as unpaired D-sequences. ORF= Open Reading Frame, ITRs= Inverted Terminal Repeat sequences, A=splice acceptor, D= splice donor.

The p40 promoter regulates the Cap gene to transcribe 2.6kb and 2.3kb mRNA

and encode capsid proteins VP1, VP2 and of VP3 as well as AAP (Figure 2). The molecular weights of VP1, VP2, VP3 are 87kDa, 73kDa and 61kDa. The three VPs exist in the capsid at the molar ratio of 1:1:10, respectively. It is known that VP2 and VP3 can package progeny single-stranded DNA without VP1, but these progeny viruses are non-infectious, suggesting that VP1 is required for the infectivity. The unique fragment at the N terminus of VP1 was shown to comprise the phospholipase A2 (PLA2) activity and particularly the change of residue 76HD/AN, severely impairs AAV infectivity (Girod *et al.* 2002). VP2 is a controversial component because it was indicated as an important capsid protein in the assembly of virus-like particles (Muralidhar *et al.* 1994). However, Warrington *et al.* showed VP2 to be unnecessary for the complete virus particle formation and an efficient infectivity and presented that VP2 can tolerate large insertions in its N-terminus, while VP1 cannot, probably because of the PLA2 domain (Warrington *et al.* 2004). Intact AAV particles can be formed with VP3 alone in the absence of helper functions and AAV genomes, provided that the VP3 is fused to a nuclear localization signal (Hoque *et al.* 1999).

1.1.2 Genetic engineering of the Adeno-Associated Virus

Site-directed mutagenesis allows the deletion or insertion of a known target gene thus affecting the amino acid sequence and protein structure.

Many studies have shown that peptides could be inserted into AAV capsids. AAV2 has a heparin-binding site around amino acid position 587 of capsid protein VP1 which can be substituted with other sequences. Consequently, the ability of this modified AAV to be neutralized with human serum is approximately 15-fold less reduced than AAV2 wild type (Huttner *et al.* 2003). Further studies also indicated some more specific sites could be used for insertion of heterologous sequences without influencing the assembly as well

as transduction activity.

In recent years, the AAV mutants' studies are more inclined towards the interaction between the amino acid on external surface and receptors. Zhong *et al.* established some modified AAV2 with tyrosine exchanging on the capsid surface (Y252F, Y272F, Y444F, Y500F, Y700F, Y704F, and Y730F) and detected increasing transduction efficiency because of the tyrosine-mutant AAV2 ubiquitination, which indicated that the main receptor binding site of AAV capsid is tyrosine (Zhong *et al.* 2008b). Moreover, they found epidermal growth factor receptor tyrosine kinase (EGFR-PTK) -mediated phosphorylation of tyrosine residues on AAV capsid protein is a prerequisite for ubiquitination of AAV2 capsids. The phosphorylated capsid could be ubiquitinated at the tyrosines and thus resulted in the reduced transduction efficiency, although the AAV entry has not been affected (Zhong *et al.* 2008a).

Apart of the AAV *Cap* genetic modification, AAV genome DNA structure could also be modified. Typical AAV genome is a single-stranded DNA template flanked by ITR at both sides, and the events like DNA replication or transcription need the second-strand DNA synthesis. The second-strand synthesis is widely known as the rate-limiting step for AAV transduction, wherefore McCarty *et al.* constructed a new lab-made AAV genome DNA, which could form an intra-molecular double-stranded DNA template, named self-complementary AAV (scAAV), to avoid second-strand synthesis (McCarty *et al.* 2001) (Figure 3). During AAV infection process, the two complementary DNA fragments of AAV genome will form the double stranded DNA (dsDNA) after viral genome release from AAV particle and it leads to replication or transcription immediately. Subsequently, Buie *et al.* and Deepak *et al.* found the scAAV can greatly transduce and express genes in the liver or be used to treat hemophilia B (Buie *et al.* 2010; Raj *et al.* 2011).

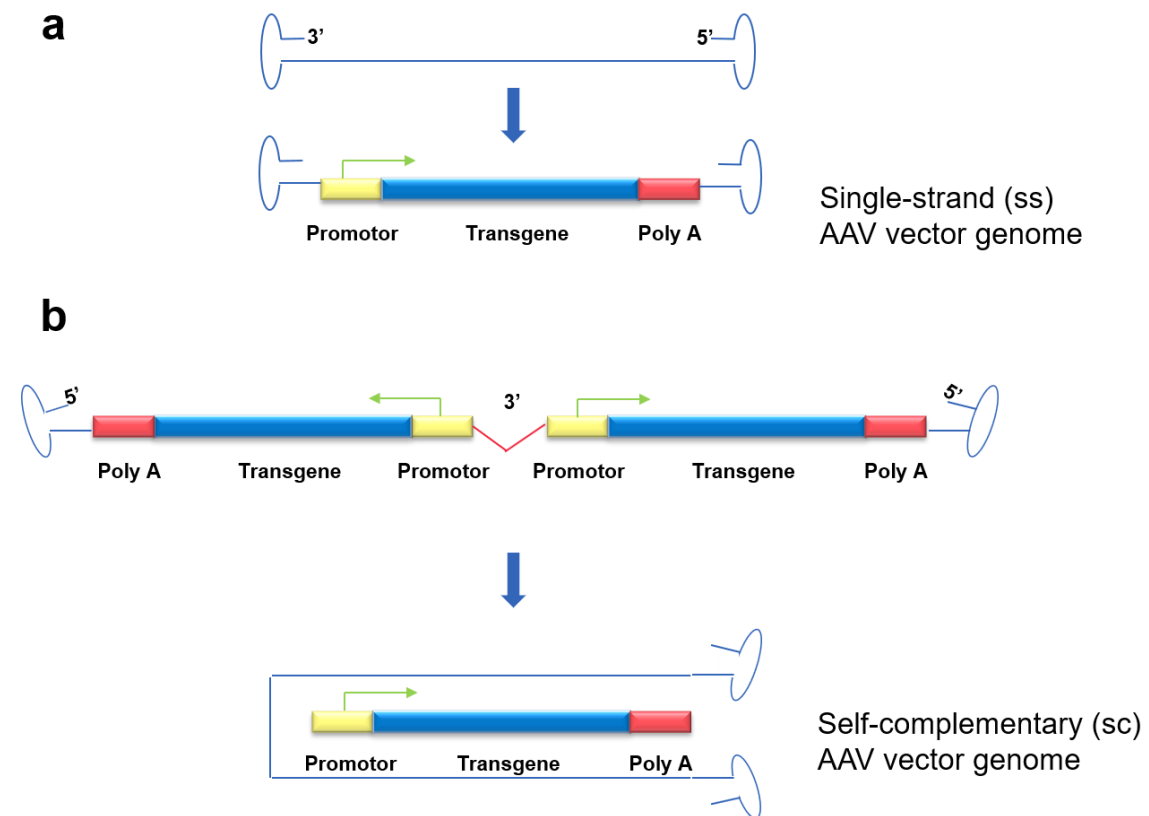


Figure 3 Single-strand AAV (ssAAV) and self-complementary AAV (scAAV) conformations. Recombinant AAV genome, where the coding sequences are replaced by a transgene, which is flanked by the 3' and 5' ITR. (b) scAAV DNA synthesis process. The recombinant transgene in scAAV is expressed as an inverted repeat DNA sequence, as well as the deleted or mutated 3' terminal repeats in the middle. This DNA is flanked by two 5' terminal repeats at both sides. After AAV transduction, the inverted repeats perform the complementary pairing followed by the double-stranded DNA transcription, thereby bypassing the synthesis of the second strand DNA. Deletion or mutation of the 3' terminal repeats prevents the function of Rep endonucleases to stabilize the self-complementary AAV genome dimeric formation. (adapted from Raj *et al.* 2011)

1.1.3 Adeno-Associated Virus Trafficking

The general process of AAV infection is carried out as follows. The external isolated AAV particles bind to the corresponding receptors or co-receptors on

the cell surface to perform the endocytosis. The low pH of the endosome leads to the exposure of the N-terminus of VP1 which is essential for endosomal escape and transportation into the nucleus. During AAV transportation, the capsid proteins are modified by phosphorylation and ubiquitination, followed by AAV degradation. However, the non-degraded viral particles enter the nucleus and are uncoated to release the AAV genome, which is converted to double-stranded (ds) DNA that is used for the expression of the encoded proteins through (Grieger and Samulski 2012; Nonnenmacher and Weber 2011; Qing *et al.* 1998; Seisenberger *et al.* 2001; Zhong *et al.* 2008b).

AAV particle attachment on the cell surface could be mediated by specific glycans or glycoconjugates which thereby provide access to specific proteinaceous co-receptors binding (Huang *et al.* 2014). The main receptor is the heparan sulfate proteoglycan (HSPG) and co-receptors include: $\alpha V\beta 5$, $\alpha 5\beta 1$, hepatocyte growth factor receptor (c-MET), fibroblast growth factor receptor I (FGFR1), laminin receptor (LamR), CD9 tetraspanin family, platelet-derived growth factor receptor (PDGFR) and the epidermal growth factor receptor (EGFR) (Summerford and Samulski 1998; Summerford *et al.* 1999; Asokan *et al.* 2006; Kashiwakura *et al.* 2005; Ling *et al.* 2010; Blackburn *et al.* 2006; Qing *et al.* 1999; Akache *et al.* 2006; Kurzeder *et al.* 2007; Di Pasquale *et al.* 2003; Weller *et al.* 2010). More recently, a genetic screen identified a previously uncharacterized transmembrane protein, KIAA0319L (denoted as AAV receptor, or AAVR) as being essential for endocytosis and Golgi trafficking of multiple AAV isolates (Pillay *et al.* 2016). Each of these receptors have been identified/verified using a facet of different methods highlighted in the follow table:

Table 1 AAV receptors and their validation (adapted from Pillay and Carette 2017)

Receptor	AAV serotype	Validation				
		siRNA knockdown	Over-expression	Ligand or ectodomain inhibition	Binding	Biodistribution/ infection correlation
aV β 5	AAV2	-	CS1 cell	-	Virus overlay assay	-
FGFR1	AAV2, 3H	-	Raji and KB cell	both	Dot blot	-
c-MET	AAV2, 3	HuH7 cell	NIH3T3 cell	ligand	Virus overlay assay	-
A5 β 1	AAV2	-	CHOB2 and CS1 cell	ectodomain	Solid phase binding profiles	-
CD9	AAV2	MCF7 and T47D cell	T47D, BT8Ca and BT12Ca cell	-	-	HSPG-low vs HSPG-high cell
Lam R	AAV2, 3, 8, 9	NIH3T3 cell	NIH3T3 cell	Ligand for AAV8	Yeast bait/prey assay	-
PDGFR	AAV5	NIH3T3	HeLa and 32D cell	both	Co-precipitation	Yes
EGFR	AAV6	NIH3T3 and NH13 cell	32D cell	-	Co-precipitation	Yes
AAVR	AAV1, 2, 3B, 5, 6, 8, 9	CRISPR/CAS9 in HAP1, HeLa, HEK293, U2OS, A549, Huh7 cell	NIH3T3, Rija, Caco-2 and HT29 cell	ectodomain	ELISA, SPR	-

After AAV particles attachment, the intracellular molecule Dynamin, Rac1 or the phosphatidylinositol kinase PI3K mediate AAV2 particles internalization into the endosome by micropinocytosis, clathrin- independent carriers/GPI-enriched endocytic compartment pathway (CLIC/GEEC) (Nonnenmacher and Weber 2011) or the clathrin-coated pathway (Bartlett *et al.* 2000; Weinberg *et al.* 2014).

After AAV enters the cell, it was identified that AAV2 traffics via the late

endosomes (Ding *et al.* 2006) but this is possibly determined by the host cell. The comprehensive microtubule network is used for the transportation of AAV2 particle which contained in the endosomal vesicles (Xiao and Samulski 2012) and localized near Golgi/ER transport proteins mediated by syntaxin-5 (Johnson *et al.* 2011; Nonnenmacher *et al.* 2015).

Virus degradation also occurs during the endocytic trafficking by multiple degradation pathways, such as ubiquitin-proteasome system, endo-lysosomal vesicles, ER-associated degradation (ERAD) and autophagy-based machinery. Previous research showed that the transduction of various AAV serotypes was enhanced after treatment with proteasome inhibitors MG132, bortezomib, N-acetyl-L-leucyl-L-leucyl-norleucinal (LLnL) or celastrol (Douar *et al.* 2001; Fisher *et al.* 1996; Madhus *et al.* 1984; Greber *et al.* 1997; Mizukami *et al.* 1996). AAV2 virions are trafficked to the lysosome through early endosomes and late endosomes (Bartlett *et al.* 2000; Ding *et al.* 2006). There is no direct evidence that AAV transport is affected by ER, although ER-associated degradation was confirmed to be active as AAV transduction enhanced after endoplasmic reticulum-associated degradation inhibitors (Eer1) treatment (Berry and Asokan 2016).

With the AAV entry non-degraded AAV particles gradually enter the cell nucleus via the Nuclear Pore Complex (NPC), followed by virus uncoating, releasing the ssDNA and utilizing free ITR 3' hydroxyl group as the primer to form the complementary DNA (Nonnenmacher and Weber 2012). In absence of the helper virus some AAV genomes could integrate in the host genome or remain as an episome in the nucleus to transcript and express proteins from the transgene cassette (Figure 4). In addition, if the helper function exists, more progeny virus will be assembled by the AAV packaging mechanism and be released from the cell.

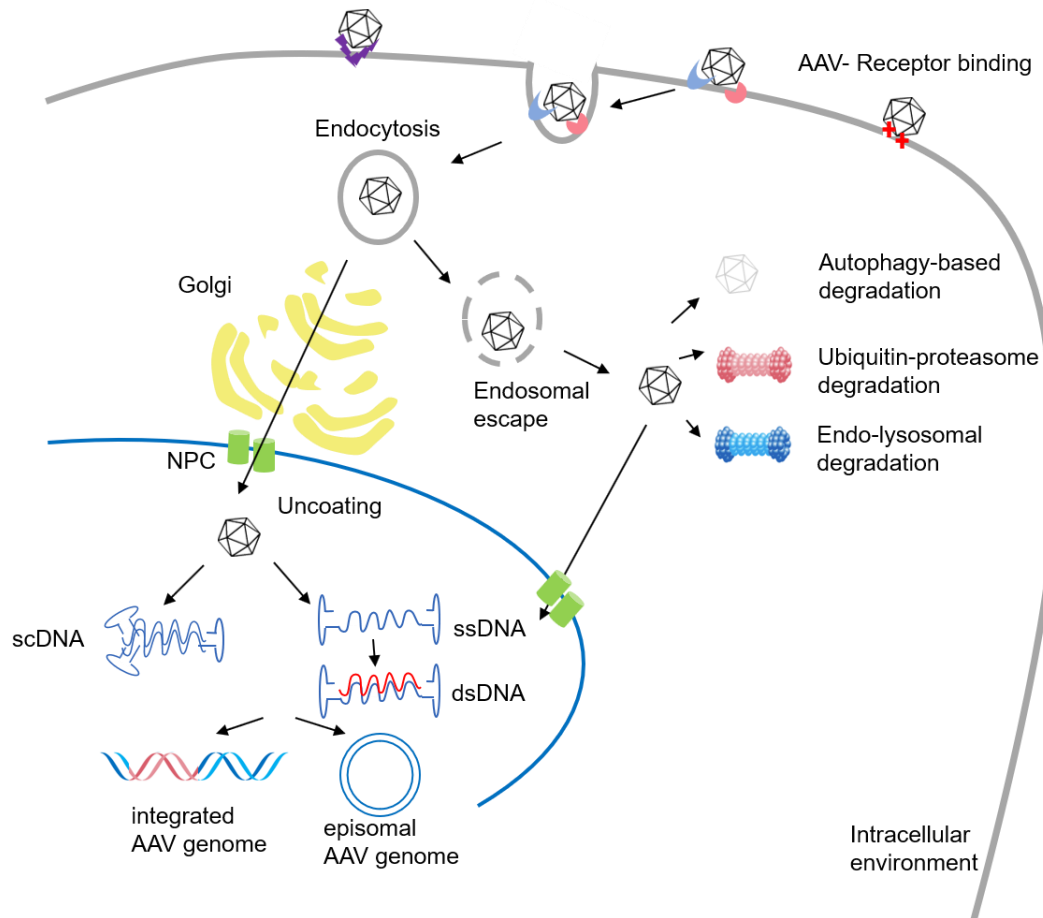


Figure 4 Schematic representation of Adeno-Associated Virus life cycle. AAV2 binds onto the surface of a target cell via receptor and/or co-receptor facilitates the internalization of the virus. Before the endosomal escape, rAAV2 undergoes a conformational change where VP1 and VP2 are exposed because of endosomal acidification. AAV particles are delivered through the trans Golgi network to accumulate in the perinuclear. In the meantime, virus degradation occurs during the endocytic trafficking by different degradation pathways. AAV transfers through the nuclear pore complex (NPC) before uncoating, followed by ssDNA release, dsDNA synthesis, genome integration or remains episomally and facilitates mRNA transcription. (adapted from Daya and Berns 2008; Pillay and Carette 2017; Colella *et al.* 2018)

1.1.4 Adeno-Associated Virus packaging mechanism

The AAV assembly includes 2 steps. Firstly, VP protein assembly by AAP. AAP is crucial in targeting newly synthesized VP proteins to the nucleolus and promoting the assembly of the AAV capsid. The exact mechanism remains elusive, but it is thought to be a scaffold to concentrate the VP proteins in the nucleolus (Naumer *et al.* 2012). This step is rapid as accumulation of the viral capsid proteins and their assembly into empty particles occurs within the first 20 min.

The second step is genome packaging, which takes several hours. After the empty particle formation, the virus genome is melted into single-stranded DNA (ssDNA) with the help of Rep factors, and then the ssDNA enters the empty particle from the top of the five-fold axis of AAV capsid, with the DNA direction being 3' to 5' (DiPrimio *et al.* 2008; King *et al.* 2001) (Figure 5). Wu *et al.* found that the empty particle can only admit the ssDNA less than 5.2 kb, otherwise the external sequence at 5' terminal of DNA could be digested by a nuclease (Wu *et al.* 2010). However, AAV 2, AAV5 and AAV8 were indicated the ability to deliver the genomes longer than 5.2 kb and expresses the proteins as long as the genome contains one ITR and the complete genome ORF. Finally, the complete virions are assembled and released from the cell (Geoffroy and Salvetti 2005).

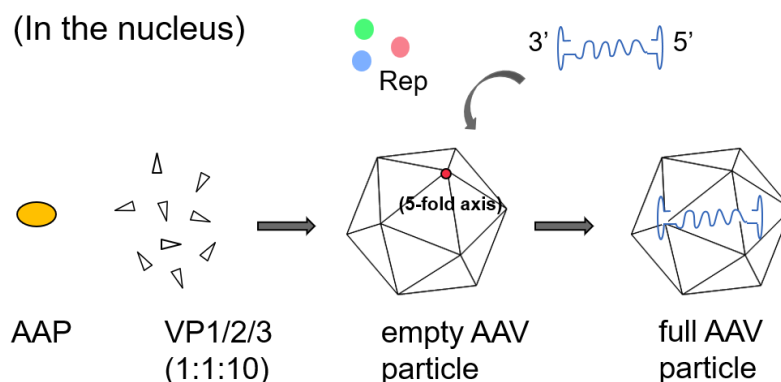


Figure 5 The Adeno-Associated Virus particle assembly process. Firstly, non- structural

proteins Reps are synthesized to regulate the AAV assembly process, followed by VP1, 2, 3 capsid proteins expression from cap ORF as well as AAP encoding by a second ORF. The viral capsid proteins are accumulated and assembled by AAP rapidly. Secondly, the single-stranded DNA enters the empty particles from the five-fold axis of AAV capsid, and the direction of ssDNA entering is from 3' to 5'.

1.2 Biology of SUMOylation

Small ubiquitin-related modifier (SUMO) was discovered as a reversible post-translational modification of proteins in the middle of 1990s. More than 3,600 proteins can be SUMOylated at 7,300 SUMOylation sites so far. SUMO modification can regulate many substrate proteins in the life process, such as intracellular sub-localization, enzyme activity, protein structure and stability, and transcriptional activity (Herrmann *et al.* 2007).

SUMO has only 18% sequence similarity to ubiquitin, but the structure after folding is highly similar that of ubiquitin (Bayer *et al.* 1998; Bernier-Villamor *et al.* 2002; Mossessova and Lima 2000). Primates could express four SUMO family members: SUMO1, 2, 3, 4 (Guo *et al.* 2004; Melchior 2000). SUMO1, SUMO2 and SUMO3 are ubiquitously expressed in all tissues, while SUMO4 is mainly expressed in organs such as kidney, lymph nodes or spleen. One study found that only SUMO2-deficient mice died of an earlier embryonic development due to severe developmental disorders, while SUMO1/SUMO3-deficient mice survived and multiplied, with no apparent abnormal phenotype (Evdokimov *et al.* 2008; Qi *et al.* 2014; Zhang *et al.* 2008).

1.2.1 SUMOylation Catalytic Pathway

SUMOylation is generally catalyzed by three enzymes (Kerscher *et al.* 2006), in which the E1 activation enzyme SAE1/SAE2 (also known as Aos1/Uba2) and

E2 binding enzyme UBC9 (Ubiquitin-Conjugating 9) are the only single enzymes, respectively. There are many kinds of E3 ligases participate in SUMOylation depending on different substrate modifications. The immature SUMO protein is modified by Sentrin-specific protease (SENp) to expose a stable di-glycine motif, followed by the activating E1 enzyme and conjugating E2 enzyme catalysis. E2 enzyme UBC9 plays a crucial role in the SUMO modification process. Apart from providing an activated SUMO protein, UBC9 can directly conjugate SUMO to the specific substrate lysine residue (Flotho and Melchior 2013) (Figure 6). The substrate with one or more multiple residues could be SUMOylated by single SUMO protein or the SUMO protein chain.

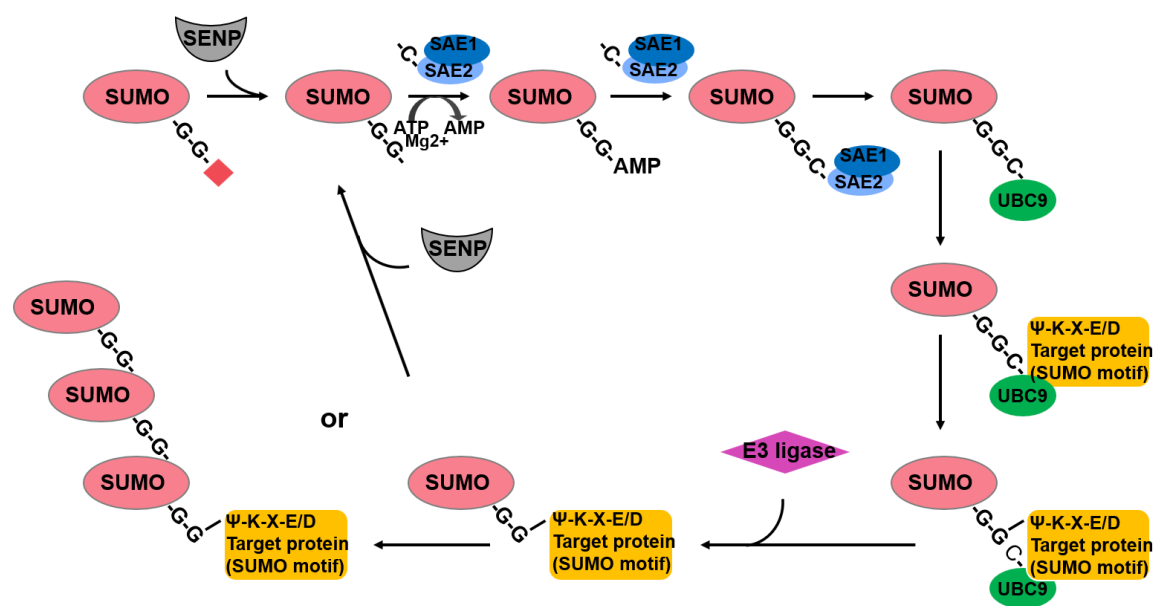


Figure 6 The SUMOylation pathway. During maturation process, 2~11 amino acids extensions of the immature SUMO protein at the C-terminus could be excised by SENP to expose the di-glycine motif Gly-Gly. The SUMO molecule is activated by a two-step hydrolysis of ATP, followed by SAE1/SAE2 complex conjugation via a thioester bond. SAE2 ship the SUMO to Ubc9 enzyme. Ubc9 recognizes the target protein which contains consensus sequence $\Psi Kx D/E$ and catalyzes the formation of SUMO to the target protein, followed by the Ubc9 detachment. Different substrate proteins determine whether they need to utilize E3

enzyme or not. Ultimately, the target protein is SUMOylated. In addition, the SUMOylation process can be reversed by SENPs, which is named deSUMOylation. (adapted from Flotho and Melchior 2013).

There are more than 600 known ubiquitin E3 ligases (Deshaies and Joazeiro 2009) but only a handful of SUMO E3 ligase have been reported, such as the protein/inhibitor of the activated STAT proteins (PIAS family), the nuclear pore protein RanBP2, human cystathionine β -synthase (CBS), the polycomb group protein Pc2, tripartite motif-containing (TRIM) proteins and so on (Werner *et al.* 2012; Yunus and Lima 2009; Kirsh *et al.* 2002; Pichler *et al.* 2002; Agrawal and Banerjee 2008; Kagey *et al.* 2003; Chu and Yang 2011; Meroni and Diez-Roux 2005). Even though UBC9 can regulate SUMO conjugation to the target protein directly, it is still an indisputable fact that different E3 ligase can promote SUMO modification by different mechanisms. The E3 enzymes do not conjugate with SUMO molecules by covalent bond but with E2 (UBC9)/SUMO complex to promote the transfer of SUMO from E2 to the substrate.

1.2.2 The SUMOylation consensus sequence

Target proteins SUMOylation by mass spectrometry-based proteomics is complicated to be dealt with because of low modification stoichiometry and incompatibility with the classical database. The SUMO regulation is more complex than previously thought, due to the post-translational modifications of SUMO family members by phosphorylation, acetylation and ubiquitination.

Most of the SUMOylated proteins have SUMO-interaction motifs (SIM) (Hecker *et al.* 2006) (Figure 7a) which are typically composed of multiple hydrophobic residues and an acidic residue (Song *et al.* 2004). SIM-containing proteins can be recruited to and immobilized on SUMOylated proteins, which may lead to their covalent SUMOylation owing to the proximity of SUMO ligases (Raman *et*

al. 2013; Silver *et al.* 2011) (Figure 7b, top), for example, SUMO group modification during the DNA damage response (DDR) in yeast was observed (Psakhye and Jentsch 2012). In the meanwhile, SIMs can facilitate the recruitment of UBC9 to the protein, resulting in covalent SUMOylation Lys residue (Figure 7b, bottom).

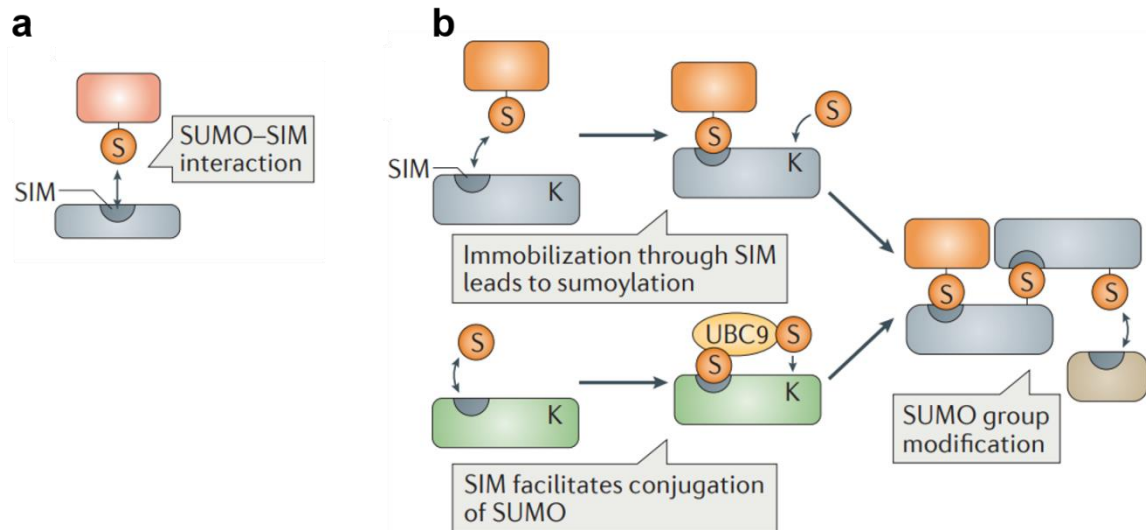


Figure 7 SUMO-interaction motifs (SIMs) role in protein SUMOylation. (a) SUMO proteins are regulated by the SUMO-interaction motifs (SIMs) for their noncovalent interaction. (b) The proteins contain SIM can be recruited to the SUMOylated proteins because of the proximity of SUMO ligases resulting in the covalent SUMOylation (top). In addition, SIMs improve the Ubc9 recruitment to the protein, leading the covalent SUMOylation of the surrounding lysine (K) residue (bottom). They both can regulate the target protein SUMOylation and keeping stability through SIM–SUMO interaction. (adapted from Hendriks and Vertegaal 2016)

The scientists found the classical SUMOylation modification motif via many protein sequence analyses of nearby SUMO sites as Ψ -K-X-E/D. Ψ is a hydrophobic amino acid, and X is an arbitrary amino acid, X is any kind of amino acid and E/D are acidic amino acids. But more recently, the consensus sequence was updated. Adherence of SUMOylation to proteins containing the

basal KXE-type motif has been widely described, which is important for direct binding of the SUMO-conjugating enzyme UBC9 (Bernier-Villamor *et al.* 2002). KXE-type SUMOylation sites are detected easier across multiple screens (structure [IVL]K and KXE account for a very large proportion) (Matic *et al.* 2010; Yang *et al.* 2006). Intriguingly, the inverted sequence [ED]XK is also observed as a SUMOylation motif (Matic *et al.* 2010), which increases the range of the sequence that can be SUMOylated (Figure 8a). Since many sequences of the SUMOylated proteins have been confirmed, Hendriks *et al.* utilized IceLogo analysis to set up a strongest reference based on the currently know SUMOylation sequence in the SUMOylated proteins, which could help the new SUMOylation sites prediction in further studies (Figure 8b).

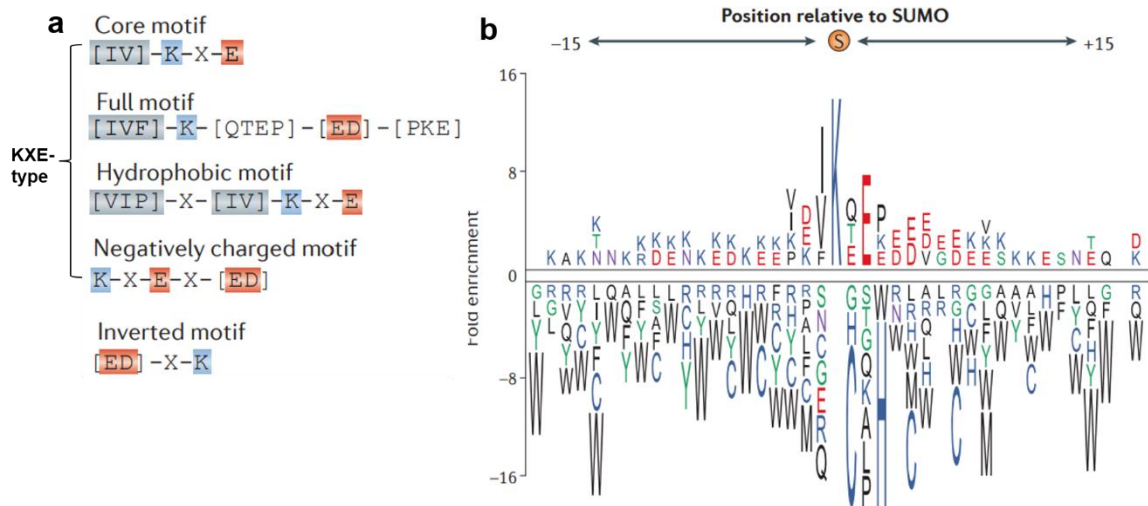


Figure 8 SUMO consensus sequences a surrounding residue. (a) Hydrophobic (grey), negatively charged (red) and phosphorylation-dependent motifs (not shown) further optimize the basic motif. The inverted motif is most often observed separately from the forward motif, but it is not mutually exclusive with the forward motif. Square parentheses indicate that any one of the listed residues is present; blue shading indicates the SUMO-modified Lys residue. (b) Amino acids surrounding SUMOylation sites were compared with randomly occurring background frequencies of amino acids in all nucleus proteins. Amino acids displayed above the x-axis are enriched, whereas amino acids displayed below the x-axis are depleted around

SUMOylation sites. (adapted from Hendriks and Vertegaal 2016)

1.2.3 SUMOylation in virus life cycles

It has been discovered that many viral components can be SUMOylated and the viral infection is affected in host cells. Adenovirus core protein V contains SUMOylation consensus motifs that could affect adenoviral replication (Freudenberger *et al.* 2018), and the capsid protein VI regulates the antiviral response by modulation of the transcription factor Daxx during infection (Schreiner *et al.* 2013). Liu *et al.* found that the 3D polymerase, an RNA-dependent RNA polymerase (RdRp) of intestinal virus type 71 (EV71), undergoes both SUMO and ubiquitin modification during infection, which act to stabilize the polymerase and promote viral replication (Liu *et al.* 2016). The following influenza virus proteins like NS1, NP and M1 contain SUMO sites and the cellular PAF1 complex component parafibromin (CDC73) is also SUMOylated to affect influenza virus replication and assembly (Ngamurulert *et al.* 2009; Santos *et al.* 2013; Han *et al.* 2014; Wu *et al.* 2011; Domingues *et al.* 2015). Numerous viral proteins have also been shown to interact with the SUMO conjugating enzyme (Ubc9) to be SUMOylated. The human papillomavirus (HPV) protein E2, which acts on viral replication and genome segregation and downregulates expression of the oncogenic E6 and E7, also interacts with Ubc9 (Wu *et al.* 2008). However, instead of using this interaction to affect the SUMOylation of other proteins, the viral E2 is itself SUMOylated.

In addition, viral proteins or components can also inhibit SUMOylation of endogenous proteins in host cells during infection. For example, avian adenovirus CELO (chicken embryo lethal orphan) infection causes the inactivation of SUMO E1 enzyme by the Gam1 protein. Gam1 mediates E1 enzyme (SAE1/SAE2) degradation by recruiting the cullin RING ubiquitin ligases and resulting in the degradation of SAE1 by the proteasome (Boggio *et*

al. 2004; Boggio *et al.* 2007). Adenovirus infection in HeLa cells could induce a reduction of SAE1 and SAE2.

Moreover, some host factors have been confirmed to be SUMOylated to affect virus infection in the host cell. For example, the promyelocytic leukemia protein (PML), a prototypical TRIM protein also known as TRIM19, is involved in a chromosomal translocation associated with the clear majority of acute promyelocytic leukemia. PML, especially PML variant II, is the eponymous and main structural component of the PML nuclear bodies (PML-NBs) (Bernardi and Pandolfi 2007; Borden 2002; Geng *et al.* 2012). Experiments have shown that SUMOylated PML plays an important role in the formation of PML-NBs and require NBs-related protein Sp100, Daxx, HDAC1, CBP, p53 and Sp3 recruitment. The death domain-associated protein (Daxx) and alpha-thalassemia retardation syndrome x-linked (ATRX) are the two components of PML oncogenic domain and are able to form a Daxx/ATRX complex by the activity of ATRX ATPase and Daxx's histone deacetylases (Hollenbach *et al.* 2002). The Daxx/ATRX complex represents an intrinsic immune mechanism acting as viral defense against different viruses, such as herpes simplex virus 1 (HSV-1), human cytomegalovirus (HCMV), human Epstein-Barr virus (EBV), and Kaposi's sarcoma-associated herpesvirus (KSHV) (Everett 2001; Preston *et al.* 1998; Tsukamoto *et al.* 2000; Everett *et al.* 2008; Everett and Murray 2005; Tsai *et al.* 2011; Kato-Noah *et al.* 2007; Lin *et al.* 1999; Wu *et al.* 2001). In return, other viruses have developed strategies to neutralize repression by Daxx/ATRX to overcome this barrier (Lukashchuk and Everett 2010; Ullman and Hearing 2008). Since most of the components in NB are transcription factors, SUMOylation and interaction in NB will have a critical influence in regulating transcription.

Altogether, post-translational modification by SUMOylation is a reversible

process and has various effects on target proteins interaction, localization, stability and activity. SUMOylation could regulate nuclear transport, DNA replication and repair as well as in mitosis and signal transduction (Herrmann *et al.* 2007).

1.3 Previous work

This thesis is based on a high throughput siRNA silencing screen performed to verify host cell factors that repress or enhance AAV2 transduction efficiency. This screen was performed by Prof. Jürgen Kleinschmidt, Dr. Florian Sonntag (DKFZ, Heidelberg, Germany) and Dr. Holger Erfle (ViroQuant core facility, Bioquant, Heidelberg, Germany) using two sub-genomic siRNA libraries (*Extended Druggable Silencer siRNA Library and the Genome Extension Silencer Select siRNA Library*) in HeLa cells. Statistical evaluation identified several proteins belonging to the SUMOylation pathway, with very high z-scores which led to follow up studies.

Subsequently, siRNA knockdown of SUMO E1 enzyme Sae2 and SUMO E2 enzyme Ubc9, which was performed by Dr. Christina Hölscher (DKFZ, Heidelberg, Germany) and Katharina Henrich (DKFZ, Heidelberg, Germany), showed an increased reporter AAV2 expression. Thus, confirming Sae2 and Ubc9 as host cell restriction factors. This work has been published in 2015 (Figure 9) (Hölscher *et al.* 2015).

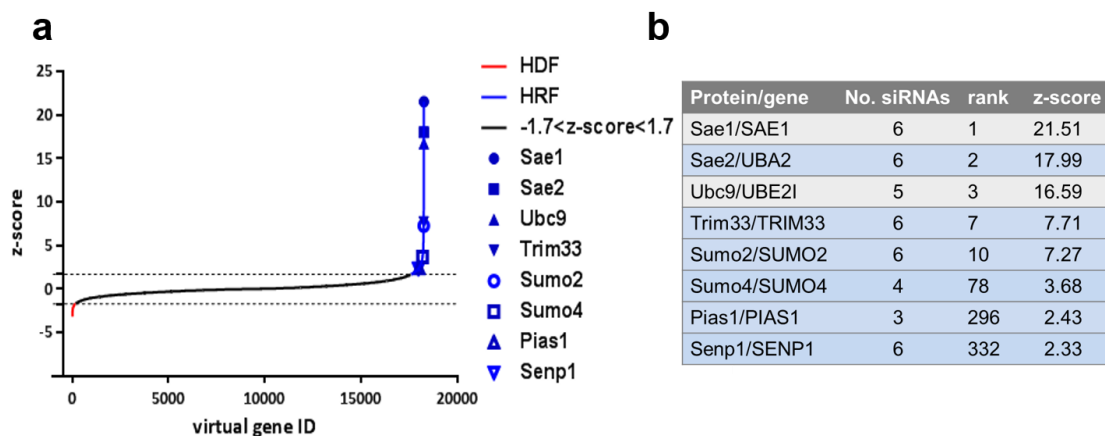


Figure 9 Two genome-wide siRNA libraries screen indicate that AAV transduction affected with SUMOylation pathway. (a) A total of 20,290 genes with their z-scores are shown in the distribution. The blue line above the dotted lines indicate 740 putative host cell restriction factors with z-score threshold of +1.7 (HRF; z-score > 1.7), and the red line below dotted lines shows 181 putative host cell dependency factors with z-score threshold of -1.7 (HDF; z-score < -1.7). (b) SUMOylation pathway related protein ranking base on the z-scores. HDF=host cell dependency factors, HRF=host cell restriction factor. (adapted from Hölischer *et al.* 2015)

1.4 Aim of study

As a result of the siRNA screen and the previous work, Sae2 (SUMO E1 enzyme) and Ubc9 (SUMO E2 enzyme) were confirmed as host cell restriction factors that affect AAV transduction. The objective of my PhD project is to identify and characterize the mechanism in which the SUMOylation pathway influences AAV transduction and challenge which step of AAV trafficking is affected by SUMOylation through the following ways:

- Confirmation of Sae2 and Ubc9 as host cell restriction factors for AAV transduction.
- Identification of the SUMO target within the AAV capsid.

- c. Determination the impact of SUMOylation on AAV transduction/trafficking in the nucleus.
- d. Identification of additional host cell factors e.g. Daxx involved in the restriction of AAV either in concert or independent of SUMOylation.

These studied should contribute to a broader understanding what exactly is SUMOylated to influence the AAV transduction and where the SUMOylation occurs. Furthermore, this study shall also give insight into some extra host cell factors that may be related to the SUMO pathway that affect AAV transduction. This serves to increase the comprehension of AAV and SUMOylation.

2 Materials

2.1 Biological materials

2.1.1 Eukaryotic Cells

Designation	Origin
HeLa	Human epithelial cervix adenocarcinoma cells containing the HPV 18 genome. These cells were cultured in supplemented Dulbecco's modified Eagle's medium (DMEM) with 10% Fetal Bovine Serum (FBS), 1% L-Glutamin (L-Glu), 1% penicillin/streptomycin (P/S).
A549	Adenocarcinomic human alveolar basal epithelial cells. These cells were cultured in supplemented with 10% FBS, 1% L-Glu, 1% P/S.
HEK 293TT	Human embryonic kidney cells expressing the simian virus T-antigen in two copies, respectively. These cells were cultured in DMEM containing 62.5 μ M Hygromycin B, 10% FBS, 1% L-Glu, 1% P/S
HeLa-Gam1	HeLa modified cell which can overexpress adenoviral protein Gam1, the inhibitor of the SUMO pathway by interfering with the activity of E1 enzyme after Doxycycline induction. These cells were cultured in DMEM containing, 10% FBS, 1% L-Glu, 62.5 μ M Hygromycin B and Blasticidin.
HeLa-Daxx KO	HeLa with Death domain-associated protein (Daxx) knock out cell line which was produced with CRISPR/CAS9 system from Robin Njenga. These cells were cultured in DMEM containing 10% FBS, 1% L-Glu, 1% P/S.

2.1.2 Prokaryotic Cells

Strain	Genotype
E. coli MegaX DH10 (Invitrogen)	This strain provides the option of blue/white screening on plates containing either X-Gal or Blue-Gal. F- mcrA Δ (mrr-hsdRMS-mcrBC) ϕ 80lacZ Δ M15 Δ lacX74 recA1 endA1 araD139 Δ (ara, leu)7697 galU galK λ - rpsL nupG tonA

E. coli XL-Blue supercompetant cells (Agilent Technologies)	The XL1-Blue strain allows blue-white color screening. recA1 endA1 gyrA96 thi-1 hsdR17 supE44 relA1 lac [F' proAB lacIqZΔM15 Tn10 (Tetr)]. (Genes listed signify mutant alleles)
---	--

2.1.3 Virus

2.1.3.1 Adeno- associated virus

Adeno-associated virus and Adeno-associated virus- mutants were produced by transfection of HEK293TT cells with the respective plasmids and purified by an Iodixanol gradient.

Virus Type	Reporter Virus	Plasmid	Source
AAV2	AAV2 wt, Firefly	#2772, #1814, #1995	This Thesis
AAV2	AAV2 wt, ss Gaussia	#2772, #1814, #3193	M. Müller
AAV2	AAV2 wt, sc Gaussia	#2772, #1814, #2485	M. Müller
AAV2	AAV2 empty	#2772, #1814	This Thesis
AAV2	AAV2 K33R, Firefly	#3588, #1814, #1995	This Thesis
AAV2	AAV2 K39R, Firefly	#3589, #1814, #1995	This Thesis
AAV2	AAV2 K51R, Firefly	#3590, #1814, #1995	This Thesis
AAV2	AAV2 K61R, Firefly	#3591, #1814, #1995	This Thesis
AAV2	AAV2 K77R, Firefly	#3592, #1814, #1995	This Thesis
AAV2	AAV2 K92R, Firefly	#3593, #1814, #1995	This Thesis
AAV2	AAV2 K105R, Firefly	#3594, #1814, #1995	This Thesis
AAV2	AAV2 K137R, Firefly	#3596, #1814, #1995	This Thesis
AAV2	AAV2 K142+ 143R, Firefly	#3597, #1814, #1995	This Thesis
AAV2	AAV2 K161R, Firefly	#3598, #1814, #1995	This Thesis
AAV2	AAV2 K169R, Firefly	#3599, #1814, #1995	This Thesis
AAV2	AAV2 K527R, Firefly	#3407, #1814, #1995	This Thesis
AAV2	AAV2 K532R, Firefly	#3419, #1814, #1995	This Thesis
AAV2	AAV2 K549R, Firefly	#3475, #1814, #1995	This Thesis
AAV2	AAV2 VP1+VP3, Firefly	#3523, #1814, #1995	This Thesis
AAV2	AAV2 VP2+VP3, Firefly	#3882, #1814, #1995	This Thesis

2 Materials

AAV2	AAV2 VP1/GFP-VP2/VP3, Firefly	#3523, #1995	#3541, #1814,	This Thesis
AAV2	AAV2 VP1/HA-VP2/VP3, Firefly	#3523, #1995	#3542, #1814,	This Thesis

2.1.3.2 Other Viruses

Virus Type	Reporter Virus	Plasmid	Source
HPV58	HPV58 wt, Gaussia	#1998	M. Müller
IAV	IAV wt, Gaussia	unknown	A. Marchini

2.1.4 Media and Supplements

2.1.4.1 Eukaryotic Cells

Media and Supplements	company
Dulbecco's Modified Eagle Medium (DMEM), low glucose	Sigma-Aldrich Deisenhofen, Germany
RPMI medium 1640	Sigma-Aldrich Deisenhofen, Germany
Fetal Bovine Serum (FBS)	PAN Biotec, Aidenbach, Germany
L-glutamin (200mM)	Genaxxon Ulm, Germany
Penicillin/Streptomycin (10.000 units/ml Pen and 10.000µg/ml Strep)	Gibco Life Technologies Paisley, UK
HiPerFect transfection reagent	Qiagen Hilden, Germany
Polyethylenimine (PEI)	Sigma-Aldrich Taufkirchen, Germany
0.25% Trypsin-EDTA	Gibco Eggenstein, Germany
Hygromycin B (62.5 µM)	Roche Mannheim, Germany
Blasticidin	Thermo Scientific Schwerte, Germany
Doxycycline (50ng/ml)	Sigma-Aldrich Taufkirchen, Germany
Heparin	Sigma-Aldrich

Corresponding growth media for each cell line

Designation	Medium	Supplements
HeLa	DMEM Low glucose	1%Glu, 1%P/S
A549	RPMI 1640	1%Glu, 1%P/S
HEK 293TT	DMEM Low glucose	1%Glu, 1%P/S
HeLa-Gam1	DMEM Low glucose	1%Glu, 0.2mg/ml Hygromycin B, 200ng/ml Blasticidin
HeLa-Daxx KO	DMEM Low glucose	1%Glu, 1%P/S

2.1.4.2 Prokaryotic Cells

Media and Supplements	Composition
LB medium	100 g Tryptone 50 g yeast extract 100 g NaCl 10L H ₂ O, pH 7.5 autoclaved
LB agar plates	98.5% LB medium 1.5% bacto-agar Autoclaved, respective antibiotics 25ml/plate
S. O. C medium	Invitrogen California, USA
Antibiotics stocks	Ampicillin (Amp): 100mg/ml Kanamycin (Kan): 25mg/ml

2.1.4.3 Long-term Storage

Designation	Composition
Eukaryotic Cells	30%FBS

	10%DMSO
	60% non-supplement
	1ml/sample
Prokaryotic Cells	0.3ml sterile glycerol (100%)
	1ml bacteria medium

2.2 Molecular biology materials

2.2.1 Plasmid

All AAV2 capsid mutation plasmids were transformed in XL-blue chemically super competent cells after Quikchange™ mutagenesis, and others are transformed in electrocompetent MxDH10 cells.

Designation	Plasmid	Source
#1814	pDGΔVP, AAV2/Ad-helper plasmid without cap-gene	M. Müller
#1995	pUF Luciferase (Luciferase reporter between AAV ITRs for production of selected clones carrying Luciferase reporter)	M. Müller
#2772	AAV2 wt capsid without ITRs (AG Grimm) for wt control multiwell peptide screening No Sfi site	M. Müller
#3193	AAV reporter, ss Gaussia	M. Müller
#2252	AAV reporter, sc Gaussia	M. Müller
#3588	mut K33R-AAV2 capsid, from #2772	This thesis
#3589	mut K39R-AAV2 capsid, from #2772	This thesis
#3590	mut K51R-AAV2 capsid, from #2772	This thesis
#3591	mut K61R-AAV2 capsid, from #2772	This thesis
#3592	mut K77R-AAV2 capsid, from #2772	This thesis
#3593	mut K92R-AAV2 capsid, from #2772	This thesis
#3594	mut K105R-AAV2 capsid, from #2772	This thesis
#3596	mut K137R-AAV2 capsid, from #2772	This thesis
#3597	mut K142+143R-AAV2 capsid, from #2772	This thesis
#3598	mut K161R-AAV2 capsid, from #2772	This thesis
#3599	mut K169R-AAV2 capsid, from #2772	This thesis
#3407	mut K527R-AAV2 capsid, from #2772	This thesis
#3419	mut K532R-AAV2 capsid, from #2772	This thesis
#3475	mut K549R-AAV2 capsid, from #2772	This thesis
#3512	N-eGFP Gateway pDEST vector	This thesis
#3513	N-HA Gateway pDEST vector	This thesis
#3523	VP1+VP3 (VP2 silence) on #2772	This thesis
#3532	VP2+VP3 sequence in pENTR1A, Sall-NotI	This thesis

2 Materials

#3541	eGFP-VP2+VP3 (gateway, #3532+#3512)	This thesis
#3542	HA-VP2+VP3 (gateway, #3532+#3513)	This thesis
#3882	VP2+VP3 (Quikchange, VP1 silence) on #2772	This thesis

2.2.2 Oligonucleotides for mutagenesis or normal PCR

All oligonucleotides were ordered and produced at MWG Eurofins in Ebersberg, Germany.

Designation	Sequence 5' to 3'
AAV2 VP-K33R-F	ACCACCACCAAGGCCCGCAGAGC
AAV2 VP-K33R-R	CGCTCTGCGGGCCTTGGTGGT
AAV2 VP-K39R-F	AGCGGCATAGGGACGACAGCAG
AAV2 VP-K39R-R	TGCTGTGTCCTATGCCGCTCT
AAV2 VP-K51R-F	TTCCTGGGTACAGGTACCTCGGAC
AAV2 VP-K51R-R	AGGGTCCGAGGTACCTGTACCCAG
AAV2 VP-K61R-F	TCAACGGACTCGACAGGGGAGAGC
AAV2 VP-K61R-R	GCTCTCCCTGTCGAGTCCGTTGA
AAV2 VP-K77R-F	TCGAGCACGACAGAGCCTACGACC
AAV2 VP-K77R-R	CGGTCGTAGGCTCTGTCGTGCT
AAV2 VP-K92R-F	AACCCGTACCTCAGGTACAACCACG
AAV2 VP-K92R-R	GTGGTTGTACCTGAGGTACGGGT
AAV2 VP-K105R-F	AGGAGCGCCTTAGAGAAGATACGTCTT
AAV2 VP-K105R-R	AAAAGACGTATCTTCTTAAGGCGCT
AAV2 VP-K137R-F	AGGAACCTGTTAGGACGGCTCC
AAV2 VP-K137R-R	CCCGGAGCCGTCTAACAGGTT
AAV2 VP-K142+143R-F	ACGGCTCCGGGAAGAAGGAGGCCGGT
AAV2 VP-K142+143R-R	CTCTACCGGCCTCCTTCTTCCCGGAG
AAV2 VP-K161R-F	TCGGGAACCGGAAGGCGGGCCA
AAV2 VP-K161R-R	TGCTGGCCCGCCCTTCCGGTTC
AAV2 VP-K169R-F	CAGCCTGCAAGAAGAAGATTGAATT
AAV2 VP-K169R-R	CAAATTCATCTTCTTCTTGACAG
AAV2 VP-K527R-F	GGCCCGGCCATGGCAAGCCACAGGACGATGAAGA AAAGTTT
AAV2 VP-K527R-R	AGGAAAAAACTTTTCTTCATCGTCCCTGTGGCTTGCC ATGGCCG
AAV2 VP-K532R-F	CGATGAAGAAAGGTTTTTCTCAGAGC
AAV2 VP-K532R-R	TCTGAGGAAAAAACCTTTCTTCATCG
AAV2 VP-K549R-F	CAAGGCTCAGAGAGAACAAATGTGGACATTG
AAV2 VP-K549R-R	TTCAATGTCCACATTTGTTCTCTGAGCCTTG
AAV2 VP1 silence-F	ATTTAAATCAGGTGCGGCTGCCGATGGTTATCT
AAV2 VP1 silence -R	AACCATCGGCAGCCGCACCTGATTTAAATCATT

AAV2 VP2 silence -F	AGGAACCTGTTAAGACCGCTC
AAV2 VP2 silence -R	TTTTCCCGGAGCGGTCTTAAC
AAV2 VP2 only-F	AAAGTCGACACGGCTCCGGGAAAAAAG
AAV2 VP2 only-R	AAAAGCGGCCGCTTACAGATTACGAGTCAGG

2.2.3 oligonucleotides for siRNA knockdown

Negative Control siRNA and all siRNAs targeting the SUMOylation pathway were purchased from Qiagen (Hamburg, Germany).

Designation	Sequence 5' to 3'	Qiagen Number
Negative control siRNA	AATTCTCCGAACGTGTCACGT	1022076
Hs_SAE2_3 (Sea2)	CACCGGTTTCTCCCACATCGA	SI04234433
Hs_UBE2L_8 (Ubc9)	ACCACCATTATTTACCCGAA	SI04185937

2.2.4 Enzymes

Designation	Company
Restriction enzymes	New England Biolabs Frankfurt, Germany
T4 DNA Ligase	New England Biolabs Frankfurt, Germany
KOD HiFi Polymerase	Merck Darmstadt, Germany
Calf intestine alkaline phosphatase (CIP)	New England Biolabs Frankfurt, Germany
RNAse	Roche Mannheim, Germany
Proteinase K	Qiagen Hilden, Germany

2.3 Virologic materials

2.3.1 Solutions for AAV production

Designation	Composition
AAV production Lysis Buffer	50 mM Tris, pH 8.5 150 mM NaCl In H ₂ O, pH 8.5 autoclave

2 Materials

PBS-MK	1 mM MgCl ₂ 2.5 mM KCl In PBS filter-sterilized
PBS-MK/NaCl	1 M NaCl in PBS-MK filter-sterilized
Iodixanol (60%)	Sigma-Aldrich Taufkirchen, Germany
Phenol red	Sigma-Aldrich Taufkirchen, Germany
Benzonase (100.000 U/ml)	Merck Darmstadt, Germany

2.3.2 Sucrose gradient for AAV separation

2.3.2.1 Iodixanol removal

Designation	Composition
Zeba Spin Desalting Column, 7K MWCO (B2162579)	Thermo Scientific Schwerte, Germany

2.3.2.2 Sucrose gradient

Designation	Composition
10% Sucrose	10% sucrose in PBS-MK 10 mM protease inhibitor cocktail filter-sterilized
30% Sucrose	30% sucrose in PBS-MK 10 mM protease inhibitor cocktail filter-sterilized
Phenol red	10ul in 1ml sample

2.4 Buffers and Solutions for DNA extraction and analysis

2.4.1 DNA plasmid extraction by phenol-chloroform

Designation	Composition
Glucose mix	50mM glucose 10mM EDTA

2 Materials

	25mM Tris HCl in H ₂ O, pH 8.0
Alkali lysis buffer	200mM NaOH 1% SDS (w/v) in H ₂ O
Sodium acetate	3M NaAc In H ₂ O, pH 5.2
Phenol mix	Phenol-CIA mix 1:1 100µg hydroxyquinoline per 100ml
Chloroform-isoamyl alcohol mix (CIA)	Chloroform-isoamyl alcohol mix 24:1
TE buffer (1x)	10mM Tris 1mM EDTA in H ₂ O, pH 8.0

2.4.2 Agarose gel electrophoresis

Designation	Composition
1% agarose gel	0.33g agarose 2ul ethidium bromide In 33ml 1x TAE buffer
Ethidium bromide	Roth Karlsruhe, Germany
TAE buffer (1x)	40mM Tris 5.71% acetic acid (v/v) 10% 500mM EDTA in H ₂ O, pH 8.0 (v/v)
6x loading buffer	New England Biolabs, Frankfurt, Germany
Quick-Load 100bp DNA ladder	New England Biolabs, Frankfurt, Germany
1 Kb Plus DNA Ladder	Thermo Scientific Schwerte, Germany

2.5 Buffers and Solutions for protein analysis

2.5.1 Protein concentration determination

Designation	Company
Bradford reagent	BioRad München, Germany

BSA standard (2 µg/µl)	Thermo Scientific Waltham, USA
------------------------	-----------------------------------

2.5.2 Electrophoresis

Designation	Composition
Tris buffer, pH 8.8	1M Tris In H ₂ O, pH 6.8
Tris buffer, pH 6.8	1 M Tris 0.03% Bromphenol blue In H ₂ O, pH 6.8
3x protein loading buffer	30% glycerol 6% SDS 15% β-mercaptoethanol 0.003% bromophenol blue 187.5mM Tris in H ₂ O, pH 6.8
Ammonium Persulfate (APS)	10%APS (w/v) In H ₂ O
Acrylamide solution (30%AA)	Roth, Karlsruhe, Germany
TEMED	Sigma-Aldrich, Deisenhofen Germany
SDS	10% SDS (w/v) In H ₂ O

2.5.3 SDS-polyacrylamide gels

Designation	Composition
12.5% separation gel (5 mini gel)	18.75ml 30% acrylamide solution 16.88ml 1M Tris/HCl buffer, 8.48ml H ₂ O pH 8.8 450µl 10% SDS 450µl 10% APS 22.5µl TEMED
2% stacking gel (5 mini gel)	1.5ml 30% acrylamide solution 1.95ml 1M Tris/HCl buffer, pH 6.8 11.25ml H ₂ O 150µl 10% SDS 150µl 10% APS 22.5µl TEMED

2.5.4 Western blot analysis

Designation	Composition
TGS buffer (1x running buffer)	2.5mM Tris 1.45% glycine 0.1% SDS in H ₂ O, pH 8.3
EMBL buffer (1x transfer buffer)	2.5mM Tris 1.45% glycine 0.1% SDS in H ₂ O, pH 8.3
Blocking buffer	5% skim milk in PBS-T
Washing buffer	0.3% Tween 20 (v/v) in 1x PBS
Prestained protein ladder color plus	NEB Biolabs Schwalbach, Germany
Amersham Hybond membranes, PVDF	GE Healthcare Buckinghamshire, UK
Nitrocellulose membrane	GE Healthcare Buckinghamshire, UK

2.6 Immunological materials

2.6.1 Antibody

Designation	Description	Source
A20	Raised against intact AAV2 particles	J. Kleinschmidt
B1	Raised against VP1, VP2 and VP3 of different AAV serotypes	J. Kleinschmidt
A69	Raised against the capsid proteins of VP1 and VP2 of different AAV serotypes	J. Kleinschmidt
A1	Raised against the capsid proteins of VP1 of different AAV serotypes	J. Kleinschmidt
Anti-SUMO1	raised against the amino acid sequence 1-101 of SUMO-1 from the human species (FL-101).	Santa Cruz
Anti-SUMO2/3	Polyclonal antibody recombinant protein encoding full length SUMO (PA5-11373).	Thermo Scientific
Anti-Daxx	Monoclonal antibody corresponds to a region surrounding Gln255 of Daxx (25C12 Rabbit mAb).	Cell Signaling Technology

2 Materials

Anti-HA probe	Raised against a peptide mapping within an internal region of the influenza hemagglutinin protein (sc-805).	Santa Cruz
Anti-LamB1	raised against adherent spleen cells of human origin (H4A3, sc-20011)	Santa Cruz
Anti-Sae2	UBA2 Rabbit mAb recognizes endogenous level of total human UBA2 protein (D15C11)	CST
Anti-Ubc9	raised against the amino acid sequence 1-81 of UBC9 of human origin (C-12, sc-271057).	Santa Cruz
Anti-Myc	Mouse monoclonal, raised against the amino acid sequence EQKLISEEDL of the human oncogene c-myc	M. Müller
Anti-Actin	Mouse monoclonal antibody detecting human actin. The detected epitope lies between amino acid 18-40.	MP Biomedicals Solon, USA
HPVK18L2	Mouse monoclonal antibody, detecting amino acid 22-30 of HPV16 L2.	M. Müller
GAMPO	HRP-coupled Goat-anti-mouse antibody	Dianova
GARPO	HRP-coupled Goat-anti-Rabbit antibody	Dianova
AlexaFlour 488	AlexaFlour 488-coupled Goat-anti-mouse antibody	Life Technologies
AlexaFlour 594	AlexaFlour 594-coupled Goat-anti-Rabbit antibody	Life Technologies
AlexaFlour 594	AlexaFlour 594-coupled Donkey-anti-Goat antibody	Life Technologies

2.6.2 Immunoprecipitation

2.6.2.1 Beads

Designation	Company
SureBead Protein G Magnetic Beads (1ml)	Bio-Rad Munich, Germany

2.6.2.2 Buffer and solutions

Designation	Composition
Non-denaturing lysis buffer	20 mM Tris-HCl, pH 8.0 137 mM NaCl 10% Glycerol 1% NP40- freshly added 2 mM EDTA In H ₂ O

2 Materials

	1x protease inhibitor tablet (Roche) per 7 ml buffer freshly added
NET-N buffer	20 mM Tris-HCl, pH 7.5 100 mM NaCl 1 mM EDTA 1% NP-40 (freshly added)
3x Loading buffer w/o β -mercapthoethanol	30% glycerol 6% SDS 0.003% bromphenol blue 187.5mM Tris in H ₂ O, pH 6.8

2.6.3 Immunofluorescence

Designation	Composition
Fixation Solution	2% PFA in 1x PBS, pH 7.4
Quenching Solution	50 mM Ammoniumchloride in 1x PBS
Permeabilization Solution	0.2% Triton 100 In 1x PBS
Blocking solution	1% BSA in 1x PBS
DAPI	100 mg/ml in 1X PBS
Mounting medium	Dianova Hamburg, Germany

2.7 General buffer and solutions

Designation	Composition
1x PBS	140 mM NaCl 2.7 mM KCl 8.1 mM Na ₂ HPO ₄ 1.5 mM KH ₂ PO ₄ In H ₂ O, pH 7.4, autoclave
H ₂ O	Millipore, autoclave
Methanol	Sigma-Aldrich Deisenhofen, Germany
Ethanol	VWR Darmstadt, Germany

2 Materials

Isopropanol	VWR Darmstadt, Germany
Hydrochloric acid	VWR Darmstadt, Germany
Sodium hydroxide	VWR Darmstadt, Germany

2.8 Chemicals

Designation	Company
Tryptone	All chemicals were purchased from Sigma-Aldrich (Taufkirchen, Germany), AppliChem (Darmstadt, Germany), Merck (Darmstadt), Roth (Karlsruhe, Germany), Serva (Heidelberg, Germany), Fluka (Neu Ulm, Germany), Gerbu (Gaiberg, Germany), VWR (Darmstadt, Germany) and Life Technologies (Karlsruhe, Germany)
Yeast extract	
NaCl	
Bacto-agar	
Ampicillin	
Kanamycin	
Zeocin (Zeo)	
Tris/Hcl	
MgCl ₂	
Kcl	
Glucose	
EDTA	
NaOH	
NaAc	
Hydroxyquinoline	
Ethidium bromide	
Acetic acid	
Bromphenol blue	
Ammonium Persulfate (APS)	
Acrylamide solut ion (30%AA)	
Glycine	
Skim milk	
Tween 20	
Protease inhibitor tablet	
PFA	
Ammonium Chloride	
Triton X 100	
BSA	
Na ₂ HPO ₄	
KH ₂ PO ₄	

2.9 Kits

Kits	Company
Beetle-Juice BIG KIT	PJK Kleinbittersdorf, Germany
Gaussia glow Juice	PJK Kleinbittersdorf, Germany
Gateway® LR Clonase™ II Enzyme mix	Life Technologies Karlsruhe, Germany
QuikChange® II Site-directed mutagenesis Kit	Agilent Technologies La Jolla, USA
Qiagen Maxi Kit	Qiagen Hilden, Germany
Qiagen Mini Kit	Qiagen Hilden, Germany
QIAquick Gel extraction kit	Qiagen Hilden, Germany
QIAquick PCR Purification Kit	Qiagen Hilden, Germany
DNeasy blood & tissue kit	Qiagen Hamburg, Germany
Qproteome cell compartment kit	Qiagen Hamburg, Germany
KOD HiFi DNA Polymerase Kit	Novagen/Merck Darmstadt, Germany
Chemiluminescence kit	Applichem Darmstadt, Germany

2.10 Laboratory equipment

2.10.1 Electrical Equipment

2.10.1.1 Cell Culture

Designation	Company
Bio GARD cell culture hood	The Baker Company Sanford, USA
Steril GARD III Advance cell culture hood	The Baker Company Sanford, USA

2 Materials

Function Line incubator	Heraeus Hanau, Germany
Sanyo CO2 incubator	Sanyo/Panasonic Healthcare Wood Dale, USA
Neubauer Counting Chamber	Neolab Migge, Heidelberg, Germany

2.10.1.2 Centrifugation

Designation	Company
Fiberlite™ F12-6 x 500 LEX Fixed Angle Rotor	Thermo Scientific Waltham, USA
Fiberlite™ F13-14 x 50cy Fixed Angle Rotor	Thermo Scientific Waltham, USA
TFT65 Fixed Angle Rotor	Thermo Scientific Waltham, USA
SW41-Ti Rotor	Beckman Coulter Krefeld, Germany
Refrigerated Sorvall RC6+ centrifuge	Thermo Scientific Waltham, USA
Refrigerated table-top centrifuge 5417R	Eppendorf Hamburg, Germany
Table top centrifuge 5415C	Eppendorf Hamburg, Germany
Megafuge 1.0 centrifuge	Heraeus Hanau, Germany

2.10.1.3 Store

Designation	Company
Liebherr Comfort	Liebherr Biberach, Germany
Liebherr MedLine	Liebherr Biberach, Germany
Liebherr Premium	Liebherr Biberach, Germany
Liebherr ProfiLine	Liebherr Biberach, Germany
Ultra-low freezer	Heraeus Hanau, Germany
Nitrogen tank	Messer Krefeld, Germany

2.10.1.4 Microscope

Designation	Company
Will Wilovert	Wilovert Hund Wetzlar, Germany
Microscope for cell culture	Diavert Leitz Wetzlar, Germany
Zeiss Cell Observer	Zeiss Jena, Germany

2.10.1.5 Plates Reader

Designation	Company
Wallac Work Station	Perkin Elmer Norwalk, USA
Multiskan GO	Thermo Scientific Waltham, USA
Gel Doc EZ Imager	BioRad Munich, Germany

2.10.1.6 Electrophoresis

Designation	Company
Polyacrylamide Gel Electrophoresis Chamber	Hoefer, San Francisco, USA
XCell SureLock™ Mini- Cell Electrophoresis System	Thermo Scientific Schwerte, Germany
Transblot SD chamber	BioRad, Munich, Germany
Agarose electrophoresis chamber	BioRad Munich, Germany
Electrophoresis power supply ST PS 305	Gibco BRL, Eggenstein, Germany

2.10.1.7 Water baths, shakers and mixers

Designation	Company
GFC Waterbaths	Grant Instruments Cambridge, UK
Bacterial culture shaker	AG

2 Materials

Informs	Bottmingen, Switzerland
Combimage Red/RET magnetic stirrer	IKA Staufen, Germany
Test-tube-rotator	Snijders Scientific Tilburg, Netherlands
IKA RW 20 Digital Dual Range Mixers	IKA® LABORTECHNIK JANKE & KUNKEL, Staufen, Germany
Thermomixer 5436	Eppendorf Hamburg, Germany
Thermomixer comfort	Eppendorf Hamburg, Germany
Duomax 1030 shaker	Heidolph Schwabach, Germany
Table-top Shaker	GFL Burgwedel, Germany
Vibramax-VXR IKA	Staufen, Germany
Vortex Genie 2TM	Bender and Hobein Ismaning, Germany

2.10.1.8 Dot Blot

Designation	Company
Stratagene's Dot Blot chamber	Stratagene California, US
Laboratory Pumps	BioRad, Munich, Germany
Silicone Vacuum Grease	Beckman Coulter GmbH Krefeld, Germany

2.10.1.9 Others

Designation	Company
Integra pipet boy	Integra Biosciences GmbH Fernwald, Germany
800 W microwave	Bosch Gerlingen-Schillerhöhe, Germany
Ice maker	Hoshizaki Willich-Munchheide, Germany
Impulse Sealer	RNS Corp Taipei, Taiwan
MicroPulser Electroporator	BioRad

2 Materials

	Munich, Germany
MilliQ ultra-pure water unit	Millipore Merck Darmstadt, Germany
Nanodrop spectrophotometer	PegLab Erlangen, Germany
pH meter	Sartorius Göttingen, Germany
Sartorius scale	Sartorius AG Göttingen, Germany
Western Blot developing machine	Agfa Mortsel, Belgium
Analytical Balance ME204E	Mettler Toledo GmbH Zwingenberg, Germany

2.10.2 Common use Equipment

Designation	Company
1.5 mL and 2.0 mL microcentrifuge tubes	Eppendorf Hamburg, Germany
10mm cover slips	Thermo Scientific Waltham, USA
10 cm culture plates	Greiner Frickenhausen, Germany
15 mL reaction tubes	TPP Klettgau, Switzerland
14 mL BD falcon round-bottom tube	BD biosciences 2 Oak Park, Bedford, USA
25, 75 and 150 cm ² Tissue culture flasks	TPP Klettgau, Switzerland
50 mL reaction tubes	Greiner Frickenhausen, Germany
6, 10 and 15 cm cell culture dishes	Sarstedt Inc. Newton, USA
6-, 12-, and 24-well test plates	TPP Klettgau, Switzerland
96-well LIA plate	Greiner Frickenhausen, Germany
96-well plate	Costar Corning, USA
Ultracentrifuge tubes (TFT65)	Beckman Coulter GmbH Krefeld, Germany
Ultracentrifuge tubes (sw41)	Beckman Coulter GmbH Krefeld, Germany

2 Materials

Cell lifter	Costar Corning
Chemiluminescence films	GE Healthcare Limited Buckinghamshire, UK
Cryo tubes, 2 ml	Roth Karlsruhe, Germany
Electroporation cuvettes (25 x 2 mm)	Peqlab Erlangen, Germany
Glass slides	Thermo Scientific Waltham, USA
Inoculating loop	Greiner Frickenhausen, Germany
One-time use filter, 0.2/0.4 µm	Renner Dannstadt, Germany
Parafilm "M"	American National Can Chicago, USA
Pipette tips	Nerbe plus GmbH Winsen/Luhe, Germany
Pipettes (1000, 200, 100, 20, 10 and 2 µL)	Gilson Middleton, USA
Syringes and needles	BD Franklin Lakes, USA
Whatman filter paper 3MM paper	Schleicher & Schuell Dassel, Germany

2.10.3 Software

Designation	Company
Microsoft Windows XP, 8.1	Microsoft Redmont, USA
Clone Manager 9.0 for Windows	Scientific & Educational Software, Cary, USA
Microsoft Office 2003, 2010	Microsoft Redmont, USA
GraphPad Prism 6.0	GraphPad Software La Jolla, USA
Wallac 1420 Workstation	Perkin Elmer Norwalk, USA
ImageJ 1.40	NIH Bethesda, USA
Citavi 5	Swiss Academic Software GmbH Wädenswil, switzerland

3 Methods

3.1 Cultivation and manipulation of cells

3.1.1 Cultivation and manipulation of prokaryotic cells

3.1.1.1 Cultivation and storage of competent cell

Glycerol stock or single colony was transferred to liquid LB medium supplemented with the respective antibiotics (Amp⁺, Kana⁺), and then shaken at 200rpm overnight at 37°C. For long-term storage of bacteria containing the transformed plasmid, glycerol stocks (2.1.4.3) were prepared with 0.3mL sterile glycerol and 1 mL of the overnight bacteria culture and stored at -80°C for further use.

3.1.1.2 Preparation of electrocompetent cell

MXDH10 E. coli bacteria were used for preparing electrocompetent cells (2.1.2). The glycerol stock was transferred to 25mL LB medium without antibiotics and shaken at 200rpm overnight at 37°C. Medium culture with 5mL were added to 400mL LB medium the following morning and shaken at 37°C 200rpm until the culture OD600 reached 0.5-0.6 (2.10.1.7), and then chilled on ice for 30min. After harvesting and centrifugation the culture was shaken at 6000rpm in 10 min at 37°C in a round-bottom tube, the pellet was resuspended in 30mL ice-cold H₂O and then transferred to a dialysis bag to dialyze in H₂O overnight at 4°C. On the third day bacterial cells were harvested by centrifugation at 4000rpm for 10min at 4°C and resuspended in 600μL ice-cold 10% glycerol solution. All the procedures were performed on ice. Aliquots of 40μL were

stored at -80°C for further use.

3.1.2 Cultivation and manipulation of eukaryotic cells

3.1.2.1 Cultivation and storage of mammalian cell lines

All mammalian cell lines were cultivated in the environment of 37°C , 5% CO_2 and 90% humidity. The cells were passaged when they reached around 90% confluency. Cell culture medium was removed, and the attached cells were washed with the 0.25% trypsin EDTA (2.1.4.1) to remove residual FBS and followed by another addition of trypsin plus incubation at 37°C to detach the cells. The flasks were tapped gently to detach the cells completely and then neutralized by adding supplemented medium. After centrifugation (1900rpm/5min), the pellet was resuspended in 10mL supplemented medium and extract 1mL suspension into new flask, then complemented medium in an adequate volume was added.

For preparing cryo-stocks, the cells at a confluency of about 80% in 150cm^2 culture flask were harvested by trypsinization and centrifugation. The cell pellet was resuspended in 3mL cryomedium (2.1.4.3) after centrifugation and then aliquoted into 3x 2mL cryotubes. The cells were stored in a cooling chamber with isopropanol at -80°C for at least 24h and then transferred to liquid nitrogen. To thaw cryopreserved cells, the tube containing the cells was incubated a in a 37°C water bath immediately until most of the suspension was thawed and then transferred to a 15mL Falcon tube containing 10mL supplemented medium and centrifuged. The cell pellet was resuspended again in an adequate volume medium and moved to a new flask.

3.1.2.2 Transfection of mammalian cell lines with polyethylenimine (PEI)

For the transfection in a 6-well plate, $0.8-2.4 \times 10^5$ cells per well were seeded in 1mL supplemented medium (Table 1) and cultivated for 24h. For preparing the transfection mix for a 6-well plate, 10 μ L H₂O were transferred into a 2mL Eppendorf tube as well as 1.5 μ g DNA (2.2.1), 0.25mL unsupplemented DMEM and 5 μ L PEI transfection reagent followed by 10sec vortex and incubating at RT for 10min. After incubation, 0.75mL supplemented medium were added to this transfection mix and vortexed again. The transfection mix was added onto the cells after removing the medium and incubated at 37°C, 5% CO₂. Four-14h after transfection the transfection mix was removed from the cells and fresh supplemented medium was added. The cells were cultivated and were ready to be used after 48h.

Table 2. Overview of the transfection procedure in different formats

Cell Culture Plate	H ₂ O Volume (μ L)	Cell Number (cell/well)	DNA amount (μ g)	Φ DMEM (mL)	PEI Volume (μ L)	Full DMEM (mL)
24-well plate	2.5 μ L	2.0-6.0 $\times 10^4$	0.4 μ g	0.07mL	1.3 μ L	0.2mL
12-well plate	5 μ L	0.4-1.2 $\times 10^5$	0.8 μ g	0.13mL	2.5 μ L	0.4mL
6-well plate	10 μ L	0.8-2.4 $\times 10^5$	1.5 μ g	0.25mL	5 μ L	0.75mL
10cm dish	61.5 μ L	2-3 $\times 10^6$	10 μ g	1.6mL	31 μ L	4.6mL
15cm dish	185 μ L	6-8 $\times 10^6$	27 μ g	4.6mL	93 μ L	13.8mL

3.1.2.3 Transfection of mammalian cell lines with siRNA

All Negative control siRNA and siRNAs targeting the SUMOylation pathway were purchased from Qiagen (Hamburg, Germany). The siRNA knockdown

was performed on 2.5×10^4 HeLa cells seeded in 0.5mL supplemented medium in a 24-well plate (Table 2). The transfection mix was prepared by dilution of 37.5ng siRNA (0.3 μ L siRNA) (2.2.3) and 3 μ L HiperFect transfection reagent in 100 μ L unsupplemented medium and incubated at RT for 10min. The transfection mix was added drop-wise to the cells evenly and cultivated the cells 48h. Thereafter the siRNA knockdown-cells were ready for harvesting or virus transduction.

Table 3. Overview of the siRNA transfection procedure in different formats

Cell Culture Plate	Volume of medium in cell (mL)	Cells Number (cell/ well)	siRNA amount (ng)	HiperFect Reagent (μ L)	Final siRNA volume (μ L)
24-well plate	0.5mL	2.5×10^4	37.5ng	3 μ L	100 μ L
12-well plate	1.1mL	8×10^4	75ng	6 μ L	100 μ L
6cm dish	4mL	3.0×10^5	256ng	20 μ L	100 μ L

3.1.2.4 Induction of a stable cell line with doxycycline

To overexpress the stably transfected myc-Gam1 protein, HeLa-Gam1 cells (Kindly provided from Susanna Chiocca) were treated for 6~12h with 50 mg/mL doxycycline (final concentration is 50ng/ μ L) after seeding and attaching.

3.2 Molecular biology methods

3.2.1 Polymerase chain reaction (PCR)

The Polymerase chain reaction (PCR) was performed to amplify DNA fragments and clone them into destination vectors. The DNA of interest was amplified from template DNA plasmid that could contain different restriction sites or necessary additional sequences with the help of primers. The primers

were designed using Clone Manager CMSuite9 and ordered from MWG Eurofins in Ebersberg of Germany. All PCRs were performed using the KOD HiFi DNA Polymerase Kit from Novagen/Merck (2.2.4), according to the manufacturer's instructions (table 3 and 4). The annealing temperature, as well as the number of DNA amplification cycles, depended on the T_m value of primers and were also optimized under different conditions.

Table 4. Constituents of PCR reaction mix and volumes

Component	Volume (50 μ L)
template DNA	(20-50ng) 1 μ L
10x KOD Buffer #2	5 μ L
dNTPs (2.5mM each)	2 μ L
MgCl ₂ (25mM)	2 μ L
Fwd Primer (100 μ M)	1 μ L
Rev Primer (100 μ M)	1 μ L
KOD Polymerase	1 μ L
H ₂ O	Add up to 50 μ L

Table 5. Standard PCR program for KOD HiFi Polymerase Kit

Process	Temperature	Time	Cycles
Pre-denaturation	98°C	3min	
Denaturation	98°C	20 sec	
Annealing	60°C	10 sec	30 cycles
Extention	72°C	25 sec	
Stabilization	72°C	5 min	
Hold	4°C	∞	

3.2.2 PCR product purification

The PCR products were purified after the polymerase chain reaction by removing all buffers and enzymes for next experiments, e.g. digestion (3.2.8) or

ligation (3.2.8). The reaction was performed using QIAquick PCR Purification Kit (2.9), following the manufacturer's protocol.

3.2.3 StrataClone™ Blunt TOPO cloning

The cloning of blunt end PCR products into the TOPO vector was carried out using the StrataClone Blunt PCR Cloning Kit (2.9) from Stratagene. It was performed according to manufacturer's instructions.

3.2.4 Gateway cloning

Genes of interest were provided as complete Gateway®-compatible entry-vectors to shuttle into a destination vector with the LR Clonase™ II enzyme mix. All the reactions were done using the Fast Gateway® LR protocol (2.9). It was performed according to manufacturer's instructions.

Table 6. Constituents of Gateway Clone reaction mix and volumes

Component	Volume
Entry clone (50-150ng)	1-7µL
Destination vector (150ng/µL)	1µL
TE Buffer	up to 8µL
LR Clonase™ II enzyme mix	2µL

The reaction was processed at 25°C for 1hr followed by the treatment with 1µL proteinase K at 37°C for 10min to stop the reaction. 1µL of the LR reaction was transformed into 40µL electrocompetent bacteria and resuspended in 500µL LB, shaken at 37°C for 1h, followed by spreading on agar plates with the appropriate antibiotic and obtain colonies at 37°C overnight. Colonies were picked and cultivated for DNA plasmid extraction, restriction digests and sequencing to confirm correct insertion. Glycerol stocks of the correct colonies were prepared and stored at -80°C.

3.2.5 Site-directed mutagenesis QuikChange® cloning

To mutate the nucleotide of interest in the sequence, a pair of complementary primers was designed containing the mutation in their target sequence. The reaction was performed using the QuikChange® II XL Site-Directed Mutagenesis Kit (2.9), It was performed according to manufacturer's instructions. The reaction mix was prepared as follows:

Table 7. Constituents of QuikChange® cloning reaction mix and volumes

Component	Volume (50µL)
10x reaction buffer	5µL
F-Primer	125ng
R-Primer	125ng
DNA template	20ng
dNTPs (2.5mM each)	1µL
PfuMLtra High Fidelity DNA polymerase (2.5U/µL)	1µL
H ₂ O	Add up to 50µL

Table 8. Standard QuikChange® amplification program

Process	Temperature	Time	Cycles
Pre-denaturation	95°C	30 sec	
Denaturation	95°C	30 sec	12-18 cycles
Annealing	55°C	1 min	
Extention	68°C	1kb/ 1min	
Hold	4°C	∞	

* The point mutations need 12 cycles, single amino acid changes need 16 cycles, and multiple amino acid deletions or insertions need 18 cycles.

The PCR product was digested with 1µL of DpnI enzyme and incubated at 37°C for 1h. 1µL of each treated PCR product was transferred to a 1.5mL Eppendorf

tube containing 50µL of the XL1- Blue supercompetent cells and was gently mixed and incubated on ice for 20-30 minutes. The bacteria were transformed by heat pulsed for 90 seconds at 42°C and then placed on ice for 2 minutes followed by adding 500µL S.O.C medium, and tubes were shaken at 250rpm for 1h at 37°C. 250µL of the transformation reaction was spread on agar plates containing the appropriate antibiotic and incubated at 37°C overnight to obtain colonies. Colonies were picked and cultivated for DNA plasmid extraction and sequencing to confirm correct insertion. Glycerol stocks of the correct colonies were prepared and stored at -80°C.

3.2.6 Agarose gel-electrophoresis

Agarose gel-electrophoresis (2.4.2) was used to separate and analyze DNA fragment by size. The preparative 1% agarose gels contained 0.006% ethidium bromide and were placed into an electrophoresis chamber and filled with 1x TAE buffer, mixed loading 6x dye and DNA fragments (volume ratio 1:5) which were either produced by PCR or enzymatic restriction to cut a specific region of the plasmid DNA was loaded onto the gel together with a DNA ladder and electrophoresis was run at 120 V for 30 min. For analytical gels, the DNA was visualized with UV light at 254 nm wavelength and for preparative gels at 366 nm to avoid DNA damage.

3.2.7 DNA extraction from agarose gels

For purification of specific DNA fragments from an analytical agarose gel, the desired bands were cut out with a scalpel and the QIAquik Gel Extraction Kit (2.9) from Qiagen was used. The following purification procedure was carried out according to the manufacturer's instructions. The purified DNA was analyzed on a mini agarose gel.

3.2.8 Enzyme restriction

To test isolated plasmid DNA for the absence or presence of a specific insert, 500ng of DNA plasmids were transferred to a new Eppendorf tube. For enzymatic restriction a master mix was prepared containing the 2 μ L of the corresponding 10x buffer, 1 μ L of the specific enzyme/s per reaction as well as H₂O add up to 20 μ L. The reaction was incubated at 37°C 2-3h. To analyze the restricted plasmid DNA, 5 μ L reaction were mixed with 1 μ L 6x loading dye and run on an agarose gel electrophoresis (2.4.2).

Table 9. Constituents of Enzyme restriction reaction mix and volumes

Component	Volume (20 μ L)
10x reaction buffer	2 μ L
Enzyme I (20,000U/mL)	1 μ L
Enzyme II (20,000U/mL)	1 μ L
Plasmid DNA	100-500ng
H ₂ O	Add up to 20 μ L

3.2.9 Dephosphorylation of DNA backbone 5'

Dephosphorylation is mainly to prevent the self-ligation of the plasmid vector and is most commonly used for plasmids for blunt end ligation. Thus, after the enzymatic restriction, the 5'-phosphate group of the cleavage vector was removed by adding 2 units of calf-alkaline phosphatase (CIP) (2.2.4). The reaction was incubated at 37°C for 15min, followed by a second incubation at 58°C for another 15min. The dephosphorylated vector was purified by agarose gel-electrophoresis as described.

3.2.10 Ligation

Vector DNA and insert DNA were used in a molar ratio of 1:3. The ligation mix was prepared according to manufacturer's instruction from NEB and incubated

at 4°C overnight.

Table 10. Overview of the ligation mix

Component	Volume (20µL)
10x T4 DNA Ligase Buffer	2µL
Vector DNA	0.02pmol
Insert DNA	0.06pmol
T4 DNA Ligase (400,000U/mL)	1µL
H ₂ O	Add up to 20µL

3.2.11 Transformation of *E. coli* bacteria

3.2.11.1 Transformation of *E. coli* using the heat-shock method

To transform into XL-Blue supercompetent cells (2.1.2), the DNA plasmid was mixed with bacteria and incubated for 90 seconds at 42°C in water bath and then the reaction was put on ice for 2 minutes, followed by adding 500µL S.O.C medium at 37°C for 1h shaking.

250µL of the transformation reaction was spread on agar plates containing the appropriate antibiotic and incubated at 37°C overnight to obtain colonies. Colonies were cultivated, DNA plasmid extracted, enzyme digested and sequenced to confirm correct insertion. Glycerol stocks of the correct colonies were prepared and stored at -80°C.

3.2.11.2 Transformation of *E. coli* using the Electroporation

For the transformation of electrocompetent bacteria, 1µL of the ligation (3.2.10) was mixed with 40µL of electrocompetent bacteria and transferred into a cooled electroporation cuvette. 2.5 kV for 5ms pulsing was set up for electroporation and 500µL of LB-medium were added to the transformed bacteria and the mix

was incubated at 37°C for 1h, followed by plating 10-150µL on a LB-agar plate with the respective antibiotic and incubated at 37°C overnight.

3.2.12 DNA extraction from bacterial cultures

3.2.12.1 Mini-preparation using the alkaline lysis and phenol-chloroform extraction

The bacteria containing plasmid DNA were harvested from 1.5mL culture medium in Eppendorf by centrifugation at 13.000rpm for 2min. To resuspend the pellet the 100µL glucose (2.4.1) was used and shaken for 10min at RT. 200µL lysis buffer were added and incubated for 5-10min on ice and followed by a 150µL 3M NaAc ice incubation for 5-10min to stop the reaction. Afterwards, 450µL phenol were added to the lysed cells and the sample was incubated 5-10min on a shaker at RT, centrifugation at 13,000rpm for 5min. 380µL of the supernatant were transferred to a fresh tube which contains 450µL isopropanol already. The sample was then incubated at -70°C for 10min to precipitate plasmid DNA followed by centrifugation at 13.000rpm for 30min on ice and washed with 500µL 70% ethanol and 500µL 99% EtOH afterwards. After quick drying the pellet was resuspended in 50µL H₂O and stored at 4°C. This prep needs to be treated with RNase (2.2.4) during digesting process.

3.2.12.2 Mini-preparation using the Qiagen mini-prep kit

Plasmid DNA isolation was performed by QIAprep Spin Mini Prep Kit cultured from 2mL bacteria culture. The preparation of plasmid DNA was performed according to manufacturer's instructions.

3.2.12.3 Maxi-preparation using the Qiagen maxi-prep kit

Plasmid DNA isolation was performed by Qiagen MaxiPrep Kit cultured from 2mL bacteria culture. The preparation of plasmid DNA was performed according to manufacturer's instructions.

3.2.13 DNA quantification

Nanodrop was used to test plasmid DNA concentration. 1 μ L DNA sample was measured in relation to a blank sample.

3.2.14 DNA-Sequencing

Sequencing was performed by GATC Biotech in Konstanz, Germany.

3.3 Protein analysis methods

3.3.1 Bradford assay

To make a calibration curve to determine the target protein concentration, 10 μ g/ μ L BSA stock solution was diluted in H₂O to get a final concentration of 2 μ g/ μ L as the working solution. The BSA standard was titrated 1:2 in duplicates in a 96-well plate, starting with a concentration of 2 μ g/ μ L to 0.016 μ g/ μ L. H₂O was used as well as blank within the Bradford assay (2.5.1). The protein samples were used in 3 different dilutions (in H₂O), by sequential 1:1 dilution.

3.3.2 SDS-Polyacrylamide gel electrophoresis (SDS-PAGE)

SDS-PAGE was performed to separate different protein according to the difference of protein molecular weight. Each sample (Cell lysate or viral particles) was mixed with 3x SDS loading buffer (2.6.2.2) and boiled for 10 minutes at 95°C. 5 μ L of the denatured cell lysates or 15 μ L denatured viral

particles, as well as protein ladder, were loaded on fixed SDS gel (2.5.2) in chamber. Proteins were separated on the SDS gels in 1x TGS running buffer at 80 V for 30min for the stacking gel and 120 V (2.5.4) for separating gel.

3.3.3 Western Blot analysis

The protein has been separated by SDS-PAGE gel (2.5.3). It is necessary to transfer the proteins to the solid phase for the further study, so the proteins were blotted onto activated PVDF or nitrocellulose (NC) membrane using the wet blot (2.10.1.6) method. Three soaked blotting pads were placed into the blot module and followed with 1 piece of filter paper, then the gel covered with NC or activated PVDF membrane. Air bubbles were removed by rolling a glass pipette over the membrane surface and covered with another filter paper afterwards. After another three soaked blotting pads on the top, the blot module was closed with the lid and fixed into the X Cell II™ Blot Module. The transfer was performed at 30 mV 90min for proteins with a molecular weight around 80-150 kDa, or 30min for protein smaller than 50 kDa. The membrane was blocked for 1h in 5% milk PBS-T at room temperature (RT) on a shaker and then incubated with the desired primary antibody (2.6.1) which was diluted in 5% PBS-T milk overnight at 4°C. After incubation the membrane was washed three times for 10 minutes with PBS-T and incubated for 1h at RT with the diluted secondary antibody. Then the membrane was washed three times for 10 minutes with PBS-T and proteins were detected by chemiluminescent kit (2.9) according to the manufacturer's protocol by adding 0.5 mL of each solution onto the membrane and incubate it for 1 minute at RT. The chemiluminescence was detected using developing machine (2.10.1.7) in a dark room.

3.3.4 Dot Blot

Protein detection using the dot blot protocol is like western blotting in that both

methods allow for the identification and analysis of proteins of interest. Protein samples are instead spotted onto membranes and hybridized with an antibody probe. The nitrocellulose membrane or PVDF membrane activated in methanol for 20 min are put together with two pieces of filter papers on the plate which is fixed on the base of dot blot chamber and covered with the 96-fine hole cap (2.10.1.8) which can allow each sample across the hole. The chamber was sealed by parafilm and connected to the pump to suck liquid sample into the membrane. The pump was turned on and 5-50 μ l from each sample or fraction was pipetted onto the membrane, the samples could go through the membrane. After the membrane becomes dry after several minutes, it was blocked in 5% milk PBS-T in RT and shaken for 1h. After blocking, the membrane was incubated with the desired primary antibody (diluted in blocking solution) (2.6.1), for 2 hours at RT. After primary antibody incubation the membrane was washed three times for 10 minutes with PBS-T and incubated for 1h at RT with the secondary antibody. Then, the membrane was washed three times for 10 minutes with PBS-T and proteins were detected using the chemiluminescent kit (2.9) according to the manufacturer's protocol by adding 0.5 mL of each solution onto the membrane and incubate it for 1 minute at RT. The chemiluminescence was detected using developing machine in a dark room.

3.4 Immunological methods

3.4.1 Immunoprecipitation of virus

To investigate the interaction of AAV and proteins, immunoprecipitation was performed using SureBeads™ Protein G Magnetic Beads. 25 μ L of SureBeads per sample were added to a 1.5mL tube to be magnetized and then supernatant was discarded. The beads were washed three times by 1mL NET-N buffer with 1% NP-40 freshly added (2.6.2.2) followed by resuspension and subsequent

magnetization. Purified antibody of interest was added to beads in 1% NET-N buffer up to 750 μ L as final volume and incubated on a rotating wheel at 4°C overnight. The beads were washed three times with 1% NET-N buffer on second day and incubated with a total of 5×10^9 purified AAV2 particles overnight on a rotating wheel at 4°C. On the third day, the beads containing AAV particles were washed three times with 1% NET-N buffer by resuspension and subsequent magnetization, then moved into a new tube with 40 μ L of 1x SDS buffer (2.6.2.2). The beads were incubated at 95 °C for 10 min and moving the eluent to a new tube which was either loaded directly for analysis via western blot (3.3.3) or stored at 20°C for further use.

3.4.2 Immunofluorescence

To visualize AAV trafficking at different time points after down regulation of SUMOylation, indirect immunofluorescence was performed. 4×10^5 HeLa-Gam1 cells were plated on coverslips in a 12-well plate, and then Gam1 was overexpressed by Dox induction (3.1.8). AAV2 transduction was performed on the HeLa-Gam1 cells with MOI 10^5 and incubated at 4°C 1h on shaker. After 3 times PBS washing, fresh medium was supplemented onto cells and transferred to 37°C, 5% CO₂. To test the AAV infection in cells at different time points, slides were collected at 1h, 3h, 6h, 9h, 12h and 24h incubation at 37°C, 5% CO₂. The slides with cells were washed 3 times 5 minutes with 1x PBS and fixed with 2% paraformaldehyde (PFA) (2.6.3) for 15 minutes at RT. The cells were quenched in 50mM ammonium chloride (50mM NH₄Cl) (2.6.3) twice for 10 minutes to avoid dye artefacts, then permeabilized in 0.2% Triton-X100 (2.6.3) for 10 minutes. Followed by another 3 times washing with 1x PBS the cells were blocked in 1% BSA for 1hr at RT. Thereafter the cells were incubated with

desired primary antibody (2.6.1) diluted 1:100 in 100 μ L 1% BSA 1h at 37°C on a shaker. The cells were washed 3 times for 5 minutes with 1x PBS and were incubated with secondary antibody and DAPI (1:200) diluted in 1% BSA in PBS at 37°C for 1 hour. Subsequently the coverslips were washed three times with 1x PBS and mounted onto slides using mounting medium (2.6.3) before being sealed with nail polish. The slides were visualized using the Zeiss Cell Observer or confocal microscope and the images were processed using Image J (2.10.1.4).

3.5 Virological methods

3.5.1 Production of AAV particles in HEK293TT cells

To produce AAV particles, 5 x 10⁷ HEK293TT cells we plated on five 15cm dishes and transfected as described before (3.1.2.2) using the three-plasmid system with AAV capsid plasmid, helper plasmid, as well as reporter plasmid (2.1.3.1) at a molar ratio of 1: 1: 1 using a total of 135 μ g plasmid DNA. After 48 hours the cells were harvested by cell scrapper and collected with medium into 2x 50mL tube, washing the empty plates to remove the transfected cells completely. After centrifugation at 1900rpm for 10 minutes, the medium was removed, and the pellet was resuspended by 20mL 1x PBS and centrifuged again. The washed pellet was resuspended in 5mL AAV-lysis buffer (2.3.1) before undergoing 5 freeze-thaw cycles in liquid nitrogen and 37°C process alternately. Benzonase, which was used to degrade all forms of DNA and RNA but having no proteolytic activity, was added 1 μ L (50U/mL) per prep and incubated at 37°C for 30 minutes, followed by a centrifugation at 5000rpm for 10 minutes. The cell crude lysate containing AAV particles was either purified immediately or stored in -80°C for less up to one week.

3.5.2 AAV particle purification from 293TT cell extracts

Five mL crude lysate containing AAV particles were added through a long Pasteur pipette into a Quickseal-Tube first, followed by 1.5mL of iodixanol in PBS-MK/NaCl, 1.5mL of 25% iodixanol in PBS-MK with 3 μ L phenol red solution, 1.5mL of 40% iodixanol in PBS-MK and 3.8mL of 60% iodixanol in PBS-MK with 5 μ L phenol red solution (2.3.1). All samples were balanced to 0.000g difference with AAV-Lysis buffer and sealed by heating device and centrifuged at 50,000 rpm for 2 hours at 10°C with rotor TFT65, Accel=9, Decel=1. Lastly, the tubes were gently fixed onto a metal stand and poked with a needle from the top to relieve pressure and siphon 1mL of AAV particles from 40% iodixanol phase using a needle and syringe. The white band in between of 25% and 40% iodixanol phase was avoided during collection. Purified AAV particles were stored in -20°C or -80°C for the long-term preservation.

Table 11. Overview of the Iodixanol gradient for AAV particles purification

Component	PBS-MK/NaCl (mL)	PBS-MK (mL)	Iodixanol (mL)	Phenol red (μ L)
15% phase	1.5mL	-	0.5mL	-
25% phase	-	1.332mL	0.833mL	3 μ L
40% phase	-	0.667mL	1.333mL	-
60% phase	-	-	3.8mL	5 μ L

3.5.3 AAV particle separation by continuous sucrose gradient.

Iodixanol present in AAV particle preparation was removed by desalting spin column and before loading on sucrose gradient. Spin desalting column (2.3.2.1) was washed 3 times by PBS-MK and spun down with the speed of 1200rpm/min for 2 mins to remove Iodixanol completely. Beckman mixer was used to prepare the 10-30% sucrose gradient, with 4.5mL of 30% sucrose in the front groove and 4.5mL of 10% sucrose in behind (2.3.2.2). Setting up the speed of the mixer as 90rpm and dropping into a Beckman tube (14 x 89 mm) at

1 drop/2sec. Sucrose gradient can be stored at 4°C less than 2 days. A total of 1×10^{11} purified AAV capsids was obtained after iodixanol removal and dissolved in 1mL PBS-MK which were mixed with 10 μ L of phenol red and loaded on the top of a Beckman tubes which contain 9mL 10-30% sucrose gradient. After ultracentrifugation with the rotor SW41 at 160,000g (or 37,000rpm) for 2 h at 10°C, 400 μ L fractions were collected and detected by either Dot Blot (3.3.4), Western Blot (3.3.3) or viral infectivity assay (3.3.5).

3.5.4 AAV particle quantification

AAV particles containing a CMV- firefly reporter gene aliquots were prepared, and titer was determined via quantitative real time PCR (by Barbara Leuchs, DKFZ, Heidelberg).

3.5.5 Viral transduction assay (for Firefly and Gaussia luciferase assay)

Viral transduction assay was performed to analyze the infectivity of the viruses containing Firefly or Gaussia reporter gene on different cell lines at different conditions, e.g. siRNA knockdown treatment (Table 11). For this, cells were seeded at least one day prior transduction and incubated at 37°C. The transduction was done at different MOIs (10^3 , 10^4 or 10^5) depending on the experiment (3.1.2.3). Luciferase analysis could be done in 24h transduction with a Kit (3.5.7).

3.5.6 Viral transduction assay (qPCR)

3.5.6.1 qPCR for time course experiment

HeLa cells were seeded in 6cm dish with 3×10^5 and incubated at 37°C, 5% CO₂

o/n. The next day Scramble or Sae2 siRNA were prepared for knockdown as described before and cultured 48h (Table 2). The cells were transduced and incubated in 4°C 1h on shaker. After 3 times PBS washing, cells were harvested directly (1h) or incubated longer (5h) at 37°C. Cells were harvested by scraping or treatment with trypsin and proteinase K (1000µL Trypsin+ 50µL Proteinase K). For trypsin and proteinase K harvesting, the cells were treated for 30min at 4°C, harvested and washed with ice-cold 1xPBS. Centrifugation was performed at 1,900rpm for 5min. AAV vector genomes were quantified by qPCR afterwards.

3.5.6.2 qPCR for subcellular fractionation

HeLa cells were treated with siRNA and transduced with AAV2 as described before (3.5.6.1). After 4°C incubation 1h followed by 3 times PBS washing to remove the free AAV2, the cells were incubated at 37°C for 12h. Samples were harvested by subcellular fractionation with the Cell Compartment Kit. AAV vector genomes were quantified by qPCR afterwards.

Table 12. overview of AAV transduction in cells

Experiment	Cell number	Culture plate	MOI	Detection method
Untreated	10x10 ⁴	24-well plate	10 ⁵	Western Blot
siRNA KD	10x10 ⁴	24-well plate	10 ³	Luciferase assay
siRNA KD	2.0x10 ⁵	12-well plate	10 ⁵	IF
siRNA KD	3.0x10 ⁵	6cm dish	10 ⁵	qPCR

3.5.7 Luciferase assay

3.5.7.1 Firefly luciferase assay

The medium was discarded after 24h AAV2 transduction, and 100µL of specialized 1x lysis buffer from Beetle Juice BIG Kit (2.9) was added in the

24-well plate and shaken for 15 minutes at RT. Subsequently, 20 μ L of the lysate were transferred into white LIA 96-well plate and all samples were triplicated. For the firefly luciferase detection, 100 μ L of Beetle juice BIG Kit (2.9) were added to each well and readout after 1min. The luminescence was analyzed via the Wallac Work Station (2.10.1.5).

3.5.7.2 Gaussia luciferase assay

Unlike the firefly luciferase assay which tests the crude lysate, the 10 μ L cell culture medium was transferred into white LIA 96-well plate and all samples were triplicated. For the Gaussia luciferase detection, readout was performed after adding 100 μ L of Gaussia glow juice (2.9) with 1:50 coelenterazine to each well and readout was performed after 1min. The luminescence was analyzed via the Wallac Work Station.

4 Results

4.1 The role of SUMO as host restriction factors effecting AAV transduction

4.1.1 Knockdown of SUMOylation results in increased AAV transduction

AAV is worldwide used as gene therapy vector in the past years but it is still limited by the length of carriable gene fragments as well as the poor virus transduction efficiency. In order to find out the host cell factors effecting AAV transduction, screening of siRNA libraries was used to identify that putative SUMOylation pathway proteins play an important role as AAV restriction factors. This work was performed by our colleague Christina Hölscher *et al.*. The genome wide siRNA libraries screen identified the key players of the SUMOylation pathway- which are the E1 enzyme: Sae1/Sae2 complex and the E2 enzyme: Ubc9. After 48h knockdown in HeLa cells with siRNA targeting Sae2 or Ubc9, AAV2 particles encoding firefly luciferase reporter gene driven by a CMV promoter was used to transduce the cells for 24h followed by harvesting and testing luciferase assay.

The data shows the Sae2 or Ubc9 siRNA knockdown *in vitro* increases the transduction of AAV2 (Figure 10b), and the protein level detection confirmed the decreased amount of Sae2 or Ubc9 in HeLa cells (Figure 10a), thus confirming that SUMOylation catalyzing enzyme Sae2 and Ubc9 are restriction factors of AAV2 infection.

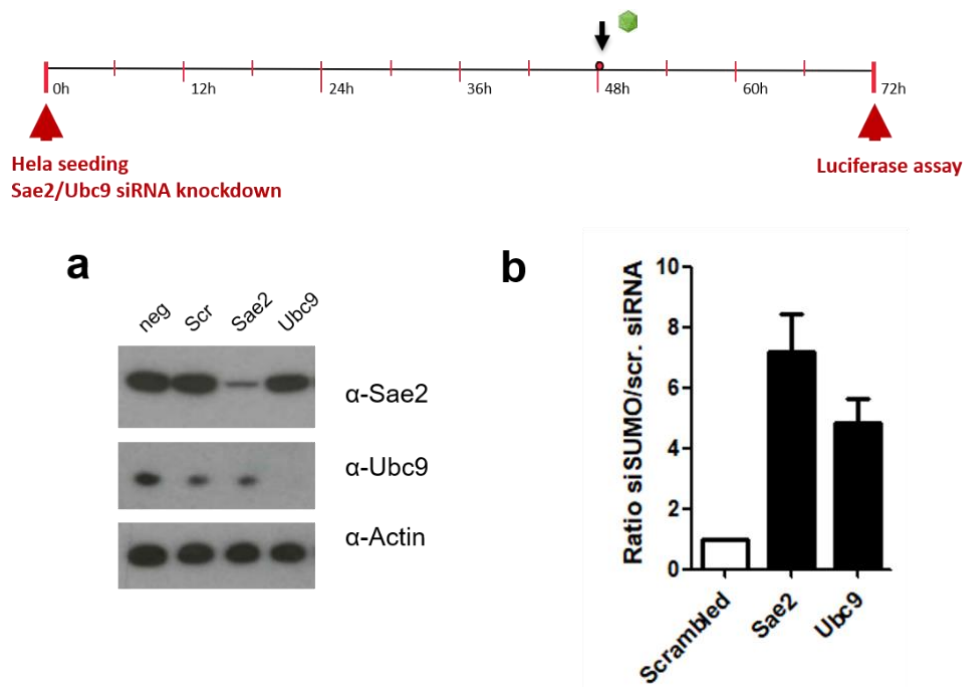


Figure 10 SUMOylation enzyme Sae2 or Ubc9 knockdown increases AAV transduction.

(a) Sae2 or Ubc9 protein expression was down-regulated by siRNA transfection *in vitro*. HeLa cells were seeded into 24-well plate with 2.5×10^4 /well and transfected with 37.5ng siRNA targeting Sae2 or Ubc9 siRNA, and then harvested after 48h to test the protein level, (b) or continually transduced by AAV2-CMV-firefly at MOI=1000 for the next 24h. All samples for western blot test was treated with 1x SDS loading buffer. Firefly luciferase assay was intended for AAV transduction test, and the standard deviation of the mean of three independent experiments is indicated.

4.1.2 Inhibition of AAV transduction by SUMOylation depends on the time point of the knockdown

The previous work carried out by Katharina Henrich indicated that varying the time between knockdown and the next infection by 36h, 24h or 12h (all with Sae2 knockdown before transduction) still resulted in enhanced transduction rates, but all transductions at these three time points are lower than that of the 48h period between knockdown and AAV infection (data not shown). So, the

next challenge was whether knockdown even after AAV infection would still influence transduction efficiency. Cells were infected with AAV2-firefly reporter for 24 hours followed by Sae2 knockdown for 72 hours. At the same time this was compared to the standard protocol of knockdown before AAV infection, in which a Sae2 knockdown for 24h or 48h was accompanied by AAV infection and the luciferase assay was performed at 72h. The data shows no increase in AAV2 transduction efficiency when infection was done before siRNA knockdown (Figure 11a). The kinetics of Sae2 siRNA knockdown shows the amount of Sae2 protein decreased over time, and this was indicated by western blot and analyzed by ImageJ (Figure 11b).

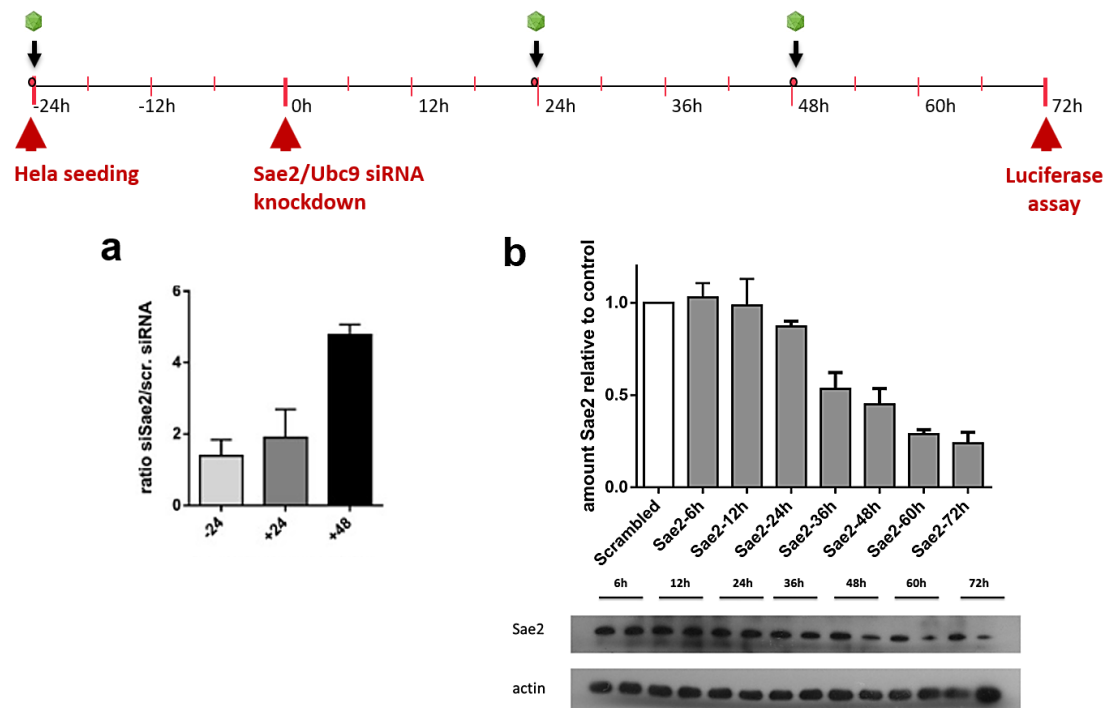


Figure 11 Influence of the time point of Sae2 knockdown on AAV transduction. (a) Sae2 knockdown after infection have no effect on transduction efficiency. HeLa cells were seeded into 24-well plate with 2.5×10^4 /well and transfected with Sae2 or Scr siRNA as described before. AAV2-firefly MOI=1000 was prepared and transduced before (-24h) or after siRNA transfection (+24h, +48h). (b) To test the kinetics of Sae2 knockdown, HeLa cell were transfected with 0.3ul Sae2 or scrambled siRNA and samples were washed with 1x PBS

before harvesting at different time points. Sae2 protein levels were determined by western blot, and time point experiment was quantified by ImageJ. All samples were quantified by Bradford and treated with 1x SDS loading buffer and boiled. The graph shows relative expression levels normalized for each time point to housekeeping gene alpha-actin and to Sae2 signals of cells transfected with scrambled siRNA.

4.1.3 SUMOylation affects transduction of single stranded and self-complementary AAV vectors

The previous experiments described above were performed with self-complementary (sc) AAV2 vectors carrying CMV-firefly reporter genes and resulted in around 5 to 7-fold increase in Sae2 or Ubc9 siRNA knockdown. These vectors deliver a vector genome into the cells that can anneal to a double strand (ds) DNA bypassing the requirement of second strand DNA synthesis. Given that wildtype AAV carries single stranded genomic DNA in nature, whether SUMOylation also affects single stranded (ss) AAV2 vectors was previously undetermined. ssAAV as well as scAAV encoding gaussia luciferase (ssAAV2-GL and scAAV2-GL) were used side by side in a transduction experiment (Figure 12). Similar results were obtained for Ubc9 or Sae2 knockdown, the data show that SUMOylation pathway could affect ssAAV and scAAV vectors.

4 Results

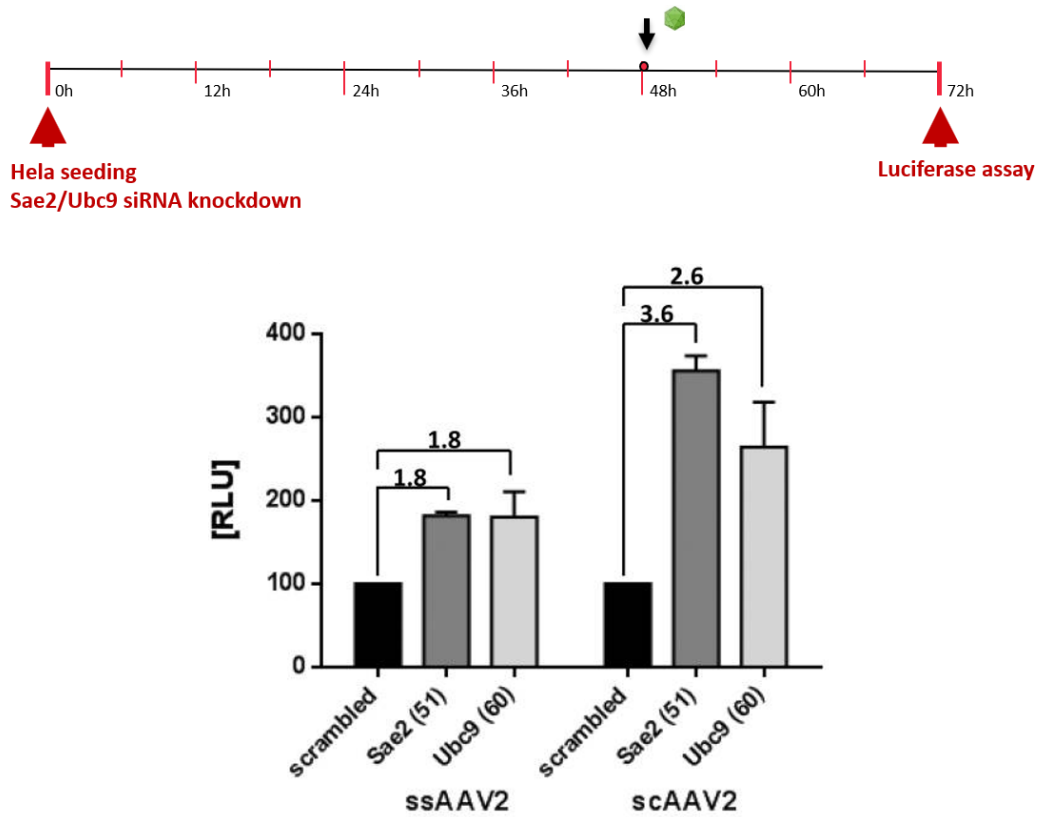


Figure 12 Sae2 or Ubc9 knockdown enhances transduction of ssAAV and scAAV vectors. HeLa cells were seeded into 24-well plate with 2.5×10^4 /well and transfected with 0.3ul siRNA targeting Sae2 or Ubc9 siRNA as well as scrambled siRNA, followed by ssAAV2 or scAAV2 infection with MOI=1000 and tested via the gaussia luciferase assay. The mean values and standard deviations of the RLU of three independent experiments were normalized for treatment with scrambled siRNA.

4.1.4 Total SUMOylation activity increases after AAV transduction

The previous work indicated knockdown of either the E1 or E2 enzymes of the SUMOylation pathway results in an increased transduction efficiency of AAV2. However, it is interest to know whether AAV infection would also affect total SUMOylation activity in the host cell. Domingues *et al.* determined the SUMOylation activity increased after influenza A virus (IAV) with the type A/WSN/33 infection in A549 cells (Domingues *et al.* 2015). Therefore, influenza

A virus was used to infect A549 cells as positive control to see whether AAV transduction enhanced SUMO activity in A549 cells, as well as HeLa cells, in a similar manner.

A549 and HeLa cell lines were infected/transduced by IAV with 5 PFU/cell or AAV2 with MOI=100000, and samples were harvested at 4h, 8h and 24h post-infection. The data shows that SUMO2/3 protein (including SUMO2/3 molecules and SUMO conjugates) increased over time after AAV transduction, which indicated the similar trend with SUMO level after IAV infection in A549 cell. At the same time, the data revealed SUMO2/3 protein levels in HeLa cells increased significantly over time after AAV2 infection as well (Figure 13).

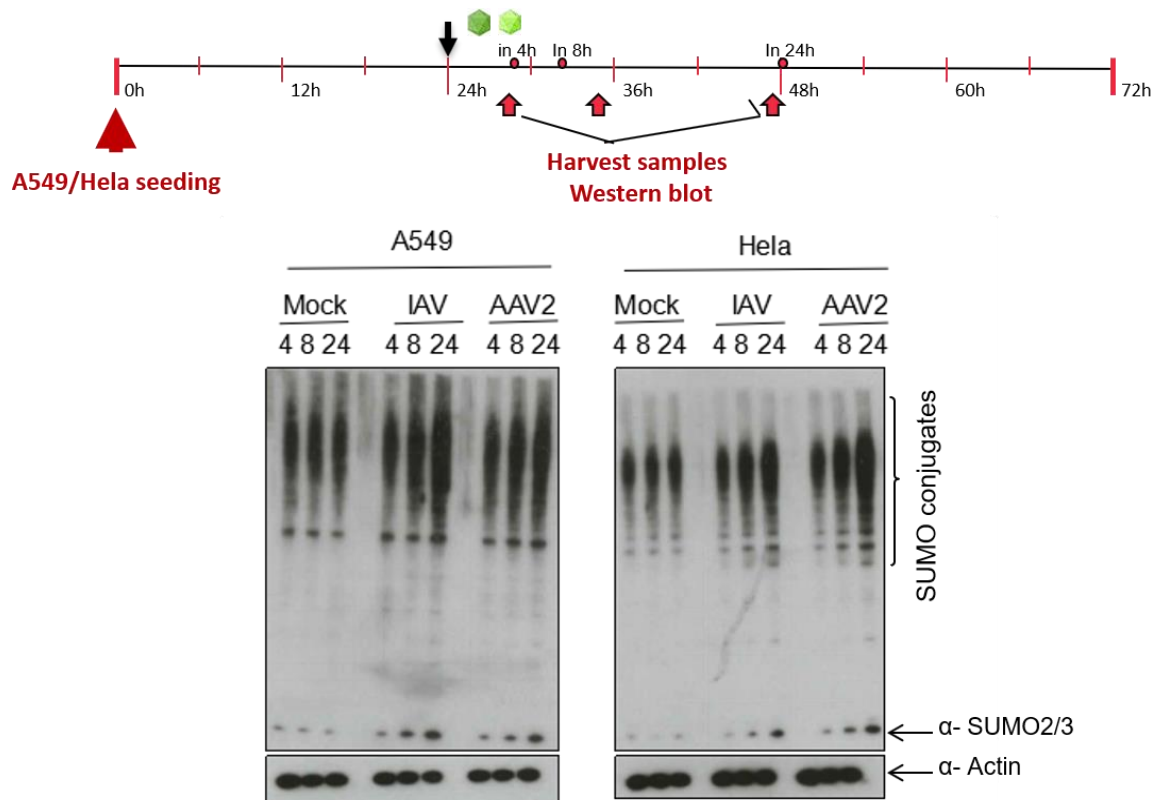


Figure 13 Total SUMOylation activity increases after AAV transduction. HeLa or A549 cells were seeded into 24-well plate at 1×10^5 /well and incubated with either mock (PBS), IAV with 5 PFU/cell, or AAV2 vectors at MOI=10000 for 1h at 4°C. After washing to remove the free virus, cells were transferred into 37°C and harvested after 4h, 8h, 24h incubation. All samples

were quantified by Bradford and harvested with 1x SDS loading buffer.

4.2 SUMOylation influences infection efficiency by affecting the AAV capsid

4.2.1 AAV2 particles can be SUMOylated

Previous work showed the knockdown of SUMOylation enzymes E1 or E2 siRNA could increase AAV transduction *in vitro*, but how the SUMOylation pathway influences AAV was unidentified. To determine the target of SUMOylation, the AAV capsid is hypothesized as the target of SUMOylation and I tried to find out whether SUMO proteins could conjugate the AAV particles capsid directly.

VP1 (87 kDa), VP2 (73 kDa) and VP3 (62 kDa) proteins assemble to form the AAV capsid. AAV particles production was performed by co-transfecting 3 plasmids into HEK293TT cells (AAV2 VP plasmid which encodes the capsid proteins, PDGΔVP helper gene which provides different helper functions to produce the particles, as well as the ITR- firefly-ITR reporter gene which allows a read out of AAV transduction) and purifying via iodixanol/PBS-MK gradient. The hypothesis is that during the AAV production in HEK293TT cells, the intact mature AAV2 particles are already modified with SUMOylation, means the purified AAV2 particles could be detected with SUMO directly.

When the purified AAV2 particles were probed with an anti-SUMO antibody, a band around 85kDa was detected (Figure 14a), and this can be reproduced with different batches of AAV2 preps (Figure 14b). To confirm this was a specific band and not a contaminating protein from the AAV production process, purified AAV particles were immune precipitated by different antibodies: The human papillomavirus-specific antibody K18L2 (as negative control), intact AAV2

particle capsid-specific antibody A20, and SUMO1 polyclonal antibody, and then tested by western blot. SUMO can be detected on purified AAV2 particles after A20 pull down, and in the other way around AAV capsid protein could be detected in a SUMO1 pull down. The presence of the SUMO-specific band only in the AAV lane and not with Human Papillomavirus 58 (HPV58) plus the lack of a SUMO band in the K18L2 pull down confirms the specificity of the SUMO protein conjugation to AAV particles (Figure 14c).

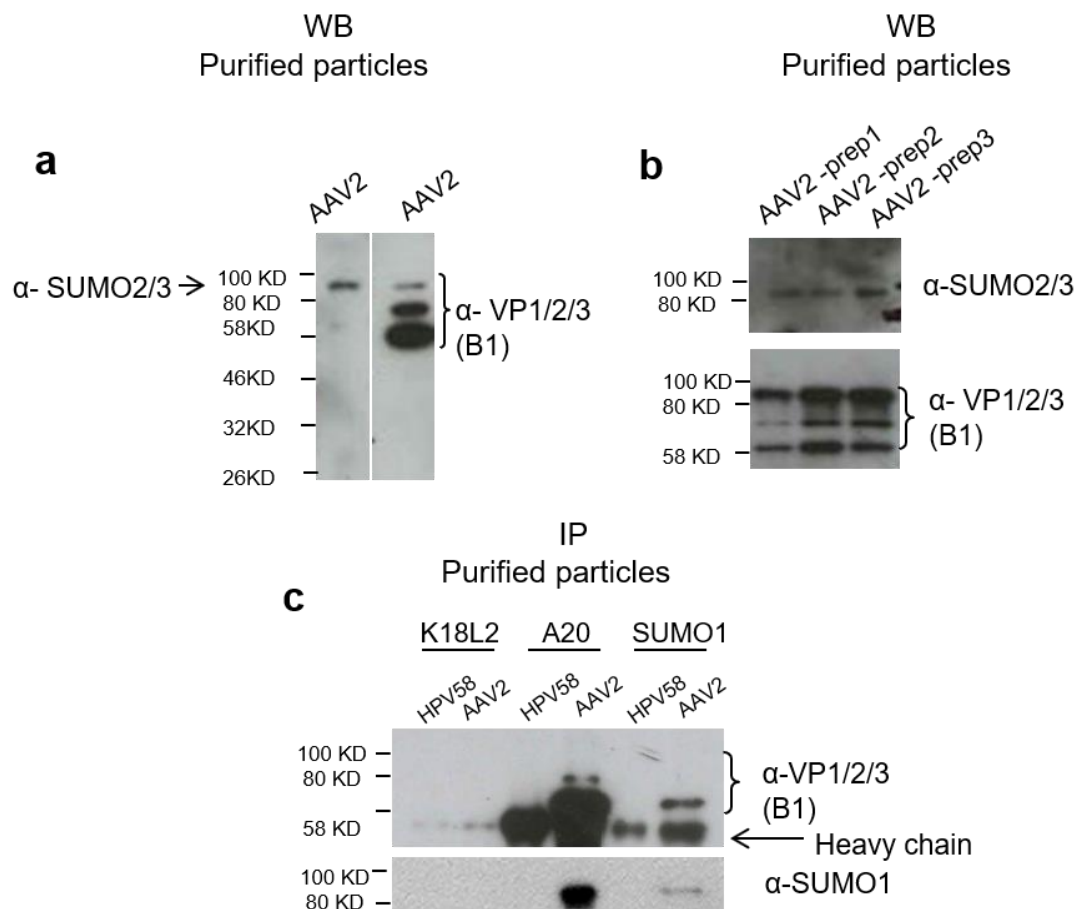


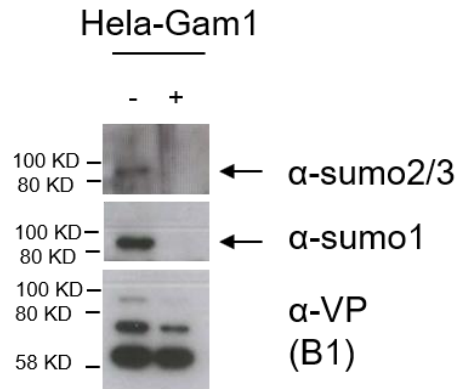
Figure 14 AAV2 purified particles SUMOylation specificity confirmation. (a) Purified AAV2 particles can be SUMOylated after the viral production process. AAV2 particles were harvested from transfected HEK293TT cells and purified by iodixanol gradient. These purified AAV particles were mixed with 3x SDS loading buffer and boiled, and 5×10^8 particles were loaded for western blot test. Primary antibody B1 was used to detect AAV2 capsid proteins

VP1, VP2, VP3, and α -SUMO2/3 antibody for SUMO detection. (b) VP conjugated SUMO was detected on different batches of purified AAV2 particles. Purified AAV2 particles were prepared as described before and western blot shows the VPs and SUMO detection. (c) After A20 antibody pull down, SUMO can be detected on purified AAV particles, meanwhile SUMO1 antibodies are able to pull down AAV2 particles. Samples were treated as described before (3.4.1).

4.2.2 AAV2 particles cannot be SUMOylated in a SUMO-inhibited cell line

Given the above result it appears that purified AAV2 particles were already SUMOylated during the virus production process. Therefore, whether the produced AAV2 from SUMO-impaired cell line could be SUMOylated or not needs to be challenged.

HeLa-Gam1 cell are an inducible HeLa cell line whereby the Gam1 protein (with Myc-tag) of the adenovirus CELO is expressed after 50ng/ml Doxycycline (Dox) induction. The Gam1 protein interferes with the activity of E1 enzyme (Sae1/Sae2) inhibiting the SUMOylation pathway, and thus it is utilized here to block the SUMOylation and produce AAV2 particles in this cell line to see whether the produced particles can be SUMOylated. The SUMO-specific band seen before in western blot when particles were produced in regular cells was no longer observed in virus produced from induced HeLa-Gam1 cells (Figure 15). The data provides further evidence that in normal cells AAV particles are SUMOylated.



- : no Dox induction in HeLa-Gam1 cell before transfection
 +: with Dox induction in HeLa-Gam1 cell before transfection

Figure 15 SUMO cannot be detected on purified AAV2 particles produced in Gam1 expressing (SUMO inhibited) cells. 5×10^6 HeLa-Gam1 cells were seeded in 5x 15cm dish and cultured until cells attached completely, followed by a 12h 50ng/ml Doxycycline incubation. The medium mixed with doxycycline was removed before 3-plasmid transfection to produce AAV particles and changing new fresh medium after transfection 4-5h. AAV2 particles were harvested in 48h and purified by iodixanol gradient. There were 5×10^8 particles loaded for western blot test. Primary antibody B1 was used to detect AAV2 capsid protein VP1 VP2 and VP3, and α -SUMO1 and α -SUMO2/3 were used for SUMO detection.

4.2.3 Empty AAV2 particles are SUMOylated to a higher extent in comparison to full AAV2 particles

During the AAV full particles production process there are still 10%- 20% empty AAV particles contained in the products (Benskey *et al.* 2016), which means the 'full AAV particles' production utilized 3-plasmids transfection are not the pure full AAV particles but contaminated with empty AAV. It was obtained that empty AAV2 particles might be more efficiently be SUMOylated than full particles (Figure 16a). To determine whether full AAV2 or empty AAV2 are SUMOylated, sucrose gradient sedimentation was used to separate the empty AAV particles

from the produced 'full AAV particle'. Thereafter AAV particles were detected by dot blot and western blot.

Full AAV particle is always heavier than empty AAV because of the DNA-containing. After sucrose gradient sedimentation, the purer full AAV particles gather in 110S area, and the contaminated empty AAV from production are more likely to stay in 60S (Figure 16b, upper layer). A total of 24 fractions (400ul/sample) were harvested from the sucrose gradient and detected by dot blot. The data shows all AAV particles appeared in the fractions in #4 ~ #13 (Figure 16b, upper layer). In order to determine where accurately the purer empty AAV particle was in the sucrose gradient, the complete empty AAV particles (without AAV reporter) were centrifuged in the sucrose gradient as a reference, and most of the empty particles were detected in the fractions in #9 ~ #12 in 60S area (Figure 16b, bottle layer). It confirms the purer AAV full particles are more inclined to appear in the fractions close to #4~#7 and empty particles are in #8~#13.

In order to know whether the empty AAV particles in fractions are indeed SUMOylated to a higher extent in comparison to full AAV2 particles, fractions #1~#15 were picked out and tested by western blot with anti-SUMO1 detection (fractions from #16 ~ #24 were indicated had no AAV particles exist). Fractions #10, #11, #12 showed the obvious SUMO signals stronger than others (Figure 16c). In the meanwhile, firefly luciferase assay indicates the fractions #10, #11, #12 which had weak infectivity were the empty AAV (Figure 16d). These data indicated the empty AAV particles SUMOylation are more extensively than full particles.

4 Results

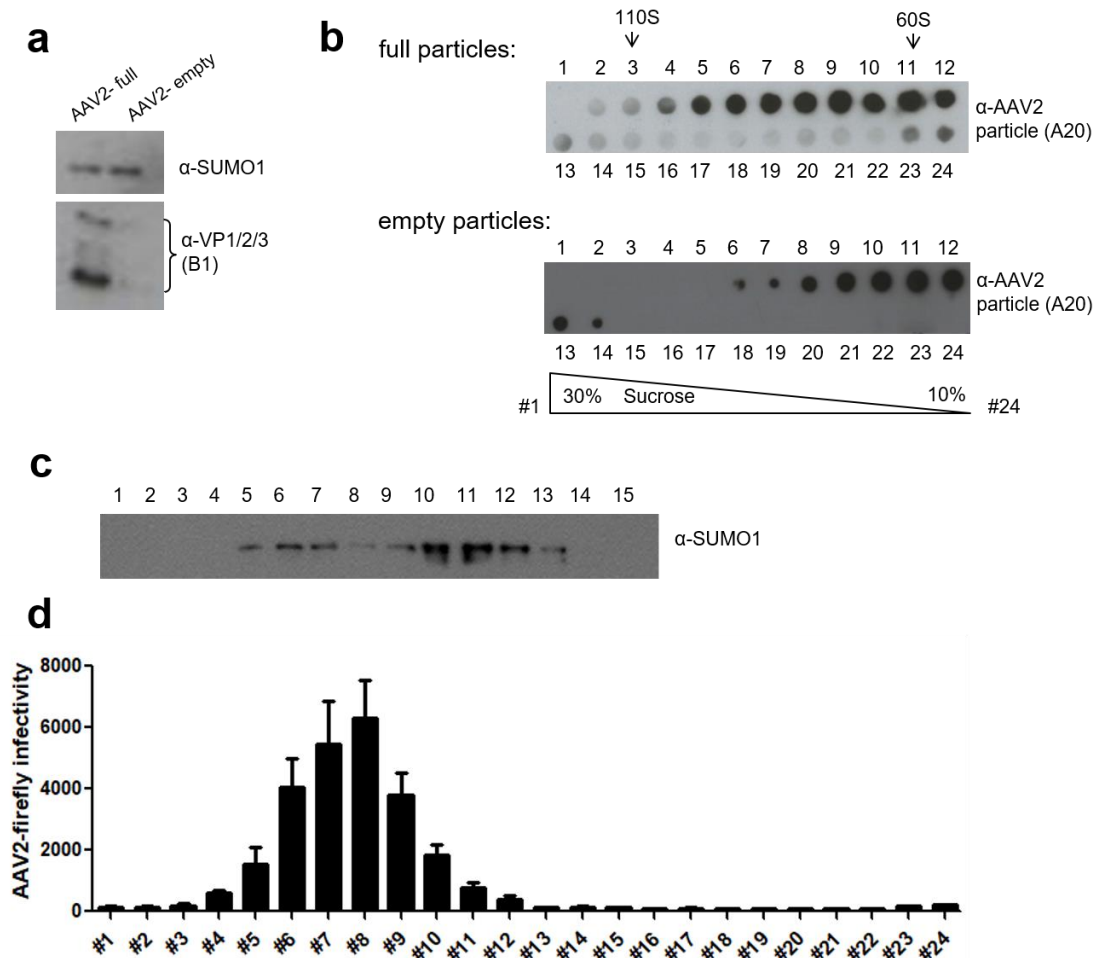


Figure 16 Empty AAV2 particles are SUMOylated more than full (DNA-containing) AAV2 particles. (a) Empty AAV2 particle shows higher extent to be SUMOylated than full particles. There were 5×10^8 AAV particles purified from iodixanol mixed with loading buffer for western blot test. B1 and α -SUMO1 antibody were used for AAV2 capsid and SUMO1 protein detection, respectively. (b) The confirmation of full particles and empty particles in sucrose gradient fractions. Dot blot assay confirmed the full particles were in the fractions #4~#7 and empty AAV2 particles in #8~#13. Primary antibody A20 was used for intact AAV2 particles detection. (c) A stronger SUMO modification was shown in the purer empty AAV particles than the purer full AAV particles. Full AAV2 fractions, especially for #10, #11 or #12 which were indicated as empty AAV particles, shown the stronger SUMO detection. Fractions #1 to #15 were loaded on SDS gel for western blot and B1 antibody was used for AAV2 capsid protein detection (d) The AAV transduction of each fractions. HeLa cells were seeded in 24-well plate and infected with

each fraction for firefly luciferase assay. Standard deviation of three independent experiments mean is indicated.

4.2.4 K142/143 and/or K169 residues play a role in AAV particles SUMOylation

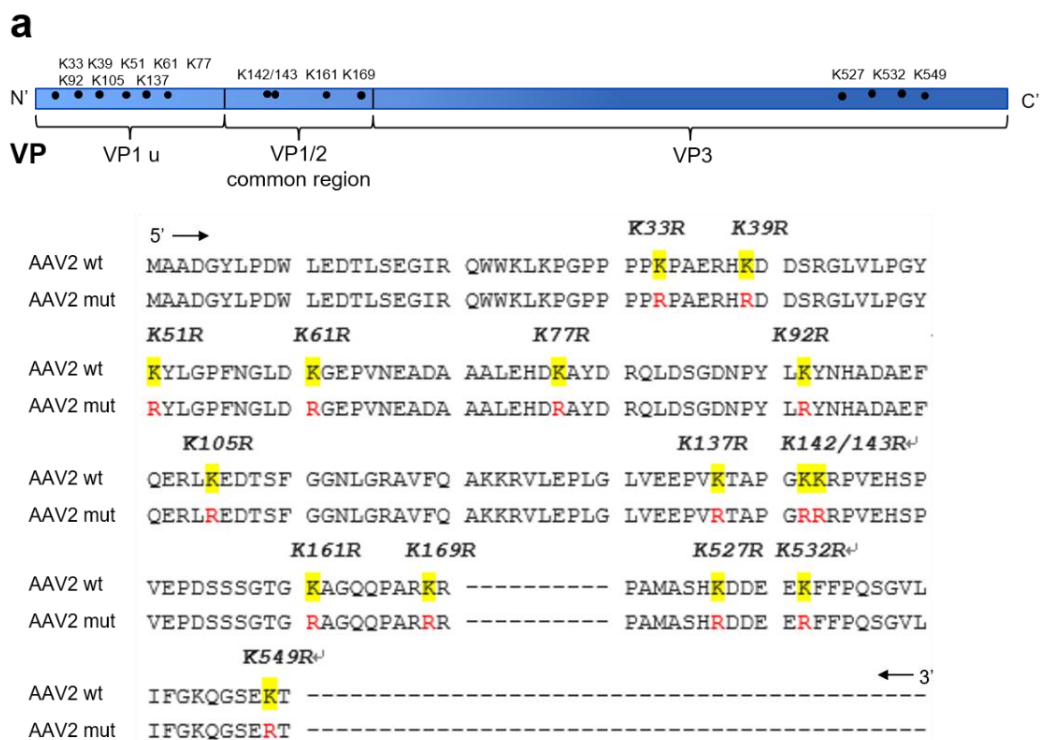
As is known that amino acid lysines (K) is the target of SUMOylation. There are 34 lysines in AAV2 VP1 and the prediction is that one/some of them might be SUMOylated: The comparison of amino acid sequence in serotype AAV1, 2, 3, 6, 7, 8, 9, 10 and 13 prompts the possibility of the potential lysine (K527) at C-terminus of VP could be the candidate, and the modified AAV2 at K532 and K549 aa exchange were published because of the enhanced/reduced transduction efficiency compared with AAV2 wt *in vitro*; In addition, some lysines in N-terminal of AAV particles VP1/2 are also considered as candidates of SUMOylation targets. Base on the above information, the lysine (K) on AAV capsid protein was exchanged to Arginine (R) to avoid SUMOylation, followed by the modified AAV2 production: in VP1 unique protein sequence (VP1u) - K33R, K39R, K51R, K61R, K77R, K92R, K105R, K137R; in VP1/2 common region - K142+143R, K161R, K169R; and in VP C-terminal - K527R, K532R, K549R (Figure 17a). If any of lysines were the targets, SUMO proteins would not conjugate on AAV VP after amino acid exchange, and thus no SUMO could be detected after probing the modified AAV2 capsids with anti-SUMO antibody.

The data shows that SUMO can still be detected on the modified AAV2 with VP1 unique sequence mutation (K33R, K39R, K51R, K61R, K77R, K92R, K105R and K137R) as well as the modified AAV2 with C-terminal mutation (K527R, K532R, K549R) (Figure 17b), but the AAV2 bearing the K142/143R and K169R exchanges were unable to be SUMOylated (Figure 17b, sample 9, 11), and the weak SUMO detection of AAV2-K161R was observed. Noticeably, K142/143, K161 and K169 are all in the VP1/2 common region. This data

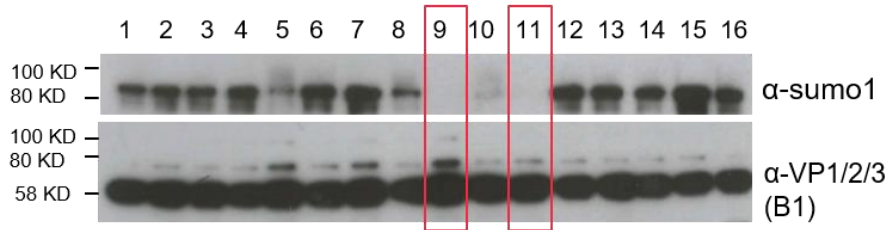
alludes that the AAV capsid VP amino acid K142/143, K169 might be SUMOylation targets.

If K142, K143, K169 of VP are the targets of SUMOylation then the enhancing effect of modified AAV particles would be lost after SUMOylation impairment. Therefore, modified AAV2s transduction were measured and it was expected that AAV2-K142/143R and AAV2-K169R transduction have no enhancing affect upon knockdown of Sae2 or Ubc9.

Luciferase assay exhibited the infectivity of modified and wt AAV2 (Figure 17c) and the enhancing effect of Sae2 knockdown was partially reduced (from ~15-fold increasing to ~5-fold increasing) compared with wt AAV2 (Figure 17d). However, the enhancing effect was nearly completely disappeared after Ubc9 knockdown in AAV2-K142/143R and AAV2-K169R transduction (from ~6-fold increasing to ~1.7-fold increasing) (Figure 17e). These data demonstrated that K142/143 and K169 residues play a role in AAV particles SUMOylation, particularly when the SUMOylation pathway impaired via Ubc9 knockdown.



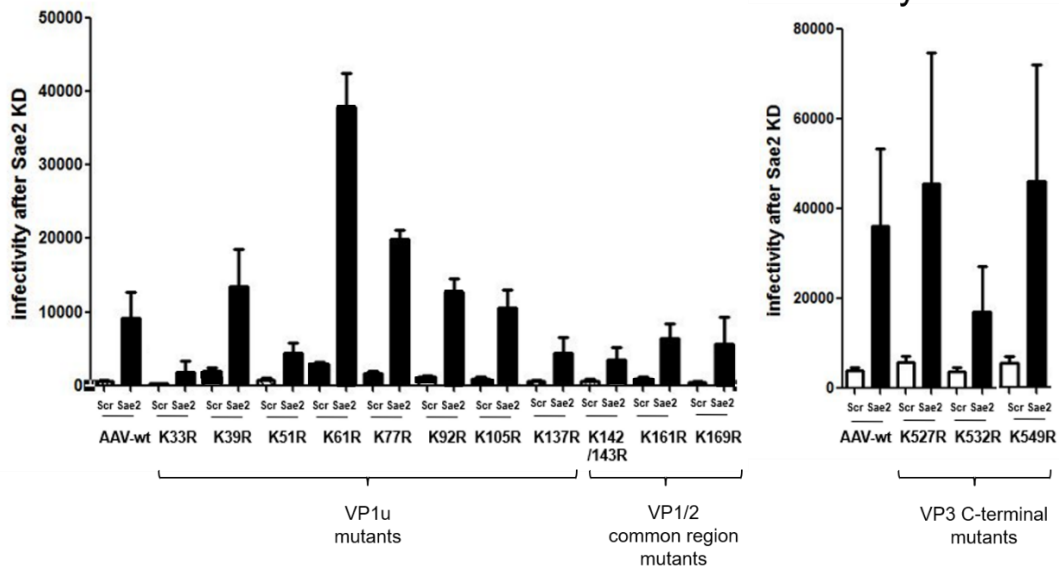
b



- | | |
|----------------|--------------------|
| 1. AAV2- K33R | 9. AAV2- K142/143R |
| 2. AAV2- K39R | 10. AAV2- K161R |
| 3. AAV2- K51R | 11. AAV2- K169R |
| 4. AAV2- K61R | 12. AAV2- K527R |
| 5. AAV2- K77R | 13. AAV2- K532R |
| 6. AAV2- K92R | 14. AAV2- K549R |
| 7. AAV2- K105R | 15. AAV2- empty |
| 8. AAV2- K137R | 16. AAV2- wt |

c

Absolute value of AAV2 mutants infectivity



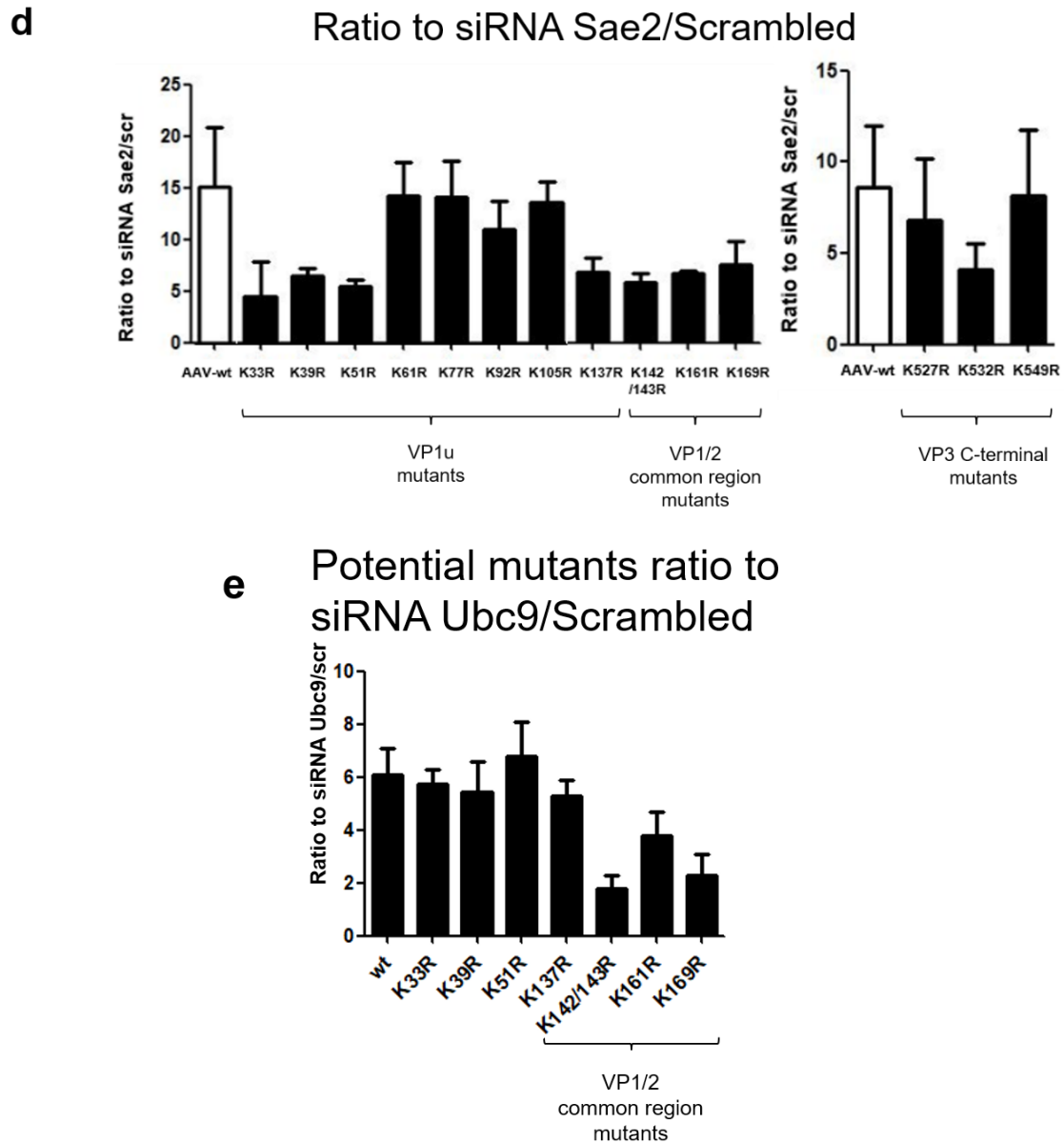


Figure 17 SUMO detection of wt and modified AAV2 indicate K142/143 and K169 are not SUMOylated, and their transduction efficiency is not greatly affected by SUMO knockdown. (a) Schematic illustration of the AAV2 mutants used in the experiments. K (yellow) is the wild type amino acid and R (red) is the exchanged amino acid. (b) SUMO was detected by western blot from AAV2 wt particles as well as most modified AAV2 except AAV2-K142/143R and AAV2-K169R. Purified wt or modified AAV2 particles were prepared for western blot. Primary antibody B1 and SUMO1 were used to detect AAV2 capsid SUMO protein, respectively. (c) The Infectivity of wt and modified AAV2 after the impairment of

SUMOylation via Sae2 or Ubc9 knockdown. (d) The relative ratio of Sae2/scr shows that modified AAV2 at K33R, K39R, K51R, K137R, K142/143R, K161R, K169R partially reduce the enhancing effect after Sae2 knockdown compared with AAV2 wt. (e) The enhancing effect of modified AAV2 K142/143R and K169R nearly completely disappeared after Ubc9 knockdown, and the relative ratio decreased to 1.7 and 2, respectively. Standard deviation of the mean of three independent experiments is indicated.

4.2.5 AAV2 capsid protein VP2 is SUMOylated but not VP1

The data indicated that the K142/143 and K169 of VP which could be targets of SUMO are located within the VP1/2 common region. So, the next question is whether either VP1 or VP2, or both are SUMOylated in the common region. AAV particles encoding the firefly luciferase reporter gene were produced with VP1+VP3 (no VP2), VP2+VP3 (no VP1) as well as wt capsid protein. The data showed SUMO cannot be detected on AAV2 VP1+VP3 (no VP2) particles but it still can be detected on AAV2- VP2+VP3 (no VP1) particles (Figure 18a). As expected, luciferase assay data indicated AAV2- VP2+VP3 (no VP1) had no infectivity. Although AAV2 wt and AAV2- VP1+VP3 (no VP2) showed similar transduction activity, but the enhancing effect of Ubc9 knockdown was reduced a lot compared with AAV2 wt (Figure 18b).

VP1 plays a very important role in AAV trafficking. The AAV2 particles with VP1 unique region (VP1u) deletion have no infectivity due to the absence of the complete phospholipase A2 (PLA2) domain. It was identified that modified AAV2 particles at PLA2 domain (76,77HD/AN) are defective for trafficking in a step following perinuclear accumulation (Girod *et al.* 2002). So, because of losing VP1, AAV2- VP2+VP3 (no VP1) particles cannot deliver their vector genome into the nucleus (Figure 18b, left).

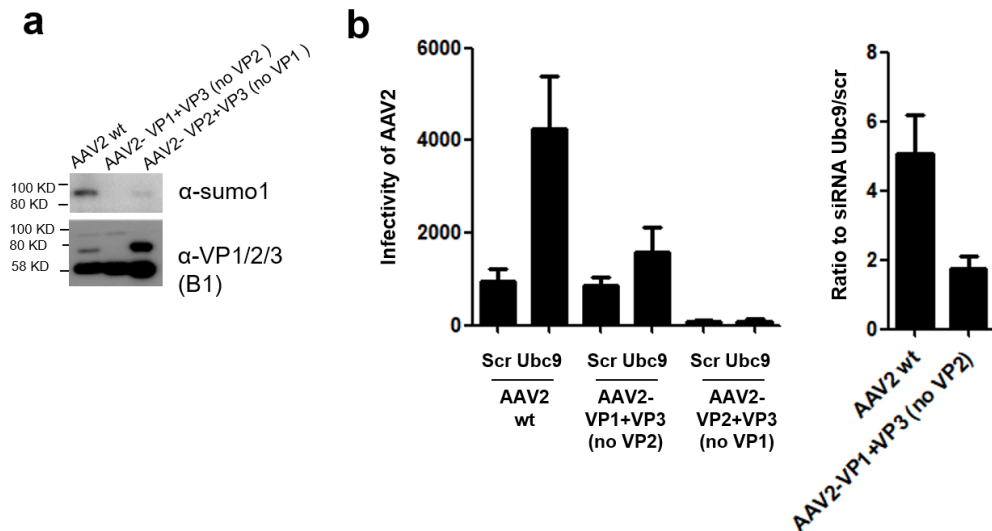


Figure 18 SUMO cannot be detected on AAV2- VP1+VP3 particles lacking VP2. (a) AAV2 particles lacking VP2 are not SUMOylated but AAV2 wt and AAV-VP1 deletion-particles are. Wildtype or VP2-lacking AAV2 particles were prepared and loaded for western blot test. B1 and SUMO1 antibody were used for AAV2 capsid protein SUMO detection, respectively. (b) AAV2 wt and AAV2- VP1+VP3 (no VP2) particles infectivity without siRNA treatment were similar, but the enhancing effect of AAV2- VP1+VP3 (no VP2) reduced a lot in Ubc9 knockdown albeit slightly elevated. HeLa cells were transfected with the siRNA targeting Ubc9, and then transduced by wt AAV2 or VP2-lacking AAV2 at MOI=1000 in next 24h. Firefly luciferase assay was intended for AAV infection test.

4.2.6 AAV2 capsid protein SUMOylation related to the VP2 spatial structure

AAV is an icosahedral virus and it was proposed that the N-termini of VP1 and VP2 were hidden inside the particle. The SUMOylation candidates K142, K143 or K169 are located within this part of the capsid. So, the hypothesis is that the AAV particles can be SUMOylated due to the spatial structure of VP2 capsid protein. Based on this assumption AAV2 particles is produced comprising VP1 and VP3, and either GFP-VP2 or HA-VP2: particle 'AAV2- VP1/GFP-VP2/VP3' and particle 'AAV2- VP1/HA-VP2/VP3'. GFP or HA tags were conjugated

N-terminally to VP2 capsid protein. Western blot data showed 'AAV2-VP1/GFP-VP2/VP3' and 'AAV2-VP1/HA-VP2/VP3' particles containing extended VP2 with either GFP or HA tag are not SUMOylated (Figure 19a). Luciferase assay also shows 'AAV2-VP1/GFP-VP2/VP3' and 'AAV2-VP1/HA-VP2/VP3' had similar transduction efficiency compared to AAV2 wt. However, the enhancing effect of Ubc9 knockdown was reduced significantly if compared with AAV2 wt. (Figure 19b). This experiment was only performed once.

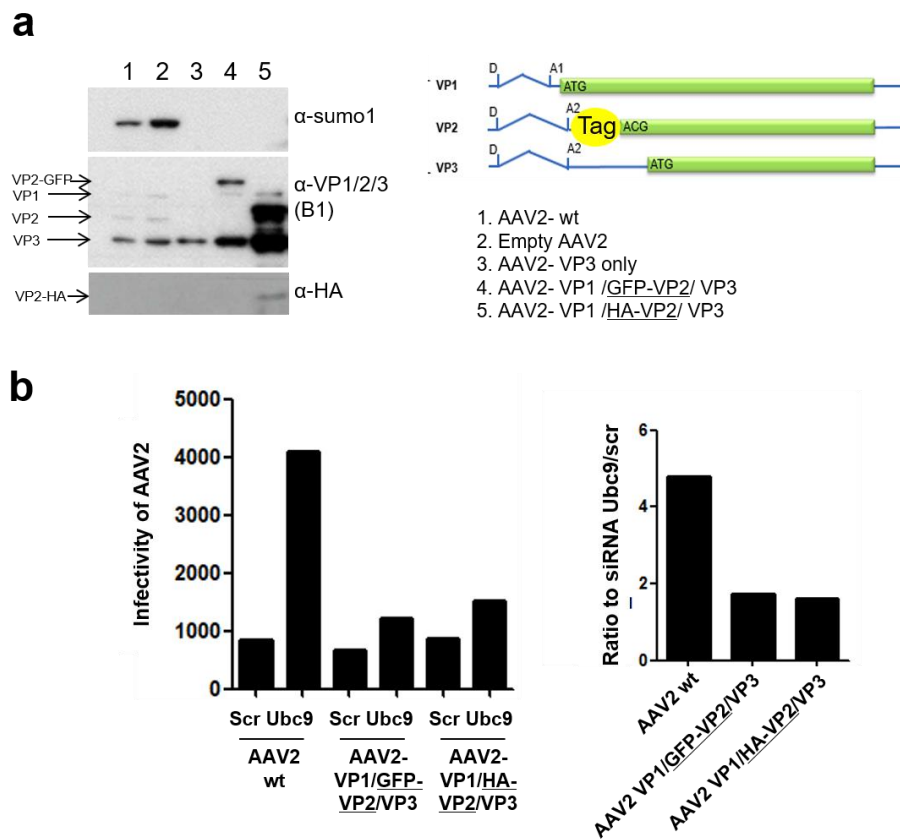


Figure 19 AAV2- VP1/GFP-VP2/VP3 and AAV2- VP1/HA-VP2/VP3 capsids are not SUMOylated. (a) 'AAV2- VP1/GFP-VP2/VP3' and 'AAV2- VP1/HA-VP2/VP3' particles are not SUMOylated. Wildtype AAV2, empty AAV2 and AAV2-VP3 only particles were purified and prepared for western blot. Anti- HA antibody was used for the HA-VP2 detection and B1 was used to detect AAV2 capsid protein VP1, VP2 and VP3, and α -SUMO1 was used for SUMO

detection. (b) AAV2 wt, 'AAV2- VP1/GFP-VP2/VP3' and 'AAV2- VP1/HA-VP2/VP3' particles infectivity without siRNA treatment were similar, but the enhancing effect of 'AAV2- VP1/GFP-VP2/VP3' and 'AAV2- VP1/HA-VP2/VP3' particles reduced a lot in Ubc9 knockdown albeit slightly elevated. HeLa cells were transfected with Ubc9 siRNA, and then transduced by AAV2 wt, 'AAV2- VP1/GFP-VP2/VP3' and 'AAV2- VP1/HA-VP2/VP3' at MOI=1000 for the next 24h. Firefly luciferase assay was performed to determine transduction efficiency.

4.3 The effect of SUMOylation pathway on AAV trafficking *in vitro*

4.3.1 AAV transduction after SUMOylation knockdown is not due to increased binding or uptake

In general, the AAV transduction process includes cell binding and uptake, endocytosis, post-endocytic trafficking, endosomal escape, nuclear translocation and single stranded DNA conversion, but the exact step of the AAV transduction process that is affected by the SUMOylation pathway is still unknown.

Therefore, whether AAV2 binding and uptake could be the rate limiting step affected by SUMOylation is the first question to be answered. To quantify the amount of AAV2 particles binding and entering, HeLa cells, which were transfected with Scr or Sae2 siRNA as described before, were incubated with AAV vectors for 1h at 4°C. After washing cells, free AAV2 were removed and AAV bound on the cell surface would be either harvested directly (1h) or harvested after incubation (5h) at 37°C. AAV2 genome was then quantified by qPCR and the luciferase assay shows the Sae2 knockdown effect on AAV transduction was increased over Scr siRNA as before (3.5.6.1).

Since no increase was observed in the number of transduced cells upon

SUMOylation knockdown either in 1h which is AAV2 binding step (Figure 20, 1h) or in 5h uptake step (Figure 20, 5h), using different harvesting methods (cell scraper, or trypsin/proteinase K treatment) direct to the same experimental results. A regular luciferase assay was performed in 24h post-infection in order to ensure the impairment of SUMOylation via Sae2 siRNA knockdown (Figure 10b). The data showed SUMOylation would not restrict early events of cell entry of AAV.

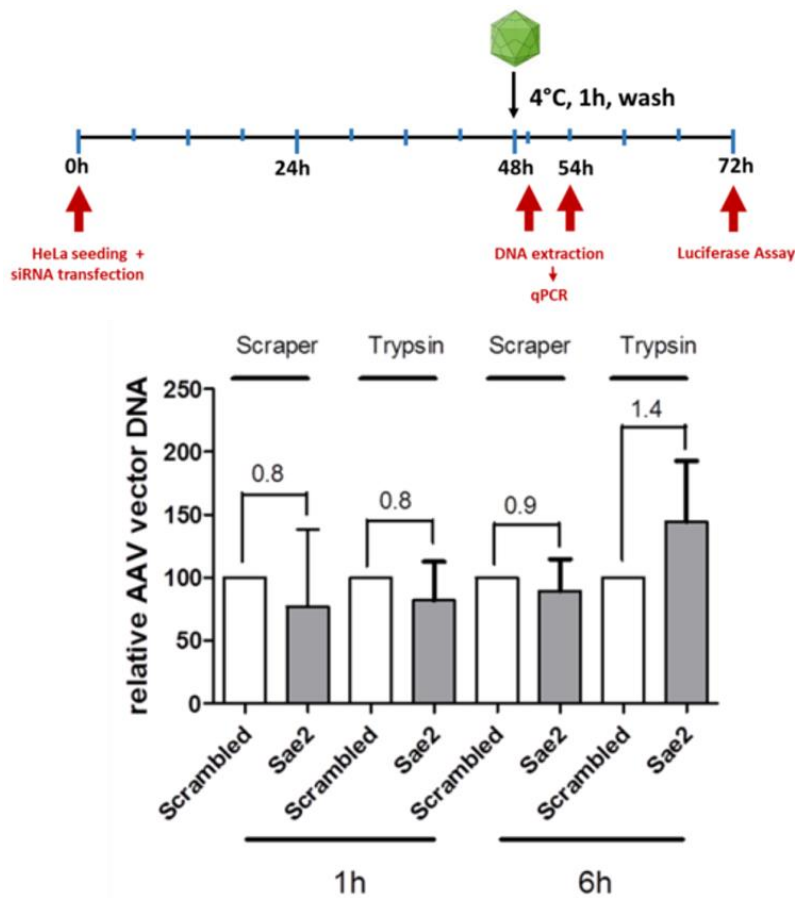


Figure 20 Enhanced AAV transduction by inhibition of SUMOylation is not due to increased binding or uptake of capsids. HeLa cells were transfected with scr or Sae2 siRNAs for 48h and then incubated with AAV vectors at MOI=10000 for 1h at 4°C. After washing, cells were harvested directly (1h) or incubated for 5h. Cells were harvested by scraping or treatment with trypsin and proteinase K. AAV vector genomes were quantified by qPCR. The graph shows the mean of two independent experiments with triplicates each. The

AAV vector DNA was quantified by qPCR and normalized to the corresponding siRNA control (scrambled).

4.3.2 Inhibition of SUMOylation does not affect the AAV2 vector DNA distribution in cell membrane, cytoplasm or nucleus

Next, whether the AAV2 particles are affected by SUMOylation in different cellular components needs to be challenged, e.g. cell membrane, cytoplasm or nucleus. HeLa cells were transfected with Scr or Sae2 siRNA as described before and then incubated with AAV vectors for 1h at 4°C (to ensure consistent binding of AAV on the membrane) and then the free AAV particles were washed afterwards. The infected cells were incubated for another 12h to ensure that the virus can be distributed in various parts of cellular components, and then different cellular fractions (speed 1000g for cytosolic fraction, 6000g for membrane fraction, 6800g for nuclear fraction) were harvested using subcellular fractionation technique and quantify AAV vector DNA by qPCR (3.5.6.2). Luciferase assay was performed as well to show the AAV transduction increase indeed after Sae2 knockdown as before (Figure 10b).

The qPCR data showed Sae2 knockdown did not affect AAV2 vector DNA distribution in the membrane, cytoplasm or nucleus fractions, which are still 10%, 50% and 40%, respectively (Figure 21).

Remarkably about AAV2 in nucleus. Although there is no detectable effect of AAV2 vector DNA in the nucleus after the Sae2 knockdown, it is still unknown whether there are any other changes to the intact AAV particles in the nucleus. To be specific, the virus particles are uncoated in the nucleus accompanied by the DNA release. The nucleus was harvested by subcellular fractionation and the DNA amount detected by qPCR, but it is not clear how many AAV particles are uncoated in the nucleus and whether released ssDNA was regulated via

SUMOylation impairment. Therefore, although qPCR data suggests no effect of AAV2 vector DNA in nucleus, the possibility of AAV2 particles (capsid in particular) affected by Sae2 knockdown is still existed.

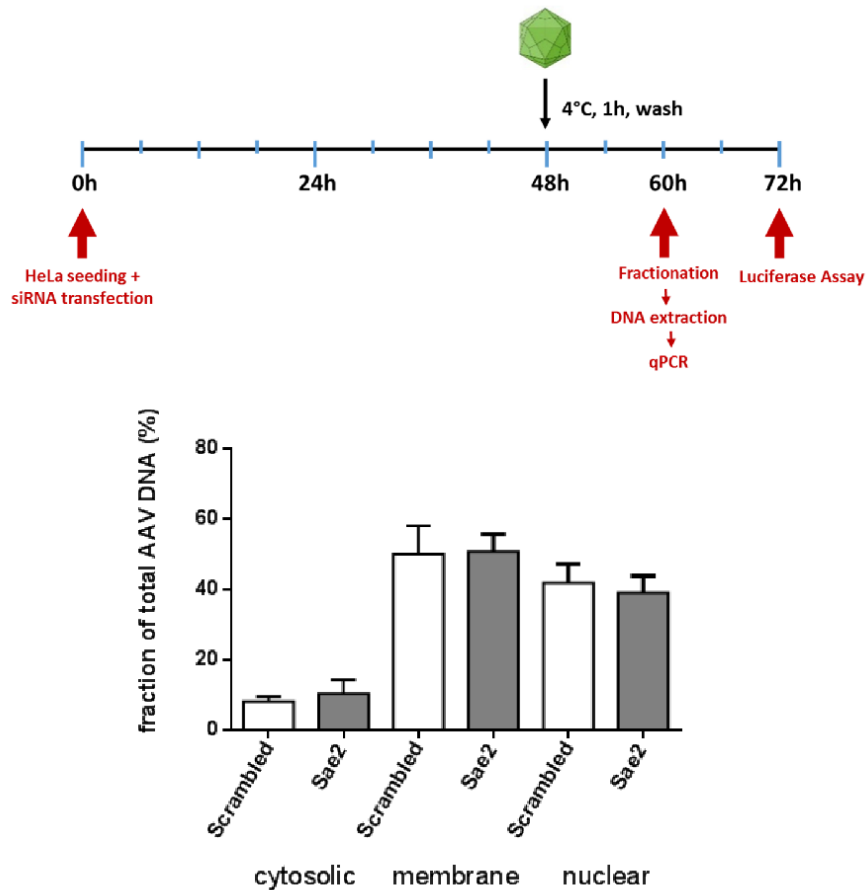


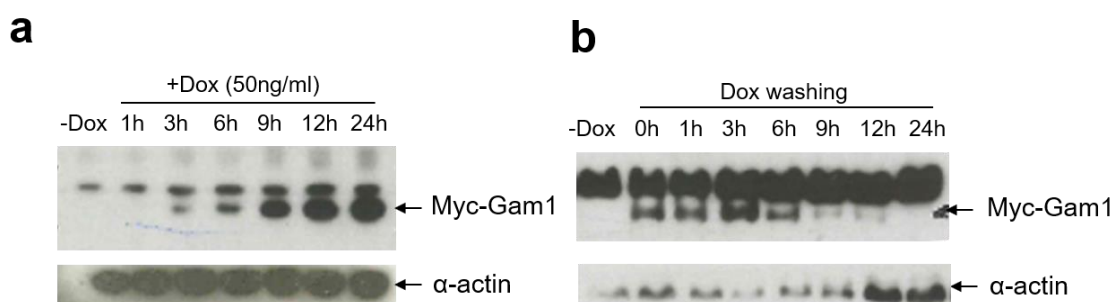
Figure 21 Inhibition of SUMOylation does not lead to gross changes in subcellular localization of AAV vectors. HeLa cells were seeded in 6cm dishes and transfected with Sae2 or scr siRNAs for 48 h and then incubated with AAV2 vectors at MOI=10000 for 1h at 4°C. After washing, cells were incubated for 12 h followed by washing steps. Cells were harvested by trypsin and extract cytosol, membrane, and nuclear compartments according to manufacturer's protocol. AAV2 genomes were quantified by qPCR. The graph shows the fraction of AAV2 DNA found in the three subcellular fractions cytosol, membrane, and nuclear.

4.3.3 SUMOylation inhibition can enhance AAV accumulation in the nucleus

Since I observed the AAV binding and uptake were not the rate limiting steps of AAV entry affected by SUMOylation, and the amount of AAV genomes DNA in cytoplasmic and membrane fractions are not altered upon SUMOylation knockdown, the nucleus is hypothesis as the important place for AAV2 SUMO modification.

HeLa-Gam1 cell was used as the stable cell line which could inhibit endogenous Sae1/Sae2 protein after Doxycycline (Dox) induction. The data showed that after Dox (50ng/ml) induction, Gam1 protein starts to be expressed and could be detected as early as 3h (Figure 22a) after induction reaching the maximum after 12 hours. When doxycycline was removed by washing Gam1 expression was undetectable after 24h (Figure 22b).

About the AAV transduction in HeLa-Gam1 cells. HeLa-Gam1 cells were induced with doxycycline overnight (12h) which was then removed from the cells. This cell line was kindly supported from Susanna Chiocca. After AAV2 incubation for 1h at 4°C, the cells were washed and transferred to 37°C. Cells lysate were harvested after 1h, 3h, 6h, 9h, 12h and 24h for firefly luciferase assay. The data showed luciferase could be tested after 6h infection, and the enhancing effect of Gam1 inhibition increases with longer AAV transduction (Figure 22c).



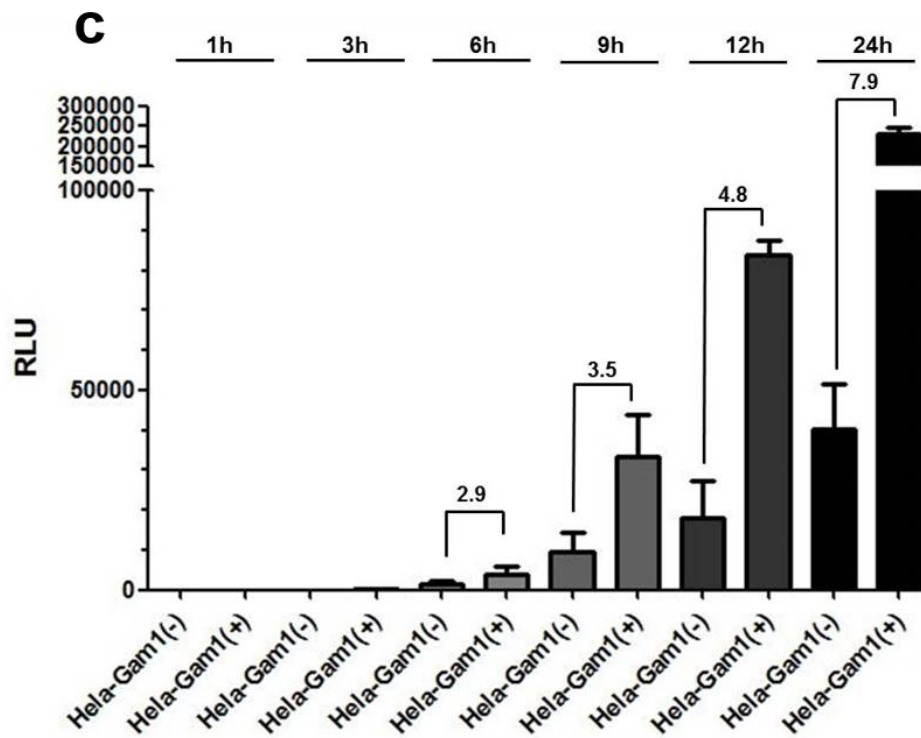


Figure 22 Detection of Gam1 expression in HeLa-Gam1 cells which increases AAV transduction. (a) HeLa-Gam1 cells were induced with final concentration 50ng/ml of Dox, harvesting cell lysate with 1x SDS buffer after induction 1h, 3h, 6h, 9h, 12h and 24h to test the Gam1 protein level against α -Myc antibody. (b) HeLa-Gam1 cells were induced with Dox 50ng/ml for 12h, after removing dox the cells were harvested in 1h, 3h, 6h, 9h, 12h and 24h. All samples for western blot were treated with 1x SDS loading buffer. (c) HeLa-Gam1 cells with/without 50ng/ml Dox induction overnight (12h) were infected with AAV2 and firefly luciferase assay was tested after 1h, 3h, 6h, 9h, 12h and 24h of transduction. Shown are the mean values and standard deviations of the RLU of three independent experiments normalized for treatment with scramble siRNA.

Next, HeLa-Gam1 cells were used to analyze intracellular translocation of AAV2 particles. The cells were treated as described before and collected 3h, 6h, 12h and 24h after AAV2 infection for immunofluorescence (3.4.2), followed by intact AAV2 particle antibody A20 detection. The data shows that after Dox

induction, the more expression of Gam1 leads to an accumulation of intact AAV particles into the nucleus over time when compared to the non-induced HeLa-Gam1 cell (Figure 23).

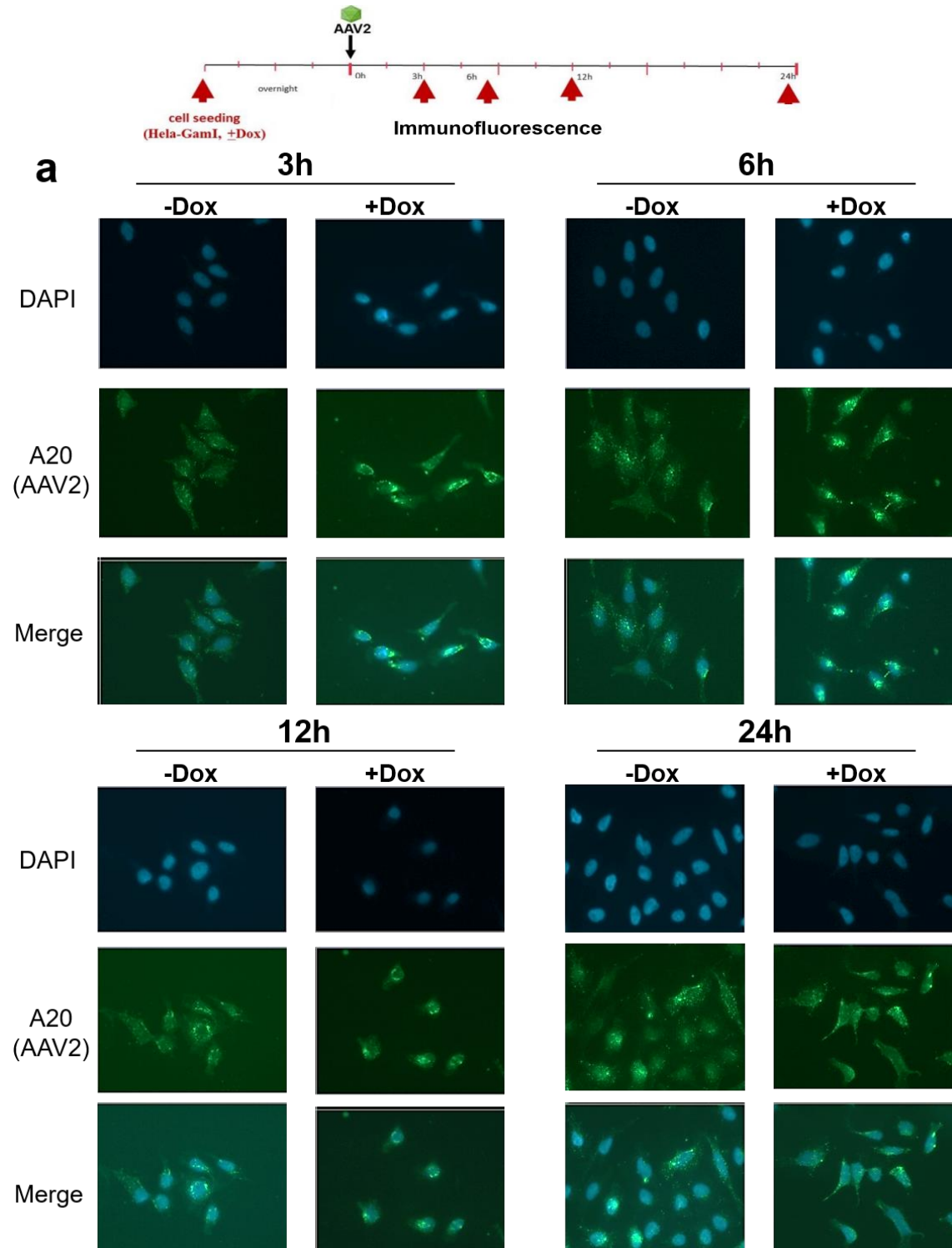


Figure 23 SUMOylation inhibition by Gam1 expression can direct more AAV particle

accumulation in the nucleus. HeLa-Gam1 cells were seeded into 24-well plate with 1×10^5 /well with cover slips and induced with 50ng/ml doxycycline overnight (12h). After changing the Dox-medium, cells were then incubated with AAV vectors at MOI=100,000 for 1h at 4°C, followed by 3 times washing to clear away the free AAV particles. Cover slips were collected after 3h, 6h, 12h and 24h AAV incubation in 37°C. AAV particles were labeled by primary antibody A20 and Alexa 488-conjugated secondary antibodies. DAPI was used as a nuclear staining. An average of 100 cells transfected with AAV and each construct were counted and classified into the patterns described.

4.4 SUMOylation is linked to other existing host cell restriction factors that affect AAV transduction

4.4.1 AAV transduction increased in a Daxx knock out cell line

During the AAV2 trafficking process, the previous data indicated that AAV particles binding or uptake were not affected by SUMOylation (Figure 20), and the amount of AAV vector genomes in cytosolic fraction shows no affect by SUMOylation either (Figure 21, cytosolic). Intriguingly, although the AAV vector DNA in the nucleus did not show the difference (Figure 21, nuclear), immunofluorescence data indicated more intact AAV particles accumulated in the nucleus after SUMOylation knockdown, which prompted us that SUMOylation pathway restricts AAV transduction may occurred in the nucleus, and some of the nuclear factors may play an important role towards this.

As a multifunctional nuclear protein, death domain-associated protein (Daxx) regulates a wide range of biological processes, including cell apoptosis and gene transcription. Daxx could be modulated by SUMOylation for its subcellular localization, and it associated with heterochromatin and promyelocytic leukemia nuclear bodies (PML-NBs). In addition, the SUMOylated PML by

either SUMO1 or SUMO2/3 could redistribute the localization of Daxx protein in the PML-NBs, and Daxx protein can be SUMOylated as well (Lin *et al.* 2006). Moreover, the previous high throughput siRNA screen lists the Daxx protein with a high z-score 5.39, which indicates the possibility of AAV transduction regulation.

Based on this assumption, the HeLa-Daxx knock out cell line was performed with CRISPR/CAS9 system to study AAV transduction and verify whether SUMOylation pathway related to Daxx or Daxx-associated proteins to regulate viral infection.

HeLa-Daxx knockout cell line was produced by Robin Njenga and two colonies were picked up successfully (HeLa-Daxx knockout cell line 04B and 06B) after Daxx knockout specificity confirmation (Figure 24a). Firefly luciferase assay shows the AAV2 transduction in HeLa-Daxx knockout cells compared to wild type HeLa cells, 5-fold elevated AAV transduction was observed in both cell lines, which indicates that Daxx protein is one of the restriction factors that affect AAV transduction *in vitro* (Figure 24b).

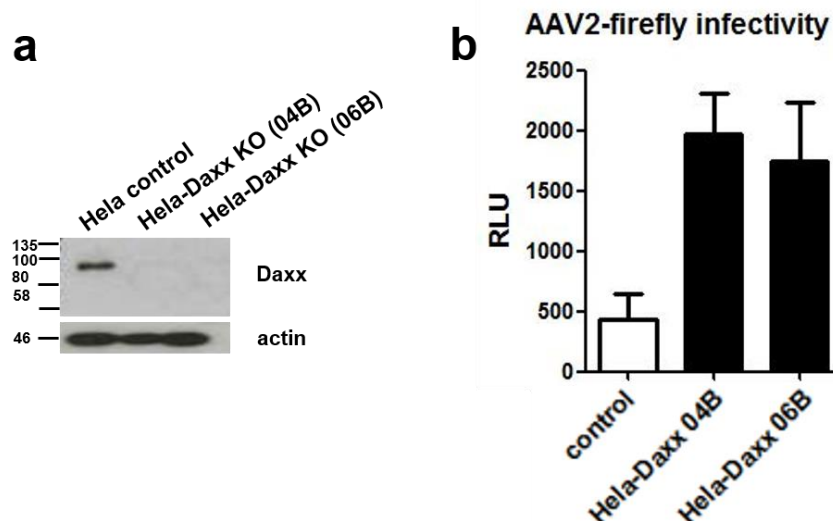


Figure 24 AAV2 infectivity enhanced in HeLa-Daxx knockout cell. (a) HeLa control and

HeLa-Daxx knockout cells 04B and 06B were seeded into 24-well plate with 1×10^5 /well overnight and then harvested and tested for protein amount, (b) or continually transduced by AAV2-CMV-firefly at MOI=1000 in next 24h. All samples for western blot were treated with 1x SDS loading buffer and boiled at 95°C for 10mins. Firefly Luciferase Assay was intended for AAV transduction test, and the standard deviation of the mean of three independent experiments is indicated.

4.4.2 SUMOylation and Daxx may work in the same pathway

The previous work indicates SUMO and Daxx both could restrict AAV transduction. To know whether SUMO and Daxx worked in the same route to affect AAV2 transduction, impairment of SUMOylation via Ubc9 siRNA knockdown was performed in the HeLa-Daxx knockout cell line and infected with AAV2-firefly afterwards.

Data showed AAV2 transduction in two Daxx knockout cell were higher than in control cell line (Figure 25a, three white column). Ubc9 knockdown enhanced AAV transduction in varying degrees in HeLa and HeLa-Daxx knockout cells (Figure 17a, black column), but the enhancing effect of Ubc9 knockdown was significantly reduced compared to HeLa wild type cells (Figure 25b) which indicates SUMO and Daxx protein may work in the same route in a sense, and the Ubc9 knockdown in HeLa-Daxx knockout cell cannot promote more on the basis of elevated AAV transduction.

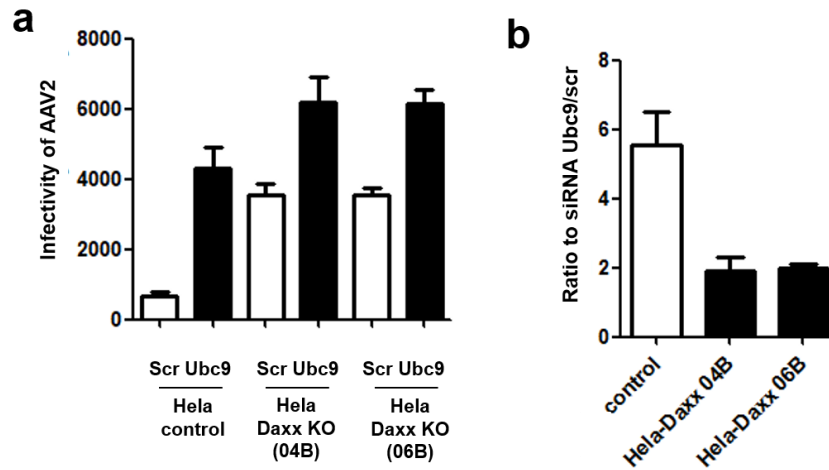


Figure 25 SUMO protein and Daxx protein work in the same pathway controlling AAV transduction. (a) AAV transduction in Daxx knockout cell is higher than in control cell line with the negative siRNA treatment. Ubc9 knockdown in HeLa-Daxx knockout cell enhance the AAV transduction but slightly. (b) The relative ratio of Ubc9/siRNA showing the transduction of AAV2 in HeLa-Daxx knockout cell after Ubc9 knock down has no significantly change compared with AAV2 infection in HeLa wt cell, albeit slightly elevated. HeLa and HeLa-Daxx knockout cells 04B and 06B were seeded into 24-well plate with 2.5×10^4 /well and transfected with 0.3ul targeting Ubc9 or scr siRNA, and then transduced by AAV2 wt or AAV mutants at MOI=1000 for the next 24h. Firefly luciferase assay was intended for AAV infection test. Standard deviation of the mean of three independent experiments is indicated.

5 Discussion

5.1 SUMOylation affects AAV transduction in a host cell dependent manner

Adeno-associated virus (AAV) is widely used as a vector for gene therapy due to the broad tissue tropism, low immune response as well as the non-pathogenicity. However, it is still limited by the poor transduction efficiency due to intercellular restriction factors. Therefore, it is of particular importance to study the role of host restriction factors with the aim to increase AAV2 transduction, thereby improving the utilization of AAV vectors for many disease treatments in the clinical trial.

A high throughput siRNA screen had been carried out previously and two candidates with very high z-scores, Sae2 and Ubc9, the catalyzing enzymes of SUMOylation pathway (Figure 10), were identified as putative AAV restriction factors. Sae2 is a subunit of the unique heterodimeric SUMO E1 activation enzyme, and Ubc9 is the unique SUMO E2 conjugating enzyme. Compared to untreated cells, HeLa cells treated with Sae2 siRNA or Ubc9 siRNA showed significantly increased rAAV2 transduction, indicating that the SUMO E1 and E2 enzymes are host restriction factors affecting AAV2 transduction (Hölscher *et al.* 2015).

Many kinds of virus proteins have been confirmed to be SUMOylated, for example adenovirus (Ad) core protein V and human papillomavirus type16 (HPV16) capsid protein L2 (Freudenberger *et al.* 2018; Marusic *et al.* 2010). Not only SUMOylation affects viral transduction of the host cell, but some experiments also showed that viral infection can change the intracellular SUMOylation activity. Pal *et al.* verified that influenza A virus (IAV) infection

triggers an increase in the abundance of proteins carrying both, SUMO1 and SUMO2/3 modifications (Pal *et al.* 2011). Base on this discovery, I also observed that the AAV2 infection increases the endogenous total SUMOylation activity in two different cell lines (Figure 13). It is conceivable that the host cell uses the SUMOylation pathway as a protective mechanism in order to resist the invasion of AAV, so more and more activated SUMO proteins can act on AAV2 to affect the transduction.

I found that SUMOylation E1 or E2 enzyme (Sae2, Ubc9) siRNA knockdown lead to an increase viral infectivity on one hand, and AAV infection can also increase global intracellular SUMOylation on the other hand, which seems to be a paradox. However, SUMO levels were also indicated to be regulated post-transcriptionally (Sahin *et al.* 2014). It was indicated that the IAV infection did not result in the increase of SUMO mRNA content but increase global SUMO1 and SUMO2/3 activity (Domingues *et al.* 2015), so it might be possible that AAV2 infection does not cause an increase in intracellular SUMO mRNA content either. Therefore, the next experiment should be determining the SUMO mRNA content after AAV2 infection via qPCR, as well as the testing after different AAV serotypes in different host cell line.

5.2 What is the target of SUMOylation?

Interaction of viruses and the SUMOylation pathway can be acting in different manners. For example, leukemia virus is SUMOylated on its capsid protein (Yueh *et al.* 2006), or HSV-1 causes a change in viral transduction through the SUMOylation of host promyelocytic leukemia protein (PML) and Sp100. So, the SUMOylation pathway is considered to restrict AAV transduction by either SUMOylating the virus itself (viral capsid/genome) or an endogenous host cell factor that interacts with the virus, or both. In this thesis, the AAV2 capsid

protein was indeed confirmed as a target for SUMOylation.

To determine whether AAV capsids can be SUMOylated, purified AAV2 particles were proven to carry a SUMO modification. The hypothesis is that the produced mature AAV2 particles are modified with SUMO already during the AAV production in HEK293TT cells. Thus, a pull-down assay of AAV2 particles which were purified by iodixanol gradient was performed and a specific SUMO signal is seen indicating the AAV2 capsid is the target of SUMOylation (Figure 14c). This, however, does not answer the question that whether AAV capsids are also further SUMOylated during the entry process. Isolation of AAV capsids from transduced cells proved to be difficult, therefore this question remains open.

Due to the characteristics of the AAV packaging process, the capsid is formed by VP1 VP2 VP3 and accompanied by ssDNA entry into the virus particles from 5-fold axis of AAV capsid (DiPrimio *et al.* 2008; King *et al.* 2001). As the DNA packaging is not a 100% efficient process, empty AAV particles are usually present in AAV vector preparations. Empty AAV exhibit some properties that are different from those of capsid viruses, e.g. empty capsids exhibiting higher thermal stability than full AAV particles (Kronenberg *et al.* 2005; Bleker *et al.* 2005). In addition, I could observe that empty AAV2 particles are SUMOylated to a higher extent in comparison to full particles, a plausible explanation for this would be better accessibility of SUMO target sequences within VP (Figure 16).

According to the analysis of more than 3,600 SUMOylated proteins, the classical SUMOylation modification motif found nearby SUMO sites is Ψ -K-X-E/D (Hendriks and Vertegaal 2016). Ψ is a hydrophobic amino acid, and X is an arbitrary amino acid, and E/D are acidic amino acids. Ubc9 recognizes the Ψ -K-X-E/D SUMO motif within a target protein and catalyzes the interaction with the substrate (Bernier-Villamor *et al.* 2002). Based on the

above information, I analyzed the AAV capsid VP sequence for the presence of the core *KXE*-type motif. The analysis of sequences shows that the AAV2 capsid VP contains a total of 34 lysines (K) residues, four of them having the basal *KXE*-type of SUMO site: K39, K61, K105 and K527. However, the data presented in this thesis indicates that none of these are actually targets for SUMOylation. Nonetheless, the Ψ -*K-X-E/D* is not the only SUMO modification motif, but the inverted sequence [ED]XK is investigated as another promising motif (Matic *et al.* 2010). Sequences analysis shows only K532 on the AAV2 capsid have this inverted sequence.

In fact, there are ten lysines (K258, K490, K507, K527, K532, K544, K549, K556, K665, and K706) at C-terminal of AAV2 VP protein are surface exposed (Xie *et al.* 2002). Lochrie *et al.* found the modified AAV2 with K527A transduction efficiency is 50% lower than wild type AAV2 (Lochrie *et al.* 2006). Li *et al.* found the modified AAV2-K527E and AAV2-K532E have no transduction activity *in vitro* but much better transduction than wt AAV2 vectors *in vivo*, and the transduction efficiency of AAV2-K549E increased *in vivo* and *in vitro* up to 5-fold compared with wt AAV2 (Li *et al.* 2015). But in this thesis the lysine at C-terminus of VP were exchanged with arginine (R) because they both have side chain which can be positively charged, and the mutants were used to produce the AAV2-K527R, AAV2-K532R and AAV2-K549R. The infection test shows these three modified AAV2 transduction have no big change compared with wt AAV2 without any treatment (Figure 17c, right, white column), confirming that different amino acid (A/E/R) after lysine exchange could impact the infectivity of AAV2. Since E1 or E2 knockdown still enhance the increase of modified AAV2-K527R, AAV2-K532R and AAV2-K549R transduction efficiency (Figure 17c, right, black column) and the SUMO signal can still be detected on these viruses capsid (Figure 17b), I concluded that the VP amino acid K527, K532 or K549 are not the targets of SUMOylation.

Not only the lysines on the capsid external surface, but also those located in the N-terminus are candidate sites for SUMOylation. During intracellular AAV trafficking, the N-terminus of the AAV2 capsid VP1 is exposed to reveal the PLA2 domain, caused by the low pH/acidic environment of the endosome or lysosome (Girod *et al.* 2002). So not only the lysine in C-terminal of VP which could be exposed on the external surface, the lysines in the N-terminal are still worth to be challenged even if the N-terminal of VP is hidden inside of the virus. Modified AAV2 (the K33, K39, K51, K61, K77, K92, K105, K137 in the VP1u, and K142/143, K161, K169 in the VP1/VP2 common region) were produced and in fact AAV2-K142/143R and AAV2-K169R were indicated to be SUMOylation targets. Interestingly, another modified AAV2-K161R was also observed to have weak SUMOylation (Figure 17b), which prompted the possibility of AAV capsid SUMOylation in the VP1/VP2 common region.

Multiple proteins which have been confirmed as SUMO substrates even if they do not have the basal motifs at all, e.g. Mdm2 protein is SUMOylated at lysine K446 (sequence GRPKNGC) which has no SUMOylation consensus sequence but is located within the RING finger domain (Buschmann 2000; Johnson 2004); and Daxx protein can also be SUMOylated at lysine K630/631 (sequence PCKKSR) but not the SUMOylation motif either, means that there are still some unknown motifs or mechanisms that could regulate target proteins SUMOylation. Although K142/143 and K169 on AAV capsid do not contain the Ψ -K-X-E/D or [ED]XK consensus sequences, these lysines are still possibly to be SUMOylated (Figure 17a).

VP1, VP2 and VP3 are being translated from one ORF, so VP1 and VP2 have an overlapping sequence which was called VP1/2 common region (from amino acid 138 to 202). Lysines K142/143 and K169 are part of this common region and modification of either site resulted in the loss of SUMO conjugation (Figure 17b). Intact AAV particles can be formed with VP1+VP3, or VP2+VP3, or VP3

alone in the absence of helper functions and AAV genomes (Warrington *et al.* 2004; Girod *et al.* 2002; Hoque *et al.* 1999). So, these defective AAV2 with SUMO detection indicated the lysines on VP2 are SUMOylation targets (Figure 18).

In addition, due to the controversial function of VP2 from the study of Muralidhar or Warrington (Muralidhar *et al.* 1994; Warrington *et al.* 2004), VP2 seems to be a good subject for AAV SUMOylation study. I observed that when AAV particles were linked with a tag (GFP or HA tag) at the N-terminus of the VP2, SUMO proteins were no longer detected on particles, which means the free N-terminal VP2 promotes SUMOylation of AAV2 particles, and the AAV2 capsid SUMOylation depends on the VP2 spatial structure (Figure 19).

5.3 Which step of the AAV transduction is affected by SUMOylation?

This thesis has provided evidence that the SUMOylation pathway restricts AAV transduction, but the exact step of AAV transduction that benefits from the impairment of SUMOylation is still unknown.

AAV2 subcellular trafficking involves multiple steps. First of all, AAV2 particles bind to different receptors or coreceptors on cell surface (Pillay and Carette 2017). In general, the AAV attachment is not recognized as rate limiting steps for AAV2 transduction (Nonnenmacher and Weber, 2012), and the data in this thesis indeed indicated the SUMOylation does not affect AAV transduction with virus binding step (Figure 20, 1h time point). Subsequently, AAV2 particles are internalized into the endosomal pathway and the comprehensive microtubule network is used for the endosomal AAV2 particle transport. Xiao *et al.* indicate the AAV particles enter the cell and escape from early endosomes within 10min after infection and viral uncoating occurs about 12 hours post-infection

(Xiao *et al.* 2002). Meanwhile the AAV2 PLA2 domain in VP1 becomes exposed in the late endosome or lysosome because of the low pH/acidic environment. Therefore, I predict that AAV has experienced endocytosis and escape from endosome after 5 hours infection. The data indicate AAV transduction does not regulated by the SUMOylation pathway in the first 5h of AAV infection (Figure 20, 5h time point). Above all, also the viral particle endocytosis and post-endocytic trafficking are always recognized as rate limiting steps for AAV2 transduction (Nonnenmacher and Weber, 2012), but they are not the bottleneck of AAV transduction regulated by the SUMOylation pathway.

AAV intracellular transport is regulated by the microtubule network as well as the trans Golgi network (Xiao and Samulski 2012; Nonnenmacher *et al.* 2015). This thesis shows that during the viral trafficking, the amount of AAV2 particles attached on the cell surface or in the cytoplasm does not change after Sae2 knockdown (Figure 21, membrane and cytoplasm). Besides, AAV virions are also known to accumulate in a perinuclear region, followed by slow entry into the cell's nucleus. Thereafter, the AAV2 particles uncoated and release their viral DNA, and the second strand DNA synthesis is promoted by the ITRs (Nonnenmacher and Weber 2012). It is clear to see that AAV2 transduction increases after Sae2 knockdown (Figure 10) and more intact AAV particles still accumulate in nucleus after 6h infection (Figure 23). This provides a possibility that SUMOylation pathway could restricts the number of particles that reach the nucleus, thus in a knockdown condition, more virus gets to the nucleus and undergoes uncoating and transduction (Figure 26a). Also given that the data collection time point of the experiment was at 12hours, this provides just a snapshot and does not rule out that the kinetics in the knockdown condition could be different leading to more viral genomes expressed either earlier or later (Figure 23).

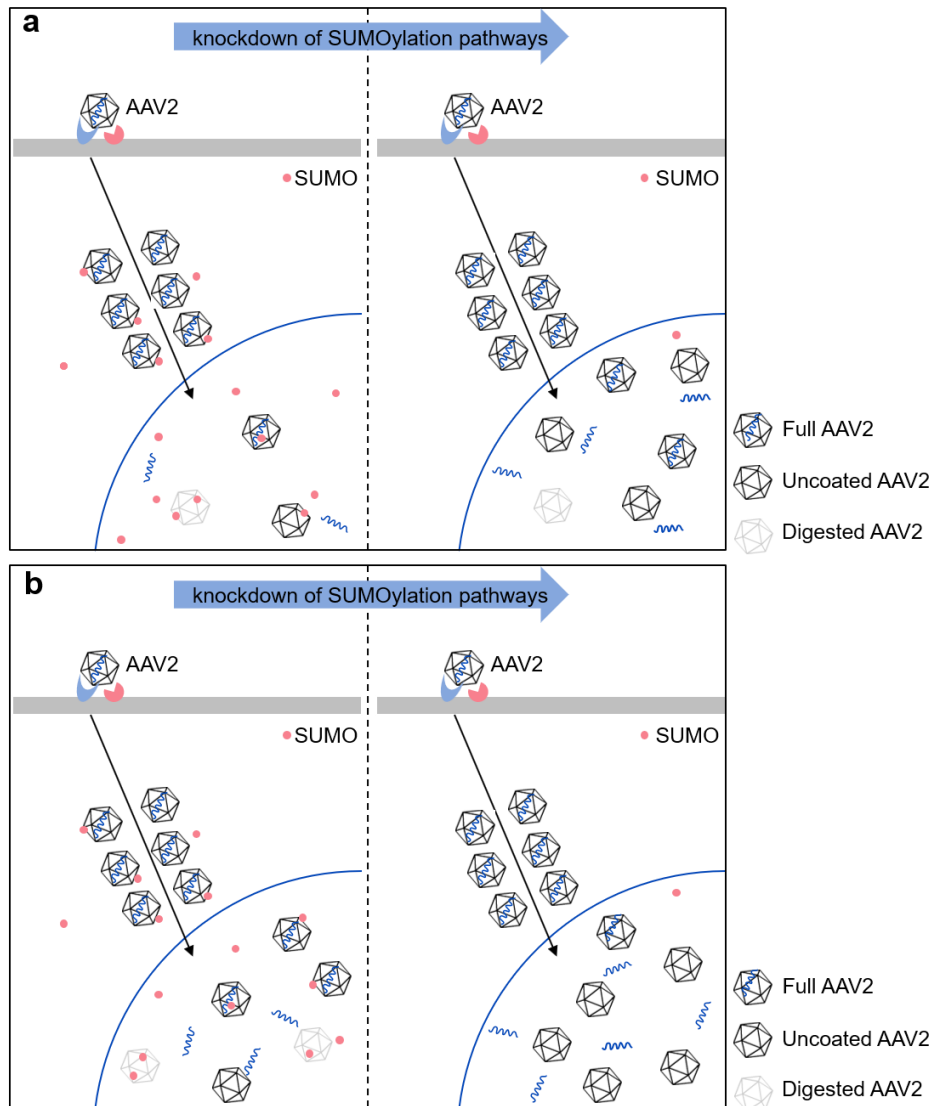


Figure 26 Hypothetical infectious pathway of AAV2 impairment of SUMOylation by Sae2 knockdown. AAV transduction at normal SUMOylation activity. From AAV2 binding, endosome, post-endocytic trafficking and virus escape, perinuclear accumulation, particle translocation into the nucleus, followed by viral capsid uncoating and ssDNA release. (a) AAV2 transduction with impairment of SUMOylation by knockdown of Sae2. In the absence of SUMOylating proteins, more capsids reach the nucleus and undergo uncoating and transduction. (b) Account of AAV particles coming into the nucleus are same, but Sae2 knockdown could promote the AAV2 genome ejection from the intact capsid, and the remaining empty particle capsid after uncoating exhibited better stability characteristic against degradation after uncoating.

In addition, if the above assumption is wrong, which means the AAV particles account coming into the nucleus are same (Figure 21, nuclear) and they are regulated by SUMOylation in the nucleus (Figure 23). Since this thesis is based on the scAAV study, the impact of the second-strand DNA synthesis is excluded. Therefore, I speculate that SUMOylation may related to the AAV uncoating and ssDNA release.

Until today, there is no study on how AAV2 is uncoated in nucleus, but it is identified that parvovirus Minute Virus of Mice (MVM) genome release mainly occurs without capsid disassembly (Ros *et al.* 2006). Viral uncoating and DNA release are important rate-limiting steps for virus transduction, and the viral genome ejection from the complete intact capsid is wide-ranging in non-enveloped viruses (Suomalainen and Greber 2013). More recently, AAV8 and AAV9 DNA release have been identified that linearized ssDNA could be ejected from the complete viral capsid (Bernaud *et al.* 2018). Therefore, combining the results of AAV capsid protein SUMOylation, the other possibility is that SUMOylation could not affect the amount of AAV2 particles but instead enhance AAV transduction by promoting AAV uncoating and ssDNA release in the nucleus (Figure 26b).

5.4 The Daxx protein affects AAV transduction via the SUMOylation pathway

Daxx is a highly conserved nuclear protein widely distributed in subcellular regions such as nucleoplasm, nucleolus, heterochromatin and promyelocytic leukemia protein nucleus bodies (PML-NBs) and acts to regulate apoptosis and transcription, and DAXX deficiency will lead to the depolymerization of PML-NBs (Bernardi and Pandolfi 2007; Borden 2002; Geng *et al.* 2012). Some studies have shown that the Daxx and ATRX, two components of the PML

oncogenic domains (PODs), in the form of a complex to represent an intrinsic immune mechanism acting as a viral defense against a large number of different viruses (Schreiner and Wodrich 2013). Moreover, the previous RNAi screen in my lab identified the protein Daxx and ATRX as putative AAV restriction factors showed the preeminent ranking No. 27 and No. 108 with high z-scores of 5.39 and 3.38, respectively (in total ~20,000 gene) (Hölscher *et al.* 2015). In consequence it reveals the possibility of AAV transduction affected by PML-NBs-related proteins.

SUMOylation is mainly occurs in the nucleus, especially high enriched in nuclear bodies and chromatin to regulate chromatin-remodeling complexes modification (Wotton *et al.* 2017). In addition, this thesis shows the possibility of AAV2 SUMOylation in the nucleus (Figure 23), so nuclear factors may play an important role in AAV transduction process.

In general, PML SUMOylation (at aa K65, K160 and K490) could distributes the localization of Daxx in PML-NBs. PML-NBs will be depolymerized when PML protein is not SUMOylated after Ubc9 downregulation, followed by the Daxx protein translocate to dense chromatin (Best *et al.* 2002; Nacerddine *et al.* 2005), In the meanwhile, the Daxx protein itself can be SUMOylation as well. It was identified that Daxx, the SUMOylation defective mutant, was able to interact with PML and co-localized in PODs at K630/631 (Lin *et al.* 2006; Jang *et al.* 2002). The PODs co-localization mediated by SUMO1 to form DAXX-SUMO1-PML complex, which is the supporting structure of PML-NBs (Chang *et al.* 2011; Hecker *et al.* 2006), and the DAXX in the cytoplasm is recruited into PML-NBs by combining with the SUMOylated PML protein. The absence of Daxx cause PML-NBs disintegration. Therefore, the AAV transduction is predicted to be affected by Daxx and/or PML protein SUMOylation.

Due to the above conjecture, Daxx is considered in this thesis to be involved in

the effect of SUMOylation on AAV transduction. The knockout of endogenous Daxx leads to the increased AAV transduction (Figure 16). Upon the impairment of SUMOylation, especially for Ubc9 siRNA knockdown in HeLa-Daxx knockout cell, the enhancing effect of Ubc9 knockdown were reduced significantly. This indicates that the Daxx protein works, at least in part, in the same pathway with SUMOylation to affect AAV transduction (Figure 25).

Based on the above data, the AAV2 capsid protein and intracellular factor Daxx could be considered as targets of SUMOylation affecting AAV2 transduction. On one hand, SUMO conjugates to the AAV2 capsid protein directly; On the other hand, the results from the AAV2 transduction experiments in the presence or absence of Daxx plus or minus SUMO knockdown would postulate that the Daxx protein is SUMOylated (Figure 28, red box), or the protein associated with Daxx can be SUMOylated thereby regulating AAV transduction. Hypothetical model is shown below (Figure 27).

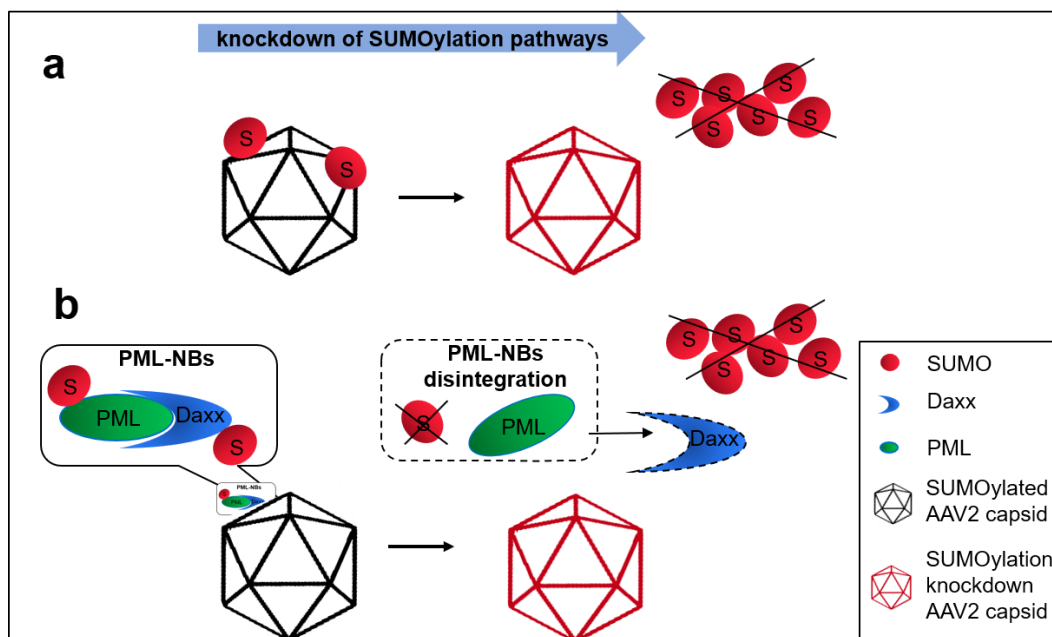


Figure 27 Hypothetical model of SUMOylation interfering with AAV. (a) Target of SUMOylation that affects AAV2 transduction is the AAV2 capsid. In general, SUMO protein would conjugate to the AAV2 capsid for the inhibition leading to reduced intra cellular transport

or uncoating, but the knockdown of enzymes in the SUMOylation cascade results in an active form of the AAV2 virus. (b) Target of SUMOylation is the host factors thus affecting AAV transduction. PML-NBs will be disintegrated when PML protein is not SUMOylated, and the Daxx would translocate from PML-NBs to the dense chromatin; And the absence of Daxx protein would also cause the disintegration of PML-NBs to affect AAV2 transduction.

Since neither of the components (AAV capsid protein at K142/143 and K169, Daxx protein) can be determined as the sole target of SUMOylation, the synergism of the multiple SUMOylation targets that affect AAV transduction needs to be further investigated. The transduction of the lysine-mutant AAV2: AAV2-K142/143R and AAV-K169R could be tested in the HeLa-Daxx knockout cell line with or without knockdown of Sae2 or Ubc9 (Figure 28). This pre-test shows the infectivity of modified AAV2 with K142/143R or K169R infectivity in Daxx knockout cell line is lower than wt AAV in wt cells. Although it still has a very weak elevated trend, but it reveals the possibility of multiple factors cooperation on AAV transduction by SUMOylation regulation.

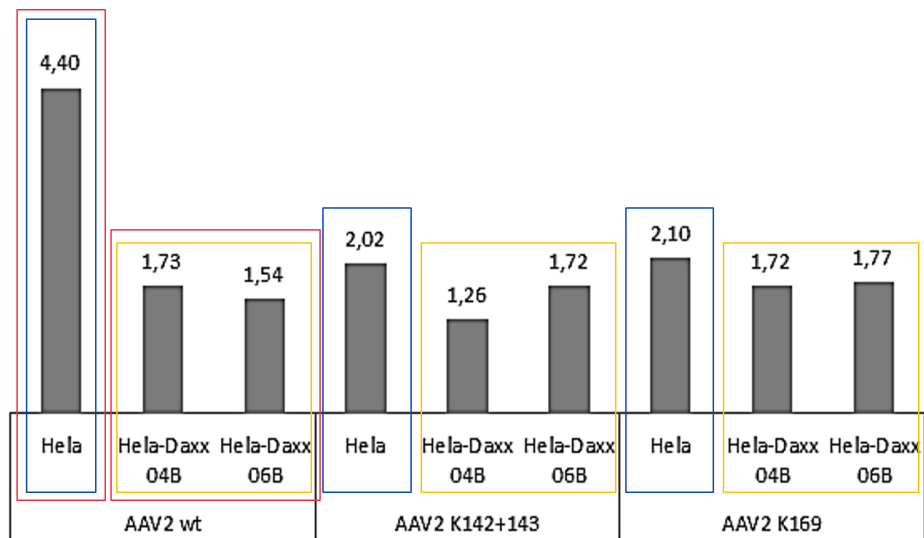


Figure 28 Multiple factors control AAV2 transduction. AAV wt infectivity in HeLa-Daxx knockout cells is lower than in HeLa wt cells, and the modified AAV2 at K142/143R or K169R show even lower infectivity in HeLa-Daxx knockout cells. There are two Daxx knockout cell line were used for infection test (04B, 06B). Blue box, the comparison of AAV2 wt and modified

AAV2 (K142/143R, K169R) transduction efficiency. Red box, the comparison of AAV2 wt transduction efficiency in wt or Daxx knockout cell line. Yellow box, the comparison of modified AAV2 (K142/143R, K169R) in Daxx knockout cell line.

5.5 AAV gene therapy

Gene therapy vectors have been approved in succession around the world. In 2017, the United States successively approved the listing of three gene therapies, two gene therapy programs and one direct-dose gene therapy drug. Apart from the latest immunotherapy using CAR-T cells which target tumor-associated cell surface antigens, various viral vectors have also been studied including lentivirus (LV), retrovirus (RV), and AAV, etc. For reasons of long-term gene expression, non-autonomous replication, transduction of dividing and non-dividing cells and especially because of the non-pathogenicity of the parental wild type AAV, recombinant AAV (rAAV) become a promising and meaningful tool in gene therapy.

Remarkably, AAV vector has been used and shall continue to be used for different clinical trials. The AAV vector alipogene tiparvovec (Glybera®) for the treatment of familial lipoprotein lipase deficiency is the first AAV-based drug licensed in Europe in October 2012 (Salmon *et al.* 2014). Recently, the US Food and Drug Administration (FDA) approved Luxturna in October 2017, which is used for the hereditary blindness genetic therapy treatment (<https://www.fda.gov/NewsEvents/Newsroom/PressAnnouncements/ucm589467.htm>). More recently, George *et al.* reported that the Hemophilia B Gene Therapy using AAV on patients was successful for the first time (George *et al.* 2017). Also, there are multiple neurological disease clinical trials that are ongoing throughout different parts of the world (Deverman *et al.* 2018). These indicate that AAV plays a pivotal role as a promising carrier of gene therapy

worldwide.

Scientists have tried to use some substances along with AAV in order to increase the transduction efficiency of AAV *in vivo*. For example, the proteasome inhibitor, Bortezomib is currently approved by the US Food and Drug Administration for clinical trial, mainly for the treatment of multiple myeloma, and scholars have utilized this chemical compound in AAV gene therapy. Monahan et al used Bortezomib to treat dogs with hemophilia accompanied by rAAV2 or rAAV8 injection which contained the eighth coagulation factor, and they found the single dose of Bortezomib can increase their transduction efficiency and return the hemophilia dogs clotting time to normal and reduced the bleeding rate by 90% (Monahan *et al.* 2010).

However, the toxicity of these chemical compounds needs to be considered despite the increase in the rAAV transduction efficiency. For example, Bortezomib would cause adverse reactions such as gastrointestinal discomfort, peripheral neuropathy, heart failure, etc., so patients have had to reduce the dose or even stop treatment (Petrucci *et al.* 2013; Rampen *et al.* 2013; Voortman and Giaccone 2006). Therefore, the cooperation of chemicals and AAV need to be balanced within a safe and effective range.

To avoid the chemical compound toxicity, I proposed an alternative scheme to use a co-infection of two viruses of the same serotype, whereby the restriction factors of SUMOylation are eliminated resulting in higher transduction efficacy. The unique enzymes (E1 and E2) of the SUMO pathway are restriction factors of AAV2 infection in this thesis, and Gam1 was indicated as the inhibitor of the SUMO E1 catalytic enzyme, such that the overexpression of Gam1 resulted in the increase of AAV transduction. To avoid toxicity caused by chemicals *in vitro*, the AAV2-Gam1 and AAV2-firefly coinfection was performed. The AAV2-Gam1 coinfecting with AAV2-firefly *in vitro* shows significantly higher transduction than

the AAV2- YFP coinfecting with AAV2-firefly (control group) and the maximum value was observed when the molar ratio of two viruses was 0.5:1 (AAV2-Gam1: AAV2-firefly= 1:2). This demonstrates a new direction for AAV vectors for use in future clinical trials (Figure 29).

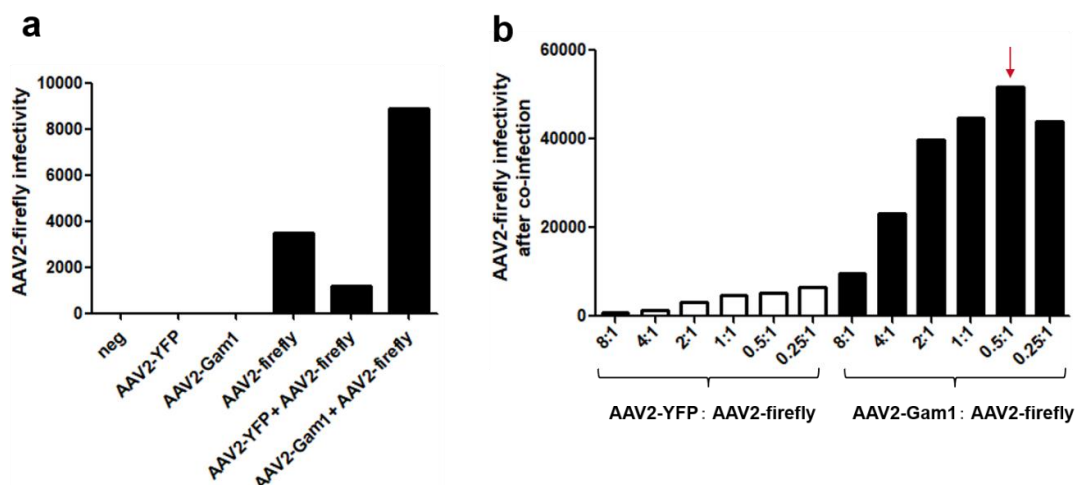


Figure 29 Coinfection with AAV2- Gam1 increases transduction efficacy of AAV2 vectors. (a) Infectivity of rAAV2-firefly coinfecting with control rAAV (AAV2-YFP) and SUMO-targeting rAAV (AAV2-Gam1). (b) Infectivity of rAAV2-firefly with different molar ratios of SUMO-targeting rAAV, and the best infectivity of rAAV2-firefly is observed at the molar ratio of 0.5:1. The molar amount of rAAV2-firefly was kept the same, and coinfecting with either AAV2-Gam1 or control rAAV2-YFP with different molar ratios.

This pre-test suggested the possibility of co-infection, i.e. rAAV2-a a gene carrying the SUMO inhibitor, and rAAV2-b carrying a target gene. The homologous AAV was used to avoid cytotoxicity caused by infection of non-homologous viruses. Further experiments should also be performed *in vitro* and *in vivo*.

5.6 Conclusion

In summary, SUMO E1 (Sae2) and SUMO E2 (Ubc9) enzymes are confirmed as host cell restriction factors for rAAV2 transduction efficiency, and total

SUMOylation activity is enhanced by AAV2 infection.

To determine the target of SUMOylation, pull-down assays were performed for AAV2 particles which indicated that the AAV2 capsid protein is the target of SUMOylation. The site-directed mutation and enhanced virus transduction show that K142/143 and K169 on VP2 play a role in capsid SUMOylation. In addition, the tag-linked VP2 N-terminus resulting in no SUMOylation, indicating that the AAV2 capsid protein SUMOylation requires a defined VP2 spatial structure.

Moreover, the increase in AAV2 transduction in Daxx knockout cell line indicated that Daxx is another restriction factor of AAV infection. Compared with wild type cell line, the enhancing effects after SUMOylation knockdown were strongly reduced, which means the Daxx protein and SUMOylation may work in the same pathway. So not only the AAV2 capsid protein but also Daxx may be a target of SUMOylation.

AAV2 subcellular trafficking involves multiple steps. SUMOylation does not have an impact on the accumulation of AAV2 vector DNA on the cell surface or in the cytoplasm after transduction. But pre-liminary data indicates two possibilities for SUMOylated AAV2 particles accumulation in the perinuclear/nucleus: More AAV2 particles reach the nucleus with the impairment of SUMOylation and undergoes uncoating and transduction; SUMOylation does not restricts the amount of AAV2 particles in the nucleus but enhance AAV transduction by promoting AAV uncoating and ssDNA release from the complete viral capsid.

6 Summary

Adeno-associated virus (AAV) is a member of the *Parvoviridae* family with a non-enveloped and icosahedral capsid structure. Recombinant AAVs (rAAV) are non-pathogenic with the low immunogenicity and broad cell/tissue tropism, thus AAV is widely used as a gene therapy tool. Currently, many clinical trials involving AAV vectors are ongoing and the marketed drug Glybera® was approved in Europe in 2012, followed by the Luxturna by FDA approval in 2017.

However, the limitation of this vector is the poor AAV transduction efficiency. To reveal the regulation of the host factors in AAV2 transduction, an RNAi screen was performed previously to identify host proteins interfering with AAV2 transduction. Sae2 and Ubc9, which are key enzymes of the SUMOylation pathway, were identified as restriction factors of AAV infection. Similar to the ubiquitination, SUMOylation is a post-translational protein modification catalyzed by an E1 activating enzyme (consisting of Sae1 and Sae2) and an E2 conjugating enzyme (Ubc9).

Further investigations in this thesis confirmed that the impairment of SUMOylation via Sae2 or Ubc9 knockdown resulted in a higher AAV transduction efficiency, and AAV2 infection can also enhance the total SUMOylation activity of host cells. Moreover, SUMOylation affects the transduction of AAV vectors with single stranded DNA (ssAAV) and self-complementary DNA (scAAV).

To determine the target of SUMOylation in the AAV life cycle, a pull-down assay was performed for AAV2 particles indicating that the AAV2 capsid protein is SUMOylated. Site-directed mutagenesis and modified virus transduction shows involvement of K142/143 and K169 of VP2 in capsid SUMOylation. In

addition, the data suggests that the N-terminus of VP2 needs to be free, as addition of protein tags such as GFP or HA abolishes SUMOylation. This indicates that the AAV2 capsid SUMOylation has VP2 spatial structure requirements.

Moreover, the observed increased AAV2 transduction in a Daxx knockout cell line indicates that Daxx is another restriction factor of AAV. Compared with wild type HeLa cell line, the enhancing effects after Ubc9 knockdown in Daxx knockout cell line was dramatically reduced, which means the Daxx protein and SUMOylation may work in the same or overlapping pathways. Thence, not only the AAV2 capsid protein, but also SUMOylated Daxx could regulate AAV transduction.

AAV2 subcellular trafficking involves multiple steps. AAV2 vector DNA in the cell membrane and cytoplasmic fractions are not altered after Sae2 knockdown indicating that impairment of the SUMOylation-pathway cannot affect AAV binding and the intracellular transport and therefore have no influence on AAV transduction. Other than this, there are two possibilities for SUMOylated AAV2 particles to accumulate in the nucleus: SUMOylation pathway could restrict the number of particles that reach the nucleus and undergo transduction; Alternatively, SUMOylation could not affect the amount of AAV2 particles but instead enhance AAV transduction by promoting AAV uncoating and ssDNA release in the nucleus.

7 Zusammenfassung

Das Adeno-assoziierte Virus (AAV) gehört zur Familie der *Parvoviridae* und besitzt eine nicht-umhüllte und ikosaedrische Kapsidstruktur. Rekombinante AAVs (rAAV) sind nicht-pathogene Vektoren, die eine geringe Immunogenität und einen breiten Zell- und Gewebstropismus aufweisen. Deshalb kann rAAV als sicherer Gentherapievektor eingesetzt werden. Zurzeit werden einige klinische Studien durchgeführt, die auf dem AAV-Vektor basieren. Das erste kommerziell verfügbare Medikament wurde 2012 in Europa zugelassen.

Eine Limitierung des AAV-Vektors ist jedoch die vergleichbar schlechte Transduktionseffizienz. Um Wirtsfaktoren zu identifizieren, die eine Rolle bei der AAV2-Transduktion spielen, wurde ein RNAi-Screen durchgeführt. Die Enzyme des SUMOylierungsweges, Sae2 und Ubc9, wurden als Restriktionsfaktoren der AAV-Infektion identifiziert. Ähnlich wie die Ubiquitinierung, ist die SUMOylierung eine posttranslationale Proteinmodifikation, die durch ein E1-aktivierendes Enzym (bestehend aus Sae1 und Sae2) und ein E2-konjugierendes Enzym (Ubc9) katalysiert wird.

Weitere Untersuchungen in dieser Arbeit bestätigen, dass der *Knockdown* der SUMOylierung zu einer höheren AAV-Transduktionsleistung führt, und die AAV2-Infektion die gesamte SUMOylierungsaktivität der Wirtszellen erhöhen kann. Darüber hinaus beeinflusst die SUMOylierung die Transduktion von AAV-Vektoren mit einzelsträngiger DNA (ssAAV) und selbstkomplementärer DNA (scAAV).

Um herauszufinden, was das Zielobjekt der SUMOylierung ist, wurde eine Ko-Immünpräzipitation für AAV2-Partikel durchgeführt, welche darauf hindeutet, dass das AAV2-Kapsidprotein SUMOyliert wird. Die ortsspezifische

Mutagenese und die Transduktion mit dem modifizierten Viruskapsid zeigen, dass die Aminosäuren K142/143 und K169 eine Rolle bei der SUMOylierung von VP2 spielen. Darüber verhindert die Fusion des N-Terminus mit verschiedenen Liganden wie GFP und HA die SUMOylierung von VP2, was darauf hindeutet, dass die AAV2-Kapsid-SUMOylierung eine bestimmte VP2 räumliche Struktur erfordert.

Darüber hinaus deutet die verstärkte AAV2-Transduktion in der Daxx Knockout-Zelllinie, im Vergleich zur wt-Zelllinie darauf hin, dass es sich bei dem Daxx-Protein um einen weiteren Restriktionsfaktor der AAV-Infektion handelt. Im Vergleich zu Wildtyp-Zelllinien wurden die verstärkenden Effekte nach dem Ubc9-Knockdown in der Daxx-Knockout-Zelllinie offensichtlich reduziert, was bedeutet, dass das Daxx-Protein und die SUMOylierung auf dem gleichem oder sich überlappenden Wegen funktionieren könnten. Ausgehend davon könnte nicht nur das AAV2-Kapsidprotein, sondern auch das SUMOylierte Daxx-Protein die AAV-Transduktion regulieren.

Der subzelluläre Transport von AAV2 umfasst mehrere Schritte. Die Menge an AAV2-Vektor-DNA in den Zellmembran- und den Zytoplasmafraktionen ändern sich nicht nach dem Sae2-Knockdown, was darauf hinweist, dass die Beeinträchtigung der SUMOylierung die Bindung von AAV an die Zellmembran, den intrazellulären Transport und damit die AAV-Transduktion nicht beeinflusst. Darüber hinaus gibt es zwei Hypothesen für die Akkumulation von SUMOylierten AAV2-Partikeln im Zellkern. Die SUMOylierung könnte die Anzahl der AAV2 Partikel begrenzen, die den Zellkern erreichen und transduzieren können. Im Gegenteil, könnte SUMOylierung die Anzahl von AAV2 Partikeln nicht beeinflussen, sondern die AAV Transduktion verbessern, indem AAV-uncoating und ssDNA Freisetzung im Zellkern gefördert werden.

8 References

- Agrawal, N. and Banerjee, R. (2008). **Human polycomb 2 protein is a SUMO E3 ligase and alleviates substrate-induced inhibition of cystathionine beta-synthase sumoylation.** PLoS ONE 3, e4032, doi: 10.1371/journal.pone.0004032.
- Akache, B., Grimm, D., Pandey, K., Yant, S. R., Xu, H. and Kay, M. A. (2006). **The 37/67-kilodalton laminin receptor is a receptor for adeno-associated virus serotypes 8, 2, 3, and 9.** J Virol 80, 9831-9836, doi: 10.1128/JVI.00878-06.
- Alam, S., Bowser, B. S., Conway, M. J., Israr, M., Tandon, A. and Meyers, C. (2011). **Adeno-associated virus type 2 infection activates caspase dependent and independent apoptosis in multiple breast cancer lines but not in normal mammary epithelial cells.** Mol Cancer 10, 97, doi: 10.1186/1476-4598-10-97.
- Alam, S. and Meyers, C. (2009). **Adeno-associated virus type 2 induces apoptosis in human papillomavirus-infected cell lines but not in normal keratinocytes.** J Virol 83, 10286-10292, doi: 10.1128/JVI.00343-09.
- Asokan, A., Hamra, J. B., Govindasamy, L., Agbandje-McKenna, M. and Samulski, R. J. (2006). **Adeno-associated virus type 2 contains an integrin alpha5beta1 binding domain essential for viral cell entry.** J Virol 80, 8961-8969, doi: 10.1128/JVI.00843-06.
- Asokan, A., Schaffer, D. V. and Samulski, R. J. (2012). **The AAV vector toolkit. Poised at the clinical crossroads.** Mol Ther 20, 699-708, doi: 10.1038/mt.2011.287.
- Atchison, R. W., Casto, B. C. and Hammon, W. M. (1965). **Adenovirus-Associated Defective Virus Particles.** Science 149, 754-755, doi: 10.1126/science.149.3685.754.
- Bartlett, J. S., Wilcher, R. and Samulski, R. J. (2000). **Infectious entry pathway of adeno-associated virus and adeno-associated virus vectors.** J Virol 74, 2777-2785.
- Bayer, P., Arndt, A., Metzger, S., Mahajan, R., Melchior, F., Jaenicke, R. and Becker, J. (1998). **Structure determination of the small ubiquitin-related modifier SUMO-1.** J Mol Biol 280, 275-286, doi: 10.1006/jmbi.1998.1839.

- Benskey, M. J., Sandoval, I. M. and Manfredsson, F. P. (2016). **Continuous Collection of Adeno-Associated Virus from Producer Cell Medium Significantly Increases Total Viral Yield.** *Hum Gene Ther Methods* 27, 32-45, doi: 10.1089/hgtb.2015.117.
- Bernardi, R. and Pandolfi, P. P. (2007). **Structure, dynamics and functions of promyelocytic leukaemia nuclear bodies.** *Nat Rev Mol Cell Biol* 8, 1006-1016, doi: 10.1038/nrm2277.
- Bernaudo, J., Rossi, A., Fis, A., Gardette, L., Aillot, L., Büning, H., Castelnovo, M., Salvetti, A. and Faivre-Moskalenko, C. (2018). **Characterization of AAV vector particle stability at the single-capsid level.** *J Biol Phys* 44, 181-194, doi: 10.1007/s10867-018-9488-5.
- Bernier-Villamor, V., Sampson, D. A., Matunis, M. J. and Lima, C. D. (2002). **Structural basis for E2-mediated SUMO conjugation revealed by a complex between ubiquitin-conjugating enzyme Ubc9 and RanGAP1.** *Cell* 108, 345-356.
- Berry, G. E. and Asokan, A. (2016). **Chemical Modulation of Endocytic Sorting Augments Adeno-associated Viral Transduction.** *J Biol Chem* 291, 939-947, doi: 10.1074/jbc.M115.687657.
- Best, J. L., Ganiatsas, S., Agarwal, S., Changou, A., Salomoni, P., Shirihai, O., Meluh, P. B., Pandolfi, P. P. and Zon, L. I. (2002). **SUMO-1 protease-1 regulates gene transcription through PML.** *Mol Cell* 10, 843-855.
- Blackburn, S. D., Steadman, R. A. and Johnson, F. B. (2006). **Attachment of adeno-associated virus type 3H to fibroblast growth factor receptor 1.** *Arch Virol* 151, 617-623, doi: 10.1007/s00705-005-0650-6.
- Bleker, S., Sonntag, F. and Kleinschmidt, J. A. (2005). **Mutational analysis of narrow pores at the fivefold symmetry axes of adeno-associated virus type 2 capsids reveals a dual role in genome packaging and activation of phospholipase A2 activity.** *J Virol* 79, 2528-2540, doi: 10.1128/JVI.79.4.2528-2540.2005.
- Boggio, R., Colombo, R., Hay, R. T., Draetta, G. F. and Chiocca, S. (2004). **A mechanism for inhibiting the SUMO pathway.** *Mol Cell* 16, 549-561, doi: 10.1016/j.molcel.2004.11.007.
- Boggio, R., Passafaro, A. and Chiocca, S. (2007). **Targeting SUMO E1 to ubiquitin ligases. A viral strategy to counteract sumoylation.** *J Biol Chem* 282, 15376-15382, doi: 10.1074/jbc.M700889200.
- Borden, K. L. B. (2002). **Pondering the promyelocytic leukemia protein (PML) puzzle. Possible functions for PML nuclear bodies.** *Mol Cell Biol*

- 22, 5259-5269.
- Buie, L. K., Rasmussen, C. A., Porterfield, E. C., Ramgolam, V. S., Choi, V. W., Markovic-Plese, S., Samulski, R. J., Kaufman, P. L. and Borrás, T. (2010). **Self-complementary AAV virus (scAAV) safe and long-term gene transfer in the trabecular meshwork of living rats and monkeys.** *Invest Ophthalmol Vis Sci* 51, 236-248, doi: 10.1167/iovs.09-3847.
- Buller, R. M., Janik, J. E., Sebring, E. D. and Rose, J. A. (1981). **Herpes simplex virus types 1 and 2 completely help adenovirus-associated virus replication.** *J Virol* 40, 241-247.
- Buschmann, T., Fuchs, S. Y., Lee, C. G., Pan, Z. Q. and Ronai, Z. (2000). **SUMO-1 modification of Mdm2 prevents its self-ubiquitination and increases Mdm2 ability to ubiquitinate p53.** *Cell* 101, 753-762.
- Chang, C.-C., Naik, M. T., Huang, Y.-S., Jeng, J.-C., Liao, P.-H., Kuo, H.-Y., Ho, C.-C., Hsieh, Y.-L., Lin, C.-H., Huang, N.-J., Naik, N. M., Kung, C. C.-H., Lin, S.-Y., Chen, R.-H., Chang, K.-S., Huang, T.-H. and Shih, H.-M. (2011). **Structural and functional roles of Daxx SIM phosphorylation in SUMO paralog-selective binding and apoptosis modulation.** *Mol Cell* 42, 62-74, doi: 10.1016/j.molcel.2011.02.022.
- Cheung, A. K., Hoggan, M. D., Hauswirth, W. W. and Berns, K. I. (1980). **Integration of the adeno-associated virus genome into cellular DNA in latently infected human Detroit 6 cells.** *J Virol* 33, 739-748.
- Chiorini, J. A., Kim, F., Yang, L. and Kotin, R. M. (1999). **Cloning and characterization of adeno-associated virus type 5.** *J Virol* 73, 1309-1319.
- Chiorini, J. A., Yang, L., Liu, Y., Safer, B. and Kotin, R. M. (1997). **Cloning of adeno-associated virus type 4 (AAV4) and generation of recombinant AAV4 particles.** *J Virol* 71, 6823-6833.
- Chu, Y. and Yang, X. (2011). **SUMO E3 ligase activity of TRIM proteins.** *Oncogene* 30, 1108-1116, doi: 10.1038/onc.2010.462.
- Colella, P., Ronzitti, G. and Mingozzi, F. (2018). **Emerging Issues in AAV-Mediated In Vivo Gene Therapy.** *Mol Ther Methods Clin Dev* 8, 87-104, doi: 10.1016/j.omtm.2017.11.007.
- Daya, S. and Berns, K. I. (2008). **Gene therapy using adeno-associated virus vectors.** *Clin Microbiol Rev* 21, 583-593, doi: 10.1128/CMR.00008-08.
- Deshaies, R. J. and Joazeiro, C. A. P. (2009). **RING domain E3 ubiquitin ligases.** *Annu Rev Biochem* 78, 399-434, doi:

- 10.1146/annurev.biochem.78.101807.093809.
- Deverman, B. E., Ravina, B. M., Bankiewicz, K. S., Paul, S. M. and Sah, D. W. Y. (2018). **Gene therapy for neurological disorders. Progress and prospects.** *Nat Rev Drug Discov* 17, 641-659, doi: 10.1038/nrd.2018.110.
- Di Pasquale, G., Davidson, B. L., Stein, C. S., Martins, I., Scudiero, D., Monks, A. and Chiorini, J. A. (2003). **Identification of PDGFR as a receptor for AAV-5 transduction.** *Nat Med* 9, 1306-1312, doi: 10.1038/nm929.
- Ding, W., Zhang, L. N., Yeaman, C. and Engelhardt, J. F. (2006). **rAAV2 traffics through both the late and the recycling endosomes in a dose-dependent fashion.** *Mol Ther* 13, 671-682, doi: 10.1016/j.ymthe.2005.12.002.
- DiPrimio, N., Asokan, A., Govindasamy, L., Agbandje-McKenna, M. and Samulski, R. J. (2008). **Surface loop dynamics in adeno-associated virus capsid assembly.** *J Virol* 82, 5178-5189, doi: 10.1128/JVI.02721-07.
- Domingues, P., Golebiowski, F., Tatham, M. H., Lopes, A. M., Taggart, A., Hay, R. T. and Hale, B. G. (2015). **Global Reprogramming of Host SUMOylation during Influenza Virus Infection.** *Cell Rep* 13, 1467-1480, doi: 10.1016/j.celrep.2015.10.001.
- Douar, A. M., Poulard, K., Stockholm, D. and Danos, O. (2001). **Intracellular trafficking of adeno-associated virus vectors. Routing to the late endosomal compartment and proteasome degradation.** *J Virol* 75, 1824-1833, doi: 10.1128/JVI.75.4.1824-1833.2001.
- Evdokimov, E., Sharma, P., Lockett, S. J., Lualdi, M. and Kuehn, M. R. (2008). **Loss of SUMO1 in mice affects RanGAP1 localization and formation of PML nuclear bodies, but is not lethal as it can be compensated by SUMO2 or SUMO3.** *J Cell Sci* 121, 4106-4113, doi: 10.1242/jcs.038570.
- Everett, R. D. (2001). **DNA viruses and viral proteins that interact with PML nuclear bodies.** *Oncogene* 20, 7266-7273, doi: 10.1038/sj.onc.1204759.
- Everett, R. D. and Murray, J. (2005). **ND10 components relocate to sites associated with herpes simplex virus type 1 nucleoprotein complexes during virus infection.** *J Virol* 79, 5078-5089, doi: 10.1128/JVI.79.8.5078-5089.2005.
- Everett, R. D., Parada, C., Gripon, P., Sirma, H. and Orr, A. (2008). **Replication of ICP0-null mutant herpes simplex virus type 1 is restricted by both PML and Sp100.** *J Virol* 82, 2661-2672, doi: 10.1128/JVI.02308-07.
- Fisher, K. J., Gao, G. P., Weitzman, M. D., DeMatteo, R., Burda, J. F. and Wilson, J. M. (1996). **Transduction with recombinant adeno-associated**

- virus for gene therapy is limited by leading-strand synthesis.** *J Virol* 70, 520-532.
- Flotho, A. and Melchior, F. (2013). **Sumoylation. A regulatory protein modification in health and disease.** *Annu Rev Biochem* 82, 357-385, doi: 10.1146/annurev-biochem-061909-093311.
- Freudenberger, N., Meyer, T., Groitl, P., Dobner, T. and Schreiner, S. (2018). **Human Adenovirus Core Protein V Is Targeted by the Host SUMOylation Machinery To Limit Essential Viral Functions.** *J Virol* 92, doi: 10.1128/JVI.01451-17.
- Gao, G., Vandenberghe, L. H., Alvira, M. R., Lu, Y., Calcedo, R., Zhou, X. and Wilson, J. M. (2004). **Clades of Adeno-associated viruses are widely disseminated in human tissues.** *J Virol* 78, 6381-6388, doi: 10.1128/JVI.78.12.6381-6388.2004.
- Gao, G.-P., Alvira, M. R., Wang, L., Calcedo, R., Johnston, J. and Wilson, J. M. (2002). **Novel adeno-associated viruses from rhesus monkeys as vectors for human gene therapy.** *Proc Natl Acad Sci U S A* 99, 11854-11859, doi: 10.1073/pnas.182412299.
- Geng, Y., Monajembashi, S., Shao, A., Di Cui, He, W., Chen, Z., Hemmerich, P. and Tang, J. (2012). **Contribution of the C-terminal regions of promyelocytic leukemia protein (PML) isoforms II and V to PML nuclear body formation.** *J Biol Chem* 287, 30729-30742, doi: 10.1074/jbc.M112.374769.
- Geoffroy, M.-C. and Salvetti, A. (2005). **Helper functions required for wild type and recombinant adeno-associated virus growth.** *Curr Gene Ther* 5, 265-271.
- George, L. A., Sullivan, S. K., Giermasz, A., Rasko, J. E. J., Samelson-Jones, B. J., Ducore, J., Cuker, A., Sullivan, L. M., Majumdar, S., Teitel, J., McGuinn, C. E., Ragni, M. V., Luk, A. Y., Hui, D., Wright, J. F., Chen, Y., Liu, Y., Wachtel, K., Winters, A., Tiefenbacher, S., Arruda, V. R., van der Loo, J. C. M., Zeleniaia, O., Takefman, D., Carr, M. E., Couto, L. B., Anguela, X. M. and High, K. A. (2017). **Hemophilia B Gene Therapy with a High-Specific-Activity Factor IX Variant.** *N Engl J Med* 377, 2215-2227, doi: 10.1056/NEJMoa1708538.
- Georg-Fries, B., Biederlack, S., Wolf, J. and Zur Hausen, H. (1984). **Analysis of proteins, helper dependence, and seroepidemiology of a new human parvovirus.** *Virology* 134, 64-71.
- Girod, A., Wobus, C. E., Zádori, Z., Ried, M., Leike, K., Tijssen, P., Kleinschmidt, J. A. and Hallek, M. (2002). **The VP1 capsid protein of adeno-associated**

- virus type 2 is carrying a phospholipase A2 domain required for virus infectivity.** *J Gen Virol* 83, 973-978, doi: 10.1099/0022-1317-83-5-973.
- Greber, U. F., Suomalainen, M., Stidwill, R. P., Boucke, K., Ebersold, M. W. and Helenius, A. (1997). **The role of the nuclear pore complex in adenovirus DNA entry.** *EMBO J* 16, 5998-6007, doi: 10.1093/emboj/16.19.5998.
- Grieger, J. C. and Samulski, R. J. (2012). **Adeno-associated virus vectorology, manufacturing, and clinical applications.** *Meth Enzymol* 507, 229-254, doi: 10.1016/B978-0-12-386509-0.00012-0.
- Guo, D., Li, M., Zhang, Y., Yang, P., Eckenrode, S., Hopkins, D., Zheng, W., Purohit, S., Podolsky, R. H., Muir, A., Wang, J., Dong, Z., Brusko, T., Atkinson, M., Pozzilli, P., Zeidler, A., Raffel, L. J., Jacob, C. O., Park, Y., Serrano-Rios, M., Larrad, M. T. M., Zhang, Z., Garchon, H.-J., Bach, J.-F., Rotter, J. I., She, J.-X. and Wang, C.-Y. (2004). **A functional variant of SUMO4, a new I kappa B alpha modifier, is associated with type 1 diabetes.** *Nat Genet* 36, 837-841, doi: 10.1038/ng1391.
- Han, Q., Chang, C., Li, L., Klenk, C., Cheng, J., Chen, Y., Xia, N., Shu, Y., Chen, Z., Gabriel, G., Sun, B. and Xu, K. (2014). **Sumoylation of influenza A virus nucleoprotein is essential for intracellular trafficking and virus growth.** *J Virol* 88, 9379-9390, doi: 10.1128/JVI.00509-14.
- Hecker, C.-M., Rabiller, M., Haglund, K., Bayer, P. and Dikic, I. (2006). **Specification of SUMO1- and SUMO2-interacting motifs.** *J Biol Chem* 281, 16117-16127, doi: 10.1074/jbc.M512757200.
- Hendriks, I. A. and Vertegaal, A. C. O. (2016). **A comprehensive compilation of SUMO proteomics.** *Nat Rev Mol Cell Biol* 17, 581-595, doi: 10.1038/nrm.2016.81.
- Herrmann, J., Lerman, L. O. and Lerman, A. (2007). **Ubiquitin and ubiquitin-like proteins in protein regulation.** *Circ Res* 100, 1276-1291, doi: 10.1161/01.RES.0000264500.11888.f0.
- Hoggan, M. D., Blacklow, N. R. and Rowe, W. P. (1966). **Studies of small DNA viruses found in various adenovirus preparations. Physical, biological, and immunological characteristics.** *Proc Natl Acad Sci U S A* 55, 1467-1474.
- Hollenbach, A. D., McPherson, C. J., Mientjes, E. J., Iyengar, R. and Grosveld, G. (2002). **Daxx and histone deacetylase II associate with chromatin through an interaction with core histones and the chromatin-associated protein Dek.** *J Cell Sci* 115, 3319-3330.
- Hölscher, C., Sonntag, F., Henrich, K., Chen, Q., Beneke, J., Matula, P., Rohr,

- K., Kaderali, L., Beil, N., Erfle, H., Kleinschmidt, J. A. and Müller, M. (2015). **The SUMOylation Pathway Restricts Gene Transduction by Adeno-Associated Viruses.** *PLoS Pathog* 11, e1005281, doi: 10.1371/journal.ppat.1005281.
- Hoque, M., Ishizu, K., Matsumoto, A., Han, S. I., Arisaka, F., Takayama, M., Suzuki, K., Kato, K., Kanda, T., Watanabe, H. and Handa, H. (1999). **Nuclear transport of the major capsid protein is essential for adeno-associated virus capsid formation.** *J Virol* 73, 7912-7915.
- Huang, L.-Y., Halder, S. and Agbandje-McKenna, M. (2014). **Parvovirus glycan interactions.** *Curr Opin Virol* 7, 108-118, doi: 10.1016/j.coviro.2014.05.007.
- Huttner, N. A., Girod, A., Perabo, L., Edbauer, D., Kleinschmidt, J. A., Büning, H. and Hallek, M. (2003). **Genetic modifications of the adeno-associated virus type 2 capsid reduce the affinity and the neutralizing effects of human serum antibodies.** *Gene Ther* 10, 2139-2147, doi: 10.1038/sj.gt.3302123.
- Jang, M.-S., Ryu, S.-W. and Kim, E. (2002). **Modification of Daxx by small ubiquitin-related modifier-1.** *Biochem Biophys Res Commun* 295, 495-500.
- Johnson, E. S. (2004). **Protein modification by SUMO.** *Annu Rev Biochem* 73, 355-382, doi: 10.1146/annurev.biochem.73.011303.074118.
- Johnson, J. S., Gentsch, M., Zhang, L., Ribeiro, C. M. P., Kantor, B., Kafri, T., Pickles, R. J. and Samulski, R. J. (2011). **AAV exploits subcellular stress associated with inflammation, endoplasmic reticulum expansion, and misfolded proteins in models of cystic fibrosis.** *PLoS Pathog* 7, e1002053, doi: 10.1371/journal.ppat.1002053.
- Kagey, M. H., Melhuish, T. A. and Wotton, D. (2003). **The polycomb protein Pc2 is a SUMO E3.** *Cell* 113, 127-137.
- Kashiwakura, Y., Tamayose, K., Iwabuchi, K., Hirai, Y., Shimada, T., Matsumoto, K., Nakamura, T., Watanabe, M., Oshimi, K. and Daida, H. (2005). **Hepatocyte growth factor receptor is a coreceptor for adeno-associated virus type 2 infection.** *J Virol* 79, 609-614, doi: 10.1128/JVI.79.1.609-614.2005.
- Kato-Noah, T., Xu, Y., Rossetto, C. C., Colletti, K., Papoušková, I. and Pari, G. S. (2007). **Overexpression of the kaposi's sarcoma-associated herpesvirus transactivator K-Rta can complement a K-bZIP deletion BACmid and yields an enhanced growth phenotype.** *J Virol* 81, 13519-13532, doi: 10.1128/JVI.00832-07.

- Kerscher, O., Felberbaum, R. and Hochstrasser, M. (2006). **Modification of proteins by ubiquitin and ubiquitin-like proteins**. *Annu Rev Cell Dev Biol* 22, 159-180, doi: 10.1146/annurev.cellbio.22.010605.093503.
- King, J. A., Dubielzig, R., Grimm, D. and Kleinschmidt, J. A. (2001). **DNA helicase-mediated packaging of adeno-associated virus type 2 genomes into preformed capsids**. *EMBO J* 20, 3282-3291, doi: 10.1093/emboj/20.12.3282.
- Kirsh, O., Seeler, J.-S., Pichler, A., Gast, A., Müller, S., Miska, E., Mathieu, M., Harel-Bellan, A., Kouzarides, T., Melchior, F. and Dejean, A. (2002). **The SUMO E3 ligase RanBP2 promotes modification of the HDAC4 deacetylase**. *EMBO J* 21, 2682-2691, doi: 10.1093/emboj/21.11.2682.
- Kotin, R. M., Siniscalco, M., Samulski, R. J., Zhu, X. D., Hunter, L., Laughlin, C. A., McLaughlin, S., Muzyczka, N., Rocchi, M. and Berns, K. I. (1990). **Site-specific integration by adeno-associated virus**. *Proc Natl Acad Sci U S A* 87, 2211-2215.
- Kronenberg, S., Böttcher, B., Lieth, C. W. von der, Bleker, S. and Kleinschmidt, J. A. (2005). **A conformational change in the adeno-associated virus type 2 capsid leads to the exposure of hidden VP1 N termini**. *J Virol* 79, 5296-5303, doi: 10.1128/JVI.79.9.5296-5303.2005.
- Kurzeder, C., Koppold, B., Sauer, G., Pabst, S., Kreienberg, R. and Deissler, H. (2007). **CD9 promotes adeno-associated virus type 2 infection of mammary carcinoma cells with low cell surface expression of heparan sulphate proteoglycans**. *Int J Mol Med* 19, 325-333.
- Li, B., Ma, W., Ling, C., van Vliet, K., Huang, L.-Y., Agbandje-McKenna, M., Srivastava, A. and Aslanidi, G. V. (2015). **Site-Directed Mutagenesis of Surface-Exposed Lysine Residues Leads to Improved Transduction by AAV2, But Not AAV8, Vectors in Murine Hepatocytes In Vivo**. *Hum Gene Ther Methods* 26, 211-220, doi: 10.1089/hgtb.2015.115.
- Lin, D.-Y., Huang, Y.-S., Jeng, J.-C., Kuo, H.-Y., Chang, C.-C., Chao, T.-T., Ho, C.-C., Chen, Y.-C., Lin, T.-P., Fang, H.-I., Hung, C.-C., Suen, C.-S., Hwang, M.-J., Chang, K.-S., Maul, G. G. and Shih, H.-M. (2006). **Role of SUMO-interacting motif in Daxx SUMO modification, subnuclear localization, and repression of sumoylated transcription factors**. *Mol Cell* 24, 341-354, doi: 10.1016/j.molcel.2006.10.019
- Lin, S. F., Robinson, D. R., Miller, G. and Kung, H. J. (1999). **Kaposi's sarcoma-associated herpesvirus encodes a bZIP protein with homology to BZLF1 of Epstein-Barr virus**. *J Virol* 73, 1909-1917.
- Ling, C., Lu, Y., Kalsi, J. K., Jayandharan, G. R., Li, B., Ma, W., Cheng, B., Gee,

-
- S. W. Y., McGoogan, K. E., Govindasamy, L., Zhong, L., Agbandje-McKenna, M. and Srivastava, A. (2010). **Human hepatocyte growth factor receptor is a cellular coreceptor for adeno-associated virus serotype 3.** *Hum Gene Ther* 21, 1741-1747, doi: 10.1089/hum.2010.075.
- Liu, Y., Zheng, Z., Shu, B., Meng, J., Zhang, Y., Zheng, C., Ke, X., Gong, P., Hu, Q. and Wang, H. (2016). **SUMO Modification Stabilizes Enterovirus 71 Polymerase 3D To Facilitate Viral Replication.** *J Virol* 90, 10472-10485, doi: 10.1128/JVI.01756-16.
- Lochrie, M. A., Tatsuno, G. P., Christie, B., McDonnell, J. W., Zhou, S., Surosky, R., Pierce, G. F. and Colosi, P. (2006). **Mutations on the external surfaces of adeno-associated virus type 2 capsids that affect transduction and neutralization.** *J Virol* 80, 821-834, doi: 10.1128/JVI.80.2.821-834.2006
- Lukashchuk, V. and Everett, R. D. (2010). **Regulation of ICP0-null mutant herpes simplex virus type 1 infection by ND10 components ATRX and hDaxx.** *J Virol* 84, 4026-4040, doi: 10.1128/JVI.02597-09.
- Madshus, I. H., Olsnes, S. and Sandvig, K. (1984). **Mechanism of entry into the cytosol of poliovirus type 1. Requirement for low pH.** *J Cell Biol* 98, 1194-1200.
- Marusic, M. B., Mencin, N., Licen, M., Banks, L. and Grm, H. S. (2010). **Modification of human papillomavirus minor capsid protein L2 by sumoylation.** *J Virol* 84, 11585-11589, doi: 10.1128/JVI.01269-10.
- Matic, I., Schimmel, J., Hendriks, I. A., van Santen, M. A., van de Rijke, F., van Dam, H., Gnad, F., Mann, M. and Vertegaal, A. C. O. (2010). **Site-specific identification of SUMO-2 targets in cells reveals an inverted SUMOylation motif and a hydrophobic cluster SUMOylation motif.** *Mol Cell* 39, 641-652, doi: 10.1016/j.molcel.2010.07.026.
- McCarty, D. M., Monahan, P. E. and Samulski, R. J. (2001). **Self-complementary recombinant adeno-associated virus (scAAV) vectors promote efficient transduction independently of DNA synthesis.** *Gene Ther* 8, 1248-1254, doi: 10.1038/sj.gt.3301514.
- McPherson, R. A., Rosenthal, L. J. and Rose, J. A. (1985). **Human cytomegalovirus completely helps adeno-associated virus replication.** *Virology* 147, 217-222.
- Melchior, F. (2000). **SUMO--nonclassical ubiquitin.** *Annu Rev Cell Dev Biol* 16, 591-626, doi: 10.1146/annurev.cellbio.16.1.591.

- Meroni, G. and Diez-Roux, G. (2005). **TRIM/RBCC, a novel class of 'single protein RING finger' E3 ubiquitin ligases.** *Bioessays* 27, 1147-1157, doi: 10.1002/bies.20304.
- Mingozzi, F. and High, K. A. (2013). **Immune responses to AAV vectors. Overcoming barriers to successful gene therapy.** *Blood* 122, 23-36, doi: 10.1182/blood-2013-01-306647.
- Mizukami, H., Young, N. S. and Brown, K. E. (1996). **Adeno-associated virus type 2 binds to a 150-kilodalton cell membrane glycoprotein.** *Virology* 217, 124-130, doi: 10.1006/viro.1996.0099.
- Monahan, P. E., Lothrop, C. D., Sun, J., Hirsch, M. L., Kafri, T., Kantor, B., Sarkar, R., Tillson, D. M., Elia, J. R. and Samulski, R. J. (2010). **Proteasome inhibitors enhance gene delivery by AAV virus vectors expressing large genomes in hemophilia mouse and dog models. A strategy for broad clinical application.** *Mol Ther* 18, 1907-1916, doi: 10.1038/mt.2010.170.
- Mori, S., Wang, L., Takeuchi, T. and Kanda, T. (2004). **Two novel adeno-associated viruses from cynomolgus monkey. Pseudotyping characterization of capsid protein.** *Virology* 330, 375-383, doi: 10.1016/j.virol.2004.10.012.
- Mossessova, E. and Lima, C. D. (2000). **Ulp1-SUMO Crystal Structure and Genetic Analysis Reveal Conserved Interactions and a Regulatory Element Essential for Cell Growth in Yeast.** *Mol Cell* 5, 865-876, doi: 10.1016/S1097-2765(00)80326-3.
- Muralidhar, S., Becerra, S. P. and Rose, J. A. (1994). **Site-directed mutagenesis of adeno-associated virus type 2 structural protein initiation codons. Effects on regulation of synthesis and biological activity.** *J Virol* 68, 170-176.
- Muramatsu, S., Mizukami, H., Young, N. S. and Brown, K. E. (1996). **Nucleotide sequencing and generation of an infectious clone of adeno-associated virus 3.** *Virology* 221, 208-217.
- Muzyczka, N. (1992). **Use of adeno-associated virus as a general transduction vector for mammalian cells.** *Curr Top Microbiol Immunol* 158, 97-129.
- Nacerddine, K., Lehembre, F., Bhaumik, M., Artus, J., Cohen-Tannoudji, M., Babinet, C., Pandolfi, P. P. and Dejean, A. (2005). **The SUMO pathway is essential for nuclear integrity and chromosome segregation in mice.** *Dev Cell* 9, 769-779, doi: 10.1016/j.devcel.2005.10.007

- Naumer, M., Sonntag, F., Schmidt, K., Nieto, K., Panke, C., Davey, N. E., Popa-Wagner, R. and Kleinschmidt, J. A. (2012). **Properties of the adeno-associated virus assembly-activating protein.** *J Virol* **86**, 13038-13048, doi: 10.1128/JVI.01675-12.
- Ngamurulert, S., Limjindaporn, T. and Auewaraku, P. (2009). **Identification of cellular partners of Influenza A virus (H5N1) non-structural protein NS1 by yeast two-hybrid system.** *Acta Virol* **53**, 153-159.
- Nonnenmacher, M. and Weber, T. (2011). **Adeno-associated virus 2 infection requires endocytosis through the CLIC/GEEC pathway.** *Cell Host Microbe* **10**, 563-576, doi: 10.1016/j.chom.2011.10.014.
- Nonnenmacher, M. and Weber, T. (2012). **Intracellular transport of recombinant adeno-associated virus vectors.** *Gene Ther* **19**, 649-658, doi: 10.1038/gt.2012.6.
- Nonnenmacher, M. E., Cintrat, J.-C., Gillet, D. and Weber, T. (2015). **Syntaxin 5-dependent retrograde transport to the trans-Golgi network is required for adeno-associated virus transduction.** *J Virol* **89**, 1673-1687, doi: 10.1128/JVI.02520-14.
- Ogston, P., Raj, K. and Beard, P. (2000). **Productive replication of adeno-associated virus can occur in human papillomavirus type 16 (HPV-16) episome-containing keratinocytes and is augmented by the HPV-16 E2 protein.** *J Virol* **74**, 3494-3504.
- Pal, S., Santos, A., Rosas, J. M., Ortiz-Guzman, J. and Rosas-Acosta, G. (2011). **Influenza A virus interacts extensively with the cellular SUMOylation system during infection.** *Virus Res* **158**, 12-27, doi: 10.1016/j.virusres.2011.02.017.
- Petrucci, M. T., Giraldo, P., Corradini, P., Teixeira, A., Dimopoulos, M. A., Blau, I. W., Drach, J., Angermund, R., Allietta, N., Broer, E., Mitchell, V. and Bladé, J. (2013). **A prospective, international phase 2 study of bortezomib retreatment in patients with relapsed multiple myeloma.** *Br J Haematol* **160**, 649-659, doi: 10.1111/bjh.12198.
- Pichler, A., Gast, A., Seeler, J. S., Dejean, A. and Melchior, F. (2002). **The nucleoporin RanBP2 has SUMO1 E3 ligase activity.** *Cell* **108**, 109-120.
- Pillay, S. and Carette, J. E. (2017). **Host determinants of adeno-associated viral vector entry.** *Curr Opin Virol* **24**, 124-131, doi: 10.1016/j.coviro.2017.06.003.
- Pillay, S., Meyer, N. L., Puschnik, A. S., Davulcu, O., Diep, J., Ishikawa, Y., Jae, L. T., Wosen, J. E., Nagamine, C. M., Chapman, M. S. and Carette, J. E.

- (2016). **An essential receptor for adeno-associated virus infection.** *Nature* 530, 108-112, doi: 10.1038/nature16465.
- Preston, C. M., Rinaldi, A. and Nicholl, M. J. (1998). **Herpes simplex virus type 1 immediate early gene expression is stimulated by inhibition of protein synthesis.** *J Gen Virol* 79 (*Pt 1*), 117-124, doi: 10.1099/0022-1317-79-1-117.
- Psakhye, I. and Jentsch, S. (2012). **Protein group modification and synergy in the SUMO pathway as exemplified in DNA repair.** *Cell* 151, 807-820, doi: 10.1016/j.cell.2012.10.021.
- Qi, Y., Wang, J., Bomben, V. C., Li, D.-P., Chen, S.-R., Sun, H., Xi, Y., Reed, J. G., Cheng, J., Pan, H.-L., Noebels, J. L. and Yeh, E. T. H. (2014). **Hyper-SUMOylation of the Kv7 potassium channel diminishes the M-current leading to seizures and sudden death.** *Neuron* 83, 1159-1171, doi: 10.1016/j.neuron.2014.07.042.
- Qing, K., Khuntirat, B., Mah, C., Kube, D. M., Wang, X. S., Ponnazhagan, S., Zhou, S., Dwarki, V. J., Yoder, M. C. and Srivastava, A. (1998). **Adeno-associated virus type 2-mediated gene transfer. Correlation of tyrosine phosphorylation of the cellular single-stranded D sequence-binding protein with transgene expression in human cells in vitro and murine tissues in vivo.** *J Virol* 72, 1593-1599.
- Qing, K., Mah, C., Hansen, J., Zhou, S., Dwarki, V. and Srivastava, A. (1999). **Human fibroblast growth factor receptor 1 is a co-receptor for infection by adeno-associated virus 2.** *Nat Med* 5, 71-77, doi: 10.1038/4758.
- Raj, D., Davidoff, A. M. and Nathwani, A. C. (2011). **Self-complementary adeno-associated viral vectors for gene therapy of hemophilia B. Progress and challenges.** *Expert Rev Hematol* 4, 539-549, doi: 10.1586/ehm.11.48.
- Raman, N., Nayak, A. and Muller, S. (2013). **The SUMO system. A master organizer of nuclear protein assemblies.** *Chromosoma* 122, 475-485, doi: 10.1007/s00412-013-0429-6.
- Rampen, A. J. J., Jongen, J. L. M., van Heuvel, I., Scheltens-de Boer, M., Sonneveld, P. and van den Bent, M. J. (2013). **Bortezomib-induced polyneuropathy.** *Neth J Med* 71, 128-133.
- Ros, C., Baltzer, C., Mani, B. and Kempf, C. (2006). **Parvovirus uncoating in vitro reveals a mechanism of DNA release without capsid disassembly and striking differences in encapsidated DNA stability.** *Virology* 345, 137-147, doi: 10.1016/j.virol.2005.09.030.

- Rutledge, E. A., Halbert, C. L. and Russell, D. W. (1998). **Infectious clones and vectors derived from adeno-associated virus (AAV) serotypes other than AAV type 2.** *J Virol* 72, 309-319.
- Ryan, C. M., Kindle, K. B., Collins, H. M. and Heery, D. M. (2010). **SUMOylation regulates the nuclear mobility of CREB binding protein and its association with nuclear bodies in live cells.** *Biochem Biophys Res Commun* 391, 1136-1141, doi: 10.1016/j.bbrc.2009.12.040.
- Sahin, U., Ferhi, O., Carnec, X., Zamborlini, A., Peres, L., Jollivet, F., Vitaliano-Prunier, A., Thé, H. de and Lallemand-Breitenbach, V. (2014). **Interferon controls SUMO availability via the Lin28 and let-7 axis to impede virus replication.** *Nat Commun* 5, 4187, doi: 10.1038/ncomms5187.
- Salmon, F., Grosios, K. and Petry, H. (2014). **Safety profile of recombinant adeno-associated viral vectors. Focus on alipogene tiparvovec (Glybera®).** *Expert Rev Clin Pharmacol* 7, 53-65, doi: 10.1586/17512433.2014.852065.
- Samulski, R. J., Berns, K. I., Tan, M. and Muzyczka, N. (1982). **Cloning of adeno-associated virus into pBR322. Rescue of intact virus from the recombinant plasmid in human cells.** *Proc Natl Acad Sci U S A* 79, 2077-2081.
- Santos, A., Pal, S., Chacón, J., Meraz, K., Gonzalez, J., Prieto, K. and Rosas-Acosta, G. (2013). **SUMOylation affects the interferon blocking activity of the influenza A nonstructural protein NS1 without affecting its stability or cellular localization.** *J Virol* 87, 5602-5620, doi: 10.1128/JVI.02063-12.
- Schmidt, M., Voutetakis, A., Afione, S., Zheng, C., Mandikian, D. and Chiorini, J. A. (2008). **Adeno-associated virus type 12 (AAV12). A novel AAV serotype with sialic acid- and heparan sulfate proteoglycan-independent transduction activity.** *J Virol* 82, 1399-1406, doi: 10.1128/JVI.02012-07.
- Schreiner, S., Bürck, C., Glass, M., Groitl, P., Wimmer, P., Kinkley, S., Mund, A., Everett, R. D. and Dobner, T. (2013). **Control of human adenovirus type 5 gene expression by cellular Daxx/ATRX chromatin-associated complexes.** *Nucleic Acids Res* 41, 3532-3550, doi: 10.1093/nar/gkt064.
- Schreiner, S. and Wodrich, H. (2013). **Virion factors that target Daxx to overcome intrinsic immunity.** *J Virol* 87, 10412-10422, doi: 10.1128/JVI.00425-13.
- Seisenberger, G., Ried, M. U., Endress, T., Büning, H., Hallek, M. and Bräuchle,

- C. (2001). **Real-time single-molecule imaging of the infection pathway of an adeno-associated virus.** *Science* 294, 1929-1932, doi: 10.1126/science.1064103.
- Silver, H. R., Nissley, J. A., Reed, S. H., Hou, Y.-M. and Johnson, E. S. (2011). **A role for SUMO in nucleotide excision repair.** *DNA Repair (Amst)* 10, 1243-1251, doi: 10.1016/j.dnarep.2011.09.013.
- Snyder, R. O., Im, D. S., Ni, T., Xiao, X., Samulski, R. J. and Muzyczka, N. (1993). **Features of the adeno-associated virus origin involved in substrate recognition by the viral Rep protein.** *J Virol* 67, 6096-6104.
- Song, J., Durrin, L. K., Wilkinson, T. A., Krontiris, T. G. and Chen, Y. (2004). **Identification of a SUMO-binding motif that recognizes SUMO-modified proteins.** *Proc Natl Acad Sci U S A* 101, 14373-14378, doi: 10.1073/pnas.0403498101.
- Srivastava, A., Lusby, E. W. and Berns, K. I. (1983). **Nucleotide sequence and organization of the adeno-associated virus 2 genome.** *J Virol* 45, 555-564.
- Summerford, C., Bartlett, J. S. and Samulski, R. J. (1999). **AlphaVbeta5 integrin. A co-receptor for adeno-associated virus type 2 infection.** *Nat Med* 5, 78-82, doi: 10.1038/4768.
- Summerford, C. and Samulski, R. J. (1998). **Membrane-associated heparan sulfate proteoglycan is a receptor for adeno-associated virus type 2 virions.** *J Virol* 72, 1438-1445.
- Suomalainen, M. and Greber, U. F. (2013). **Uncoating of non-enveloped viruses.** *Curr Opin Virol* 3, 27-33, doi: 10.1016/j.coviro.2012.12.004.
- Tsai, K., Thikmyanova, N., Wojcechowskyj, J. A., Delecluse, H.-J. and Lieberman, P. M. (2011). **EBV tegument protein BRF1 disrupts DAXX-ATRAX to activate viral early gene transcription.** *PLoS Pathog* 7, e1002376, doi: 10.1371/journal.ppat.1002376.
- Tsukamoto, T., Hashiguchi, N., Janicki, S. M., Tumber, T., Belmont, A. S. and Spector, D. L. (2000). **Visualization of gene activity in living cells.** *Nat Cell Biol* 2, 871-878, doi: 10.1038/35046510.
- Ullman, A. J. and Hearing, P. (2008). **Cellular proteins PML and Daxx mediate an innate antiviral defense antagonized by the adenovirus E4 ORF3 protein.** *J Virol* 82, 7325-7335, doi: 10.1128/JVI.00723-08.
- Voortman, J. and Giaccone, G. (2006). **Severe reversible cardiac failure after bortezomib treatment combined with chemotherapy in a non-small cell lung cancer patient. A case report.** *BMC Cancer* 6, 129,

- doi: 10.1186/1471-2407-6-129.
- Walz, C. M., Anisi, T. R., Schlehofer, J. R., Gissmann, L., Schneider, A. and Müller, M. (1998). **Detection of infectious adeno-associated virus particles in human cervical biopsies.** *Virology* 247, 97-105, doi: 10.1006/viro.1998.9226.
- Wang, X., Peng, W., Ren, J., Hu, Z., Xu, J., Lou, Z., Li, X., Yin, W., Shen, X., Porta, C., Walter, T. S., Evans, G., Axford, D., Owen, R., Rowlands, D. J., Wang, J., Stuart, D. I., Fry, E. E. and Rao, Z. (2012). **A sensor-adaptor mechanism for enterovirus uncoating from structures of EV71.** *Nat Struct Mol Biol* 19, 424-429, doi: 10.1038/nsmb.2255.
- Wang, X. S. and Srivastava, A. (1998). **Rescue and autonomous replication of adeno-associated virus type 2 genomes containing Rep-binding site mutations in the viral p5 promoter.** *J Virol* 72, 4811-4818.
- Warrington, K. H., Gorbatyuk, O. S., Harrison, J. K., Opie, S. R., Zolotukhin, S. and Muzyczka, N. (2004). **Adeno-associated virus type 2 VP2 capsid protein is nonessential and can tolerate large peptide insertions at its N terminus.** *J Virol* 78, 6595-6609, doi: 10.1128/JVI.78.12.6595-6609.2004.
- Weinberg, M. S., Nicolson, S., Bhatt, A. P., McLendon, M., Li, C. and Samulski, R. J. (2014). **Recombinant adeno-associated virus utilizes cell-specific infectious entry mechanisms.** *J Virol* 88, 12472-12484, doi: 10.1128/JVI.01971-14.
- Weindler, F. W. and Heilbronn, R. (1991). **A subset of herpes simplex virus replication genes provides helper functions for productive adeno-associated virus replication.** *J Virol* 65, 2476-2483.
- Weller, M. L., Amornphimoltham, P., Schmidt, M., Wilson, P. A., Gutkind, J. S. and Chiorini, J. A. (2010). **Epidermal growth factor receptor is a co-receptor for adeno-associated virus serotype 6.** *Nat Med* 16, 662-664, doi: 10.1038/nm.2145.
- Werner, A., Flotho, A. and Melchior, F. (2012). **The RanBP2/RanGAP1*SUMO1/Ubc9 complex is a multisubunit SUMO E3 ligase.** *Mol Cell* 46, 287-298, doi: 10.1016/j.molcel.2012.02.017.
- Wotton, D., Pemberton, L. F. and Merrill-Schools, J. (2017). **SUMO and Chromatin Remodeling.** *Adv Exp Med Biol* 963, 35-50, doi: 10.1007/978-3-319-50044-7_3.
- Wu, C.-Y., Jeng, K.-S. and Lai, M. M.-C. (2011). **The SUMOylation of matrix protein M1 modulates the assembly and morphogenesis of influenza**

- A virus.** *J Virol* 85, 6618-6628, doi: 10.1128/JVI.02401-10.
- Wu, T. T., Tong, L., Rickabaugh, T., Speck, S. and Sun, R. (2001). **Function of Rta is essential for lytic replication of murine gammaherpesvirus 68.** *J Virol* 75, 9262-9273, doi: 10.1128/JVI.75.19.9262-9273.2001.
- Wu, Y.-C., Roark, A. A., Bian, X.-L. and van Wilson, G. (2008). **Modification of papillomavirus E2 proteins by the small ubiquitin-like modifier family members (SUMOs).** *Virology* 378, 329-338, doi: 10.1016/j.virol.2008.06.008.
- Wu, Z., Yang, H. and Colosi, P. (2010). **Effect of genome size on AAV vector packaging.** *Mol Ther* 18, 80-86, doi: 10.1038/mt.2009.255.
- Xiao, P.-J. and Samulski, R. J. (2012). **Cytoplasmic trafficking, endosomal escape, and perinuclear accumulation of adeno-associated virus type 2 particles are facilitated by microtubule network.** *J Virol* 86, 10462-10473, doi: 10.1128/JVI.00935-12.
- Xiao, W., Chirmule, N., Berta, S. C., McCullough, B., Gao, G. and Wilson, J. M. (1999). **Gene therapy vectors based on adeno-associated virus type 1.** *J Virol* 73, 3994-4003.
- Xiao, W., Warrington, K. H., Hearing, P., Hughes, J. and Muzyczka, N. (2002). **Adenovirus-facilitated nuclear translocation of adeno-associated virus type 2.** *J Virol* 76, 11505-11517.
- Xie, Q., Bu, W., Bhatia, S., Hare, J., Somasundaram, T., Azzi, A. and Chapman, M. S. (2002). **The atomic structure of adeno-associated virus (AAV-2), a vector for human gene therapy.** *Proc Natl Acad Sci U S A* 99, 10405-10410, doi: 10.1073/pnas.162250899
- Yang, S.-H., Galanis, A., Witty, J. and Sharrocks, A. D. (2006). **An extended consensus motif enhances the specificity of substrate modification by SUMO.** *EMBO J* 25, 5083-5093, doi: 10.1038/sj.emboj.7601383.
- Yueh, A., Leung, J., Bhattacharyya, S., Perrone, L. A., los Santos, K. de, Pu, S.-Y. and Goff, S. P. (2006). **Interaction of moloney murine leukemia virus capsid with Ubc9 and PIASy mediates SUMO-1 addition required early in infection.** *J Virol* 80, 342-352, doi: 10.1128/JVI.80.1.342-352.2006.
- Yunus, A. A. and Lima, C. D. (2009). **Structure of the Siz/PIAS SUMO E3 ligase Siz1 and determinants required for SUMO modification of PCNA.** *Mol Cell* 35, 669-682, doi: 10.1016/j.molcel.2009.07.013.
- Zhang, F.-P., Mikkonen, L., Toppari, J., Palvimo, J. J., Thesleff, I. and Jänne, O. A. (2008). **Sumo-1 function is dispensable in normal mouse**

- development.** *Mol Cell Biol* 28, 5381-5390, doi: 10.1128/MCB.00651-08.
- Zhong, L., Li, B., Jayandharan, G., Mah, C. S., Govindasamy, L., Agbandje-McKenna, M., Herzog, R. W., Weigel-Van Aken, K. A., Hobbs, J. A., Zolotukhin, S., Muzyczka, N. and Srivastava, A. (2008a). **Tyrosine-phosphorylation of AAV2 vectors and its consequences on viral intracellular trafficking and transgene expression.** *Virology* 381, 194-202, doi: 10.1016/j.virol.2008.08.027.
- Zhong, L., Li, B., Mah, C. S., Govindasamy, L., Agbandje-McKenna, M., Cooper, M., Herzog, R. W., Zolotukhin, I., Warrington, K. H., Weigel-Van Aken, K. A., Hobbs, J. A., Zolotukhin, S., Muzyczka, N. and Srivastava, A. (2008b). **Next generation of adeno-associated virus 2 vectors. Point mutations in tyrosines lead to high-efficiency transduction at lower doses.** *Proc Natl Acad Sci U S A* 105, 7827-7832, doi: 10.1073/pnas.0802866105.

9 Publication

1. The SUMOylation Pathway Restricts Gene Transduction by Adeno-Associated Viruses. Hölscher, C., Sonntag, F., Henrich, K., Chen, Q., Beneke, J., Matula, P., Rohr, K., Kaderali, L., Beil, N., Erfle, H., Kleinschmidt, J. A. and Müller, M. (2015).

In this thesis, the data Figure 11, Figure 12, Figure 20 and Figure 21 were published in the paper 'The SUMOylation Pathway Restricts Gene Transduction by Adeno-Associated Viruses':

Thesis Figure 11 was published in paper, as Fig 6B and S4 Fig.

Thesis Figure 12 was published in paper, as Fig 4A.

Thesis Figure 20 was published in paper, as S2 Fig.

Thesis Figure 21 was published in paper, as S3 Fig.

2. Capsid protein of adeno-associated virus type 2 is the target of SUMOylation. (in preparing)

10 Curriculum Vitae

First name: Qingxin

Family name: Chen

Date of birth: 27.01.1988

Place of birth: Heilongjiang

Nationality: China

Marital Status: Single

SCHOOL EXPERIENCE

09.1994-06.1999 Xinlin No. 1 primary school, Daxinganling, Heilongjiang province

09.1999-06.2002 Xinlin No. 3 middle school, Daxinganling, Heilongjiang province

09.2002-06.2006 Mianyang Nanshan High School, Mianyang, Sichuan province.

UNIVERSITY EXPERIENCE

09.2006- 06.2011 Harbin Medical University, Harbin, Heilongjiang

Bachelor's degree (Major: Clinical Pharmacy)

09.2011- 06.2014 Harbin Medical University, Harbin, Heilongjiang

Master's degree (Major: Pharmacology)

09. 2014- German Cancer Research Center, Heidelberg, Germany

PhD. candidate (Major: Virology)

11 Acknowledgement

I hereby would like to thank everyone who supported me in producing this work.

Firstly, I would like to thank Prof. Dr. Martin Müller for giving me the opportunity to do my PhD research in his laboratory. I would like to thank him for his great supervision and input, his patience and experimental advice and help.

My sincere thank you also goes to Prof. Dr. Oliver Müller for agreeing to act as my second professor and my TAC member, thanks for his solid support for the AAV study.

I would also like to thank another TAC member Dr. Steeve Boulant for his helpful ideas during the TAC discussion, as well as the support for AAV trafficking study.

In addition, I am very thankful to Dr. Jürgen Kleinschmidt for answering all my questions and his strict logic helped me solve many problems.

Many thanks to Barbara Leuchs and her team for all AAV titer quantifications and the cell samples qPCR test, and also thanks to Dr. Susanna Chiocca for supporting Gam1 cell line.

I am also very grateful to my colleague Robin Wanjiru Njenga about improving my English skills, discussing whole AAV project with her and her experimental help always cheering me up.

Many thanks to all members of my laboratory 2.114. Thank Dr. Caroline Odenwald, Dr. Filipe Mariz, Dr. Somayeh Pouyanfard, Xueer Zhao, Fan Yang, Anja Brauchle, Lea Herkens, Moritz Koenig, Franziska Ragaller, as well as the technician Petra Galmbacher and the secretary Madeleine Sporleder for their helping hands and motivating conversations.

Moreover, I would like to thank all my great friends inside and outside of Heidelberg who have accompanied me over the last few years and have always been there to support me.

Finally, a very special thank you to my parents and Yan Zeng, who have always supported and encouraged me to find my own path and have enabled my studies in Heidelberg. Thank you all for your patience and love.

12 Thesis Declaration

Declaration according to §8 of the doctoral degree regulations

I hereby declare that I have written the submitted dissertation independently and have not used other sources and materials than those particularly indicated.

Further, I declare that I have not applied to be examined at any other institution, nor have I presented this dissertation to any other faculty, nor have I used this dissertation in any form in another examination.

Heidelberg, Germany

Qingxin Chen